UNIVERSITAT DE BARCELONA

Effective methods for recurrence solutions in delay differential equations

Joan Gimeno i Alquézar

UNIVERSITAT DE BARCELONA

Effective methods for recurrence solutions in delay differential equations

by

Joan Gimeno Alquézar

A thesis submitted
for the PhD Program in Mathematics and Computer Science

Advisors

Àngel Jorba Monte
Rafael de la Llave Canosa

Department of Mathematics and Computer Science
University of Barcelona Graduate School

Barcelona, September 2019

Tesi presentada per en **Joan Gimeno i Alquézar** per a optar al títol de

Doctor en Matemàtiques i Informàtica

per la

Universitat de Barcelona

El tutor Àngel Jorba i Monte certifica que la present tesi ha estat realitzada per en *Joan Gimeno i Alquézar* sota la direcció dels professors *Àngel Jorba i Monte* de la Universtat de Barcelona i *Rafael de la Llave i Canosa* del Georgia Institute of Technology.

Barcelona, setembre del 2019.

Contents

Agraïments

A aquells que m'han conegut fins ara. En especial i per a realització d'aquesta tesi a aquells que m'han ajudat d'una manera o altre. Des del punt acadèmic fins al punt més proper i personal.

És d'obligat començar per aquells del principi i, en aquest cas, han sigut els meus pares i el director i tutor. Pels meus pares pel suport incondicional i els seus consells tan generals i genèrics que a vegades costa acotar-los a la inquietud o decisió del moment. A l'Àngel que tot i que coneixe'l per primer cop a l'assignatura on més vaig ensopegar, vaig començar el camí de la recerca amb ell. Gairebé només bones paraules puc dir-ne i d'on el seu consell sempre li valoro i el prenc en alta consideració. Espero poder contar amb ell per un període més llarg, és realment excepcional.

Als meus amics i persones més properes que per un ordre estrictament de coneixença temporal enumeraré com segueix: Fèlix, Anna i Eli, Martí, Mònica, Berta, Axel, David, Eduard, Raquel, Unai, Narcís, Jan, Júlia, Jiaqi i el nou Fèlix Björn, sens dubte. Així com aquells que han sorgit pel camí.

A continuació, cal també els familiars, des de les meves àvies i avi fins a la meva tieta, als meus cosins, cosines i tiets. A tots ells que tot i ser el petit en tot, sempre aconsegueixen treurem un somriure encara que sigui per lo tant que em burxen. Però de qui més cal dir coses és de ma germana que tot i els caràcters diferents, costa d'imaginar-se una vida sense ella, el seu somriure i simpatia i, també el seu inseparable canvi humor en el passat.

Tot i que els anomenats fins ara van més enllà de la tesi, hi han aquells que han sigut coneguts integrament durant la tesi i dels quals espero seguir mantenint, especial cura requereixen els del xalet, que tot i no ser-hi físicament gaire cada cop que hi era ha sigut recordable. En Marc qui potser més m'ha aguantat, només coses bones li poden deparar així com per en Narcís i la Giulia, en Gladston i la Begoña, l'Arturo i l'Alex, i l'Anna!

A part de l'Àngel, aquesta tesi em marca per l'oportunitat d'haver pogut fer estades. La primera al Japó amb en Ken d'on tot i no poder-me dedicar completament al doctorat ha sigut una experiència inoblidable.

De la segona, als Estats Units d'on he pogut conèixer qui ha esdevingut

director, en Rafael de la Llave a qui aprecio i valoro més cada cop que penso en ell, és brillantment excepcional també. Gràcies a ell sento que he millorat i d'on crec poder millorar encara més. D'aquesta estada m'emporto en Yian, l'Adrián, el Bhanu, la Libia i especialment la Jiaqi.

De la tercera, al Canadà amb en Jean-Philippe vaig patir una mica pel temps però d'on hi he tornat a la meva cinquena i d'on perdura l'Alberto.

De la quarta, la més llarga m'emporto millors resultats que en la segona. M'emporto el primer contacte amb l'Alessandra i del qual espero que mai hi hagi un últim. Ha sigut la més dura, i amb diferència, a l'inici, però gràcies a en Jarod i en Huck, la Holy i la Kat, la Marie Claire, la Cary i en Tony, en Faraz i la Negar, ha passat suaument després del marcat inici.

De la cinquena on hi sóc força bé fins al moment, d'on nous resultats estan sortint i de la sisena i última estada abans d'acabar l'espero il·lusionat i d'on ben segur que anirá molt bé tot i ser la més curta.

A fi efecte de ser just i honest, vull agrair a les institucions o organismes que m'han ajudat i rebut, entre els quals enumero com segueix: a la Universitat de Barcelona, al ministeri d'economia i competitivitat, a la Barcelona Graduate Schools of Mathematics, al National Institute of Informatics of Japan, a la fundació universitària Agustí Pedro i Pons, a School Mathematics of GeorgiaTech, a McGill university i a l'Institut d'Estudis Catalans.

Montréal, setembre 2019
Joan Gimeno

Introduction

Delay differential equations (DDEs) are, in somehow, between partial differential equations (PDEs) and ordinary differential equations (ODEs). They can be used to describe the dynamics of the model expressed through those kind of equations. However, the way that the dynamical system evolves in time is different for a DDE.

There are different types of DDE from constant delay, time-depedent delay, state-dependent delay, neutral delay, retarded delays, stochastic delay, etc. The list is large and some of these types can have intersections.

While the theory of existence and uniqueness of initial value problems (IVP) for ODEs and PDEs is mostly clear and proved, there is still no a full theory for DDEs. In consequence, some of the tools or methods require a special care when one tries to translate them into DDEs because it may happen that the theoretical explanation is still not well-understood. Special attention needs the theory by J.K. Hale [HVL93] for retarded delays that, in somehow, covers plenty of the delay situations for a theoretical point of view. In parallel, numerical methods to integrate IVP-DDE has being investigated as [BZ13] summarises, at the same time that it proposes new strategies.

Many times the DDE problems are addressed by translation of similar results or techniques in ODE or PDE which are commonly more well-understood. The strong background in ODE theory and numerics for ODEs in the research group of dynamical systems of Barcelona did to point the thesis in the use of the ODEs knowledge to understand better the DDEs.

In this thesis three projects are presented. The first one which was partially started before this thesis with Àngel Jorba and it has had a working time at the National Institute of Informatics of Japan with Ken Hayami. A second one integrally developed at the School of mathematics of Georgia Institute of Technology with Rafael de la Llave and Jiaqi Yang. And a third one with Narcís Miguel, Àngel Jorba, and Marc Jorba started physically at the department of mathematics and computer science of Universitat de Barcelona and continued remotely at GeorgiaTech, Barcelona, and Milan due to

the different destinations of the members.

The structure of the thesis is then in four independent, and mostly self-contained, chapters. Chapter **1** concerns the third project. The origin of it started in the gap in how the interpretation of jet transport and automatic differentiation (AD) is. Originally we tried to understand the interpretation for DDE but we felt the need to get a better understanding in ODE first. According to our study and the state of the art, it is a novelty in this topic.

Roughly speaking, automatic differentiation gives the derivative of a computer algorithm. In particular, AD applied in a numerical integrator is sometimes called jet transport since it is like the jet at the initial condition is being transporting via automatic differentiation in the numerical integrator. Hence, there is no apparently any reason that the high order transported jet through the integrator should provide an accurate enough jet which will contain the information of the high order variational flow. What Chapter **1** does is to proof not only that the jet is accurate, also how accurate is, and gives an idea of how one can design a suitable stepsize control for jet transport.

We prove that jet transport of order say n is exactly the same like if one added to the original differential equations all the extra equations, which represents the (normalised) variational equations up to order n, and we integrate all the system of equation, in particular, it is the same step by step using the same stepsize control. Moreover, in a first glance, one could think that if, for instance, one uses the classical Runge-Kutta 4 it is kind of impossible to use jet transport of order say $n \geqslant 5$. Our proof says that it is completely independent of the numerical integrator than one uses. That is, one can use jet transport of any order with any of the classical method of integration to get the variational flow of that order, in particular, for all the Runge-Kutta methods (both implicit and explicit), multistep methods, and Taylor method which are the most commonly used numerical integrators for ODEs.

As a first application, we have focused on Poincaré mappings and high order of their derivative, which are in fact the high order variatonal flow. While the temporal Poincaré maps, sometimes referred as stroboscopic Poincaré maps, does not present any limitation, the spatial Poincaré maps, i.e. those obtained by the use of a spatial section, does. In fact, in this case one needs to perform a projection to section, even without the use of jet transport. The reason of this projection is simple. Assume, for instance, that the spatial section condition is requested to the 0th order, then while the 0th order stops when the orbit reach the section, the other orders, which represents infinitesimal variations of the initial condition may not be reached because they could have needed to reach the section in a different time. Thus, for the 1st order on, one needs to ensure that the values are the ones that in

the suitable time lie in the section too. Note that in this projection what we are doing is to correct in an infinitesimal way the time of each of the orders to reach the section, which implies to use a temporal jet transport to correct the non-temporal jet. It is exactly this temporal jet which could affect the accuracy of the spatial jet and this strongly depends on the order of the numerical integrator. While methods like Runge-Kutta methods have a fixed order, others methods like the Taylor method has not, i.e. one can fix the order as it was requested. Because of that, Taylor method seems to be the most suitable numerical integrator to perform the high order derivative of a Poincaré mapping obtained by a spatial section.

Once the high order derivative of the Poincaré mapping are well-understood we dealt with the high order manifold computation via the parametrisation method. Part of the examples have already been covered in [JC19] and we strongly recommend to take a look on it to get a best understanding in the models behind the examples.

Chapter **2** summarises the results of the first part of the first project and, in somehow, is a continuation of the master thesis [Gim15] under the supervision of Àngel Jorba. It explains how the jet transport, introduced in Chapter **1**, can be used and theoretical justify the integration of constant DDE. A numerical integration of constant DDE requires discretise the initial condition and keep track of enough history in order to get the new values of the IVP. Because of that discretisation, it may happen that interpolation can be required. Indeed, when te stepsize of the integration is not fixed, the interpolation is always needed but even for fixed steps size it may be required as well, like in the Runge-Kutta methods case. Taylor method with fixed step for only one constant DDE does not interpolate and the jet transport applies directly. In general the applicability of the jet transport will depend on how the interpolation step is performed. For instance, assume that the Taylor method is used and one uses automatic differentiation to get the jet that temporal get at an unknown previous time value. Using AD in polynomial interpolation or Hermite interpolation will not ensure a correct applicability of jet transport. However, if one uses the polynomial or the rational barycentric interpolation order-by-order, jet transport in space will work.

As an application, we discuss the results in [GJS18] which shows, for a specific model, how the stability of the equilibria of a DDE are the same of the ODE obtained setting the delay equals to zero, and it is independently of the delay. However, how much stable or unstable depends on the delay. By numerical simulations, which use jet transport, to get an approximation of the stability quantification of equilibria depends on the delay. While the

stability of an equilibrium point requires to study the eigenvalues of a transcendental equation, the use of jet transport allows us to approximate the most significant eigenvalues of that transcendental equation which quantify the stability.

Chapter **3** is a more exhaustive application of the tools discussed in Chapter **2** up to first order, and it is the second part of the first project. It introduces the delay version of the Poincaré mapping to compute periodic and quasi-periodic motions. Due to the discretisation of the initial conditions, the size of the linear system to solve in a Newton approach can become big specially in the quasi-periodic motions. However, the Poincaré map of a DDE is a compact operator and, in particular, its spectrum is clustered. The use of iterative linear solvers allows to consider a matrix-free Newton approach, i.e. the Jacobian matrix does not need to be computed fully. Moreover, we can require that each linear system is solve with an accuracy similar to the one of the right hand side of the linear system because in the Newton approach is an indicator of how far we are to the zero we want to compute. Specially in the quasi-periodic case, we can also use preconditioners to speed the convergence of the linear solvers. We illustrates all these ingredient with numerical simulations which computes the stability and continuation of those objects.

Finally, Chapter **4** contains the second project. It states *a posteriori* Theorems which prove the existence and uniqueness of a parametrisation of a part of the infinite dimensional stable manifold of a state-dependent delay differential equation (SDDE). The stable manifold of a DDE is infinite-dimensional and the unstable one is finite-dimensional. There are numerical results of the unstable one, such as [GMJ17], but the ones for the stable do not seem to be clear enough. Here we give novel results in perturbation theory with state-dependency. More concretely, starting with a planar ODE with stable limit cycle, we add a perturbative term which introduces the state-dependency. Then we prove the existence and uniqueness of a limit cycle in the perturbative model and also the slowest stable manifold, which is contained in the infinite-dimensional manifold. We believe that is the most relevant part of the manifold because the stable manifold will be governed by the slowest one. In parallel, we discuss how that manifold can numerically be computed and we illustrate it with some examples.

Chapter 1

Jet transport for ordinary differential equations

ACK: This work is a collaboration with Prof. Àngel Jorba, Dr. Marc Jorba, and Dr. Narcís Miguel.

1.1 Introduction

Since the time of Poincaré, it has been known that invariant objects organise the long time behaviour of dynamical systems. They are the skeleton of the dynamics, and hence, for a correct understanding of a concrete dynamical system it is required first to study its invariant objects. The research in dynamical systems concerns mostly with the existence, and the properties of invariant manifolds. In order to have a complete picture, both theoretical and numerical approaches must be undertaken.

A standard tool to study continuous dynamical systems is the use of suitable Poincaré sections. They allow to decrease the dimension of the invariant objects (and of the phase space) by one which usually simplifies the use of analytical and numerical tools. One of the main difficulties when working with Poincaré maps is the lack of a closed expression for such a map, so that all the explicit computations have to be done by means of numerical integration of Ordinary Differential Equations.

The parametrisation method is based on finding a suitable parametric form for the desired invariant object. For instance, for stable, and unstable manifolds of a fixed point the manifold is usually represented as a (high order) Taylor expansion w.r.t. some parameter. The coefficients of this Taylor expansion are found by solving, order by order, a sequence of linear equations coming from the invariance equation satisfied by the manifold.

As the parametrisation method deals with high order derivatives of the

dynamical system at hand, there is an extra difficulty in applying it to Poincaré maps. In this chapter we focus on the effective computation of high order derivatives of stroboscopic maps (a special kind of Poincaré maps) with the final goal of computing high order approximation of stable/unstable manifolds of fixed points of the map (which corresponds to periodic orbits of the flow). We also require the process to be efficient enough so that extended precision arithmetic can be used if necessary.

The derivative of the Poincaré mapping can be obtained by automatic differentiation (AD) which applies to the usual operations and elementary functions such as square root, trigonometry, etc. Hence, AD can be expressed as manipulation of formal power series which goes back to L. Euler, a modern reference is, for instance, the book by D. Knuth [Knu98]. This means that, given an algorithm (defined by a sequence of mathematical formulas), we can replace its arithmetic of real numbers by a power series arithmetic, and then, the same algorithm will produce not only the result but also its derivatives up to the desired order. In other words, given a computer program that outputs some results from some initial data, we can replace the floating point operations by operations with power series (truncated to a given degree, and with floating point coefficients) to produce the power series of the result w.r.t. initial data, and/or parameters.

Here we apply these ideas to the computation of the Poincaré map of a flow. As the numerical integration can be seen as the iteration of a (finite) sequence of mathematical expressions, we can replace the computer arithmetic by a truncated power series arithmetic. This can be done regardless of the numerical integrator used (Runge-Kutta, Taylor, etc). The use of automatic differentiation w.r.t. initial data (and/or parameters) of a ODE is what we called jet transport. Note that this can be viewed as an extension of the phase space to propagate, in addition to points, the derivatives of the flow. As the set of derivatives of a function on a point is sometimes called the jet of derivatives of the function at this point, we refer to this technique as "jet transport" [AFJ+08, JPN10].

1.2 Automatic differentiation and jet transport

Automatic differentiation is a computational tool to obtain (high order) derivatives of the output of an algorithm [GC91, GW08, Nau12]. This section summarises the main ideas behind automatic differentiation in its forward mode. A classical form to introduce automatic differentiation is through the

manipulation of formal power series.

1.2.1 Formal power series in one variable

A formal power series in one variable s is an expression of the form

$$\sum_{k\geqslant 0} a_k s^k, \tag{1.1}$$

where the coefficients a_k belong to a field. If f is a C^∞ function defined on a neighbourhood of 0, we can choose as a_k its k-th *normalised derivative*,

$$a_k = \frac{1}{k!} f^{(k)}(0),$$

and then eq. (1.1) can be seen as a formal series that encodes the *jet* of derivatives of f at 0. The manipulation of formal power series goes back to L. Euler. A modern reference for the topic is, for instance, the book by D. Knuth [Knu98].

To discuss the arithmetic of formal power series, let us define

$$A = \sum_{k\geqslant 0} a_k s^k, \qquad B = \sum_{k\geqslant 0} b_k s^k, \qquad C = \sum_{k\geqslant 0} c_k s^k.$$

The basic operations of power series, $A \pm B$ and AB are defined in a natural way. If $b_0 \neq 0$, the quotient $C = A/B$ is obtained by writting $BC = A$, and taking the coefficients of degree k at both sides,

$$b_0 c_k + b_1 c_{k-1} + \cdots + b_k c_0 = a_k.$$

This implies

$$c_k = \frac{1}{b_0}(a_k - b_1 c_{k-1} - \cdots - b_k c_0),$$

which allows to compute the coefficients c_k recursively, starting from $c_0 = a_0/b_0$.

Let us see how to perform other operations. For instance, let us focus on $C = A^\alpha$ for $\alpha \in \mathbb{R}$. We assume $\alpha \neq 0, 1$ (these two cases are trivial) and $a_0 \neq 0$. Taking formal derivatives w.r.t. s we obtain $C' = \alpha A^{\alpha-1} A'$ which implies $C'A = \alpha C A'$. Now we equate the coefficients of degree $k-1$ at both sides to obtain

$$\sum_{j=0}^{k} j c_j a_{k-j} = \alpha \sum_{j=0}^{k} (k-j) a_{k-j} c_j,$$

and, therefore

$$c_k = \frac{1}{ka_0}\sum_{j=0}^{k-1}[\alpha k - (\alpha+1)j]a_{k-j}c_j,$$

which allows to compute the coefficients c_k ($k \geqslant 1$) recurrently starting from $c_0 = a_0^\alpha$. We note that this formula includes the inversion ($\alpha = -1$) and the square root ($\alpha = \frac{1}{2}$).

The same idea can be used to compute $C = h(A)$ when h is any function that satisfies a simple differential equation. This includes log, exp, and the trigonometric functions. Indeed, for instance, take $\alpha(A) = A$, $\beta(A) = 0$, and $\gamma(A) = 1$ in Lemma **1.1** to get the expression for log.

LEMMA 1.1. *Let $h\colon I \subset \mathbb{R} \to \mathbb{R}$ be a derivable function verifying*

$$\alpha(A)\cdot h'(A) - \beta(A)\cdot h(A) = \gamma(A)$$

for A a formal series and for some mappings α, β, and γ. Then the evaluation $C = h(A)$, in formal series, is obtained recurrently by

$$\begin{aligned} c_0 &\coloneqq h(a_0)\\ c_k &\coloneqq \frac{1}{k\alpha_0}\left(\sum_{j=1}^{k}\left(\gamma_{k-j} + \sum_{i=0}^{k-j}\beta_i c_{k-i-j}\right)ja_j - \sum_{j=1}^{k-1} j\alpha_{k-j}c_j\right), \qquad k \geqslant 1, \end{aligned}$$

whenever $\alpha_0 \neq 0$.

Proof. By the chain's rule, $C' = h'(A)\cdot A'$, i.e., $\alpha(A)\cdot C' = \big(\gamma(A) + \beta(A)\cdot C\big)\cdot A'$. The product is just the discrete convolution. Thus,

$$\alpha_0 k c_k + \sum_{j=1}^{k-1} j\alpha_{k-j}c_j = \sum_{j=0}^{k}\alpha_{k-j}jc_j = \sum_{j=0}^{k}\left(\gamma_{k-j} + \sum_{i=0}^{k-j}\beta_{k-j-i}c_i\right)ja_j. \qquad \square$$

Remark 1.2. As a formal series A codifies the derivatives of a C^∞ function f at, say, 0, the formal series $h(A)$ codifies the derivatives of the composition $h \circ f$ at 0. In other words, the operations with formal series can be seen as the "transport" of the derivatives through these operations.

1.2.2 Formal power series in several variables

In a similar way, we can consider power series of n variables,

$$A = \sum_{m\geqslant 0}\sum_{|k|=m} a_k s^k, \tag{1.2}$$

where $k \in \mathbb{N}^n$, $|k| = k_1 + \cdots + k_n$, and $s^k = s_1^{k_1} \cdots s_n^{k_n}$. As before, if f is a C^∞ multivariate function defined on a neighbourhood of 0, then eq. (1.2) encodes the jet of partial derivatives at 0.

The arithmetic of multivariate power series is very similar to the case of one variable. As an example, let us show how to compute $C = A^\alpha$ for $\alpha \in \mathbb{R}$. As before, we assume $\alpha \neq 0, 1$. We replace s_j by $s_j z$ (z is an extra one-dimensional variable that, at the end, it will be selected equal to 1 to recover the initial form) and we obtain,

$$A = \sum_{m \geqslant 0} A_m z^m, \qquad \text{where} \qquad A_m = \sum_{|k|=m} a_k s^k.$$

Using the same notation for C, we can use the procedure derived in Section **1.2.1** to obtain,

$$C_m = \frac{1}{mA_0} \sum_{j=0}^{m-1} [\alpha m - (\alpha + 1)j] A_{m-j} C_j,$$

where now A_j and C_j denote homogeneous polynomials of degree j. As the only required operations are sums and products of homogeneous polynomials (note that A_0 appears in a denominator but it is always a number), the formula can be carried out easily. In the same way, similar formulas can be obtained for other operations. As in the one dimensional case, operations with multivariate formal series can be seen as the "transport" of partial derivatives through these operations. See, for instance, [HCF+16] for explicit recurrences in elementary functions.

1.2.3 Truncated power series

The computer implementation of these techniques is done using truncated power series. For instance, assume we are working with truncated series up to order, say, M. Then, the equality $C = A^\alpha$ means that C is a truncated power series whose coefficients coincide with the ones of A^α. Note that this does not mean that they coincide as functions of their variables (in fact they do not, since A^α contains terms of order higher than M that we are neglecting).

Remark 1.3. From now on, we are going to consider truncated power series and the equality between to truncated power series will be up to their order.

Note that the efficiency of the operations depends on the efficiency of the product of homogeneous polynomials. Moreover, note that the complexity of these operations is very low: for instance, the cost of A^α is similar to the cost of a product of two truncated power series of order M. It is not difficult to see that this is the complexity of all the standard operations.

1.3 Numerical integration of the variational flow

Consider a generic Initial Value Problem (IVP),

$$\dot{x} = f(t, x), \qquad x(t_0) = x_0, \tag{1.3}$$

where f is smooth and x belongs to a suitable domain of $\mathbb{R}^n$. In this section we first show that the use of jet transport of order 1 on a given numerical integrator for eq. (1.3) produces *exactly* the same results as the ones obtained by using this numerical integrator on the first order variational equations,

$$\begin{aligned} \dot{x} &= f(t, x), & x(t_0) &= x_0, \\ \dot{v} &= D_x f(t, x) v, & v(t_0) &= v_0, \end{aligned} \tag{1.4}$$

where $v \in \mathbb{R}^n$ and $v_0 \neq 0$ is an arbitrary direction. In other words, the two algorithms coincide.

Remark 1.4. Note that it is enough to consider eq. (1.4) in one arbitrary direction v_0. Indeed, once is proved in particular, it will be proved in the canonical basis of $\mathbb{R}^n$.

Remark 1.5. This result implies that the use of jet transport of order, say, $m \geqslant 1$, produces exactly the same results as integrating variational equations of order m. This is seen recurrently on m, using the fact that the variational flow of eq. (1.4) contains the second variational flow of eq. (1.3) and so on.

To describe the numerical methods in this section we use the notation

$$\dot{y} = F(t, y), \qquad y(t_0) = y_0, \tag{1.5}$$

to refer either to IVP eq. (1.3) or eq. (1.4). To simplify the presentation, we assume that F is smooth enough on a suitable domain. We will focus on the first step of the methods, using a given time step h. Once it is shown the equivalence between the jet transport results and the integration of the variational flow, it is clear that if we apply the same step size control strategy to both methods we also obtain the same step sizes for the integration.

1.3.1 Runge-Kutta methods

A generic σ-stage Runge-Kutta method for the IVP eq. (1.5) is defined by (see, for instance, [But87, HNrW93])

$$\begin{aligned} \kappa_i &= F\big(t_0 + c_i h, y_0 + h(a_{i,1}\kappa_1 + \cdots + a_{i,\sigma}\kappa_\sigma)\big), \quad i = 1, \ldots, \sigma, \\ y_1 &= y_0 + h(b_1\kappa_1 + \cdots + b_\sigma\kappa_\sigma), \end{aligned} \tag{1.6}$$

where a_{ij}, b_j, and c_j are suitable real coefficients, and h is the time step. It is well known that, if h is small enough, these equations have a unique solution for the vector κ_i, [HNrW93]. When $a_{ij} = 0$ for $i \leqslant j$ the method is explicit, which means that the vectors κ_j can be obtained explicitly. Otherwise the method is called implicit.

The goal of this section is to show that to use jet transport of order 1 on the σ-stage Runge-Kutta method eq. (1.6) to approximate the solution and the variational flow of eq. (1.3) is exactly the same as to apply the Runge-Kutta method eq. (1.6) to the IVP eq. (1.4). To this end, let us introduce the following notation. If $\bar{\kappa}_j$ denote the values κ_j of eq. (1.6) corresponding to the IVP eq. (1.4), then we write $\kappa_j = (\bar{\kappa}_j, \hat{\kappa}_j)$ where $\bar{\kappa}_j$ refer to the coordinates x and $\hat{\kappa}_j$ refer to the coordinates v.

PROPOSITION 1.6. *Assume that we are using jet transport of order 1 on the scheme eq.* (1.6) *when applied to the IVP eq.* (1.3). *Then, the κ_j values obtained are exactly $\bar{\kappa}_j + \hat{\kappa}_j s$.*

Proof. If we use jet transport of order 1, and then equalities up to first order, on a Runge-Kutta method applied to the IVP eq. (1.3) we obtain the equations

$$\bar{\kappa}_i' + \hat{\kappa}_i' s = f\left(t_0 + c_i h, x_0 + v_0 s + h \sum_{j=1}^{\sigma} a_{i,j}(\bar{\kappa}_j' + \hat{\kappa}_j' s)\right).$$

This equation is equivalent to

$$\bar{\kappa}_i' + \hat{\kappa}_i' s = f\left(t_0 + c_i h, x_0 + h \sum_{j=1}^{\sigma} a_{i,j} \bar{\kappa}_j'\right) + D_x f\left(t_0 + c_i h, x_0 + h \sum_{j=1}^{\sigma} a_{i,j} \bar{\kappa}_j'\right)\left(v_0 + h \sum_{j=1}^{\sigma} a_{i,j} \hat{\kappa}_j'\right) s,$$

which implies

$$\bar{\kappa}_i' = f\left(t_0 + c_i h, x_0 + h \sum_{j=1}^{\sigma} a_{i,j} \bar{\kappa}_j'\right),$$

$$\hat{\kappa}_i' = D_x f\left(t_0 + c_i h, x_0 + h \sum_{j=1}^{\sigma} a_{i,j} \bar{\kappa}_j'\right)\left(v_0 + h \sum_{j=1}^{\sigma} a_{i,j} \hat{\kappa}_j'\right).$$

These are the equations eq. (1.6) for $\kappa_j = (\bar{\kappa}_j, \hat{\kappa}_j)$ corresponding to the IVP eq. (1.4). As the solution is unique [HNrW93], we have that $\bar{\kappa}_j = \bar{\kappa}_j'$, $\hat{\kappa}_j = \hat{\kappa}_j'$. □

Note that this result implies that a single step of a RK method (either explicit or implicit) with jet transport of order 1 on eq. (1.3) produces the same result as a single step of the RK on eq. (1.4). As we want this result to be close to the exact solution of eq. (1.4), we have to choose a suitable step size h according to some prescribed threshold value. This will be discussed later on.

1.3.2 Taylor method

One of the oldest methods for the numerical integration of an IVP like eq. (1.5) is based on the computation of the Taylor series of the solution.

$$y_1 = y_0 + y_0^{[1]}h + y_0^{[2]}h^2 + \cdots + y_0^{[p]}h^p,$$

where $y_0^{[i]}$ denotes the normalised derivative of the solution of eq. (1.5) at t_0,

$$y_0^{[i]} = \frac{1}{i!}\frac{d^i y}{dt^i}(t_0).$$

The computation of the values $y_0^{[i]}$ by taking derivatives to both sides of the ODE can be a difficult process and, moreover, it produces very complex expressions for these derivatives so that the resulting method is not very efficient, specially if high orders are required. However, automatic differentiation can be used to compute these normalised derivatives very efficiently, up to high orders, giving rise to very efficient implementations of Taylor method [JZ05].

As before, we can use jet transport on the Taylor method to approximate the variational flow.

PROPOSITION 1.7. *A step of Taylor method with first order jet transport on the IVP eq.* (1.3) *produces exactly the same results as a step of Taylor method on the IVP eq.* (1.4).

Proof. The i-th normalised derivative of the orbit of eq. (1.3) is

$$x_0^{[i]} = \frac{1}{i!}\frac{d^{i-1}}{dt^{i-1}}[f(t, x(t))](t_0, x_0).$$

To apply jet transport of order 1, we replace x_0 by $x_0 + v_0 s$ and we propagate

first derivatives with respect to s,

$$\begin{aligned} x_0^{[i]} &= \frac{1}{i!}\frac{d^{i-1}}{dt^{i-1}}[f(t,x(t))](t_0, x_0 + v_0 s) \\ &= \frac{1}{i!}\frac{d^{i-1}}{dt^{i-1}}[f(t,x(t))](t_0, x_0) + D_x \frac{1}{i!}\frac{d^{i-1}}{dt^{i-1}}[f(t,x(t))](t_0, x_0) v_0 s \\ &= \frac{1}{i!}\frac{d^{i-1}}{dt^{i-1}}[f(t,x(t))](t_0, x_0) + \frac{1}{i!}\frac{d^{i-1}}{dt^{i-1}}[D_x f(t,x(t))](t_0, x_0) v_0 s. \end{aligned}$$

To finish the proof, we note that the term of degree 0 w.r.t. s is the i-th derivative of the orbit, while the coefficient of s is the i-th derivative of the variational flow. Hence, given an order and a nonzero time step h, the output of a step of Taylor integration using jet transport of order 1 on eq. (1.3) gives exactly the same results as using Taylor method on eq. (1.4). □

1.3.3 Other methods

The same result is true for methods based on linear combination of evaluations of the vector field at given points, like multistep methods (either explicit or implicit). We do not include the details since the proofs are very similar to the previous ones.

1.4 Applications

One of the first applications of jet transport was the transport of regions of uncertainty. Due to the change of shape of the first variational propagating a set of initial conditions, it may cause a loss of accuracy for long term integrations. In [WDLA+15], the authors have been presented an automatic method to split the propagated domains to increase accuracy. The method relies on detecting when the flow expansion w.r.t. initial conditions is no longer accurate enough and to split the region into two subregions. Each subregion is further propagated using the same polynomial representation before the splitting, but centred on different point (on each subregion). See, for instance, other related work [AFJ+08, AFJ+09, ADLBZB10, PPGM18].

Another application of jet transport has been the computation of collision probability of satellite [JPN10, MADLZ15]. First the authors look for close approaches (integration without jets) and then once detected closest approaches the collision probabilities are computed via propagation of uncertainties using jet transport.

In other works like [VADLL14] jet transport has been used to get higher orders and analytic extended Kalman Filters reducing the computational effort and allows to improve the accuracy.

Also jet transport allows to find expansions of the solutions of the optimal control problem around a reference trajectory. The kind of control problem should be set as the equations of motion which are affine in the controls. Examples of such systems are, for instance, in low thrust transfers [DLABZB14].

In the context of two-point boundary value problems, see [DLAL08], jet transport techniques has successfully been used. In this case, a reference solution is found via classical iterative methods, an expansion around this reference solution is computed transporting the jet to high orders to find closed new solutions, obtained via evaluation of the obtained Taylor expansions.

More recently, it is also remarkable that this technique has been used in the computer assisted proof on the applicability of KAM theory to the figure 8 solution in celestial mechanics, [KS17].

Finally, the numerical integration of high order variational flow can be used to obtain power expansions of Poincaré maps and high order approximation of invariant manifolds.

1.4.1 Power expansion of Poincaré maps

Assume that we have a flow defined by a smooth ordinary differential equation on an open subset of $\mathbb{R}^n$ and that we are using a suitable Poincaré section to study its flow. To simplify the discussion, we will consider two separate cases. In what follows, $\Phi(t; t_0, x^{(0)})$ denotes the solution at time t corresponding to the initial data $(t_0, x^{(0)})$.

Temporal Poincaré sections

This is a common situation when we have a periodically time-dependent ODE with a period, say, $T > 0$. Then, it is usual to define a Poincaré map P as the time T flow of the ODE, that is, $P(x) = \Phi(T; 0, x)$. Periodic orbits of period T appear as fixed points of P, $P(x^*) = x^*$. The linear stability of the periodic orbit follows from the monodromy matrix $D_x P(x^*)$, but to study nonlinear aspects of the dynamics higher order terms are needed. A typical example is the analysis of bifurcations [Kuz04].

The power expansion (up to order m) of P at a given point $x^{(0)} \in \mathbb{R}^n$ can be obtained by evaluating P on $x^{(0)} + s$, using a jet arithmetic of order m for the n-dimensional vector of symbols s.

Spatial Poincaré sections

To simplify the discussion, we focus on an autonomous ODE. This is in fact the usual situation in which spatial sections are used. Let us assume that the Poincaré section Σ is defined by a hyperplane in general position. Let $x^{(0)}$ be a point on the hyperplane Σ and let us denote by $\vec{n}$ the normal vector to this hyperplane. We assume that, after some integration time, say, $T(x^{(0)})$, the trajectory comes back to the section, i.e. $\Phi(T(x^{(0)}); 0, x^{(0)}) \in \Sigma$. To produce the expansion, we have to define coordinates on the hyperplane. Without loss of generality, let us choose $x^{(0)}$ as the origin of coordinates and let us choose suitable linearly independent unitary vectors $v_1, \ldots, v_{n-1}$ such that $x^{(0)} + v_1 s_1 + \cdots + v_{n-1} s_{n-1}$ is a parametric representation of Σ.

Now we start the integration of the ODE at the point $x^{(0)} + v_1 s_1 + \cdots + v_{n-1} s_{n-1}$ using a jet arithmetic of order, say, m, with the symbols $s = (s_1, \ldots, s_{n-1})$. Note that if we stop the integration at time $T(x^{(0)})$ what we obtain is the power expansion of the flow at time $T(x^{(0)})$ w.r.t. the $n-1$ variables that are the coordinates on Σ, but this is not the power expansion of the Poincaré map $P\colon \Sigma \to \Sigma$ because this expansion does not lay inside Σ. To produce the power expansion of the Poincaré map up to a given order m, we stress that the time needed for an orbit to return to the section Σ depends on the initial point. This means that the return time also depends on s, that is, we have to write the return time as a formal series on s,

$$T(x^{(0)} + s) = T(x^{(0)}) + \sum_{|k|=1}^{m} \tau_k s^k, \tag{1.7}$$

whose coefficients τ_k are real numbers that have to be determined from the condition

$$\Phi(T(x^{(0)} + v_1 s_1 + \cdots + v_{n-1} s_{n-1}); 0, x^{(0)} + v_1 s_1 + \cdots + v_{n-1} s_{n-1}) \in \Sigma. \tag{1.8}$$

As usual, this condition must hold up to order m in s. In other words, we expect that the distance between the evaluation of the power expansion of the Poincaré map and Σ behaves like $O_{m+1}(\|s\|)$. As we will see, the coefficients τ_k in eq. (1.7) can be computed recurrently, degree by degree. To shorten the following formulas, we denote $T_0 = T(x^{(0)})$ and

$$\bar{s} = v_1 s_1 + \cdots + v_{n-1} s_{n-1}.$$

Let us denote $x^{(1)} = \Phi(T_0; 0, x^{(0)}) \in \Sigma$ and we recall that the ODE is $\dot{x} = f(x)$. Let us start by degree $m = 1$. The flow $\Phi(T_0 + \sum_{|k|=1} \tau_k s^k; 0, x^{(0)} + \bar{s})$

at time $t = T_0 + \sum_{|k|=1} \tau_k s^k$ can be written as

$$\begin{aligned}
&\Phi(T_0; 0, x^{(0)} + \bar{s}) + D_t\Phi(T_0; 0, x^{(0)} + \bar{s}) \sum_{|k|=1} \tau_k s^k \\
&= \Phi(T_0; 0, x^{(0)}) + \sum_{|k|=1} a_k s^k + D_t\Phi(T_0; 0, x^{(0)}) \sum_{|k|=1} \tau_k s^k \\
&= x^{(1)} + \sum_{|k|=1} a_k s^k + f(x^{(1)}) \sum_{|k|=1} \tau_k s^k,
\end{aligned}$$

where the values a_k come from the first order expansion of $\Phi(T_0; 0, x^{(0)} + \bar{s})$ w.r.t. s,

$$\Phi(T_0; 0, x^{(0)} + \bar{s}) = x^{(1)} + \sum_{|k|=1} a_k s^k.$$

Hence, to impose condition eq. (1.8) at first order (at order 0 is already satisfied) we have to ask that

$$\sum_{|k|=1} \left\langle a_k + \tau_k f(x^{(1)}), \vec{n} \right\rangle = 0,$$

where $\langle \cdot, \cdot \rangle$ denotes the standard scalar product. This condition implies that

$$\tau_k = -\frac{\langle a_k, \vec{n} \rangle}{\langle f(x^{(1)}), \vec{n} \rangle}.$$

From a geometric point of view, this is equivalent to project the directional derivatives w.r.t. each component of s on the Poincaré section, following the flow (see Figure **1.1**).

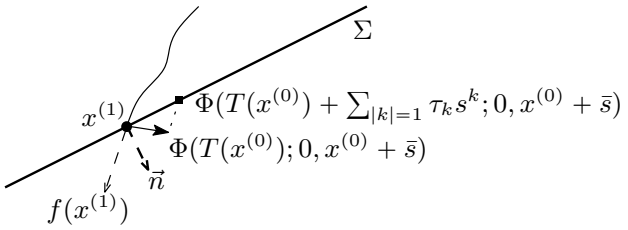

Figure 1.1. Projection of a directional derivative of the flow on the Poincaré section.

The computation of the higher order terms is more involved. In particular, it requires to perform integration steps with step sizes that also depend on $\bar{s}$. This introduces a limitation: if, for instance, we have to perform the step size $h = \sum_{|k|=1} \tau_k s^k$, and the numerical integration has a local truncation error of

$O(h^p)$, then the resulting power expansion in s will have an error of the order of $O(|s|^p)$ and this means that we cannot trust the resulting expansion in s for orders equal and higher than p. Therefore, we have to limit the degree of these expansions by the order of the local truncation error. We note that this is not a limitation for Taylor methods, since the order of integration can be easily increased to the desired value.

Now let us focus in the computation of high order derivatives, assuming that the order of the local integration error is large enough for the derivatives we want to obtain. We proceed in a recurrent way. Assume now that we have computed the values τ_k for $|k| \leqslant m$ and we want to compute them for $|k| = m + 1$:

$$\begin{aligned}
&\Phi\left(T(x^{(0)}) + \sum_{|k|=1}^{m} \tau_k s^k + \sum_{|k|=m+1} \tau_k s^k; 0, x^{(0)} + \bar{s}\right) \\
&= \Phi\left(T(x^{(0)}) + \sum_{|k|=1}^{m} \tau_k s^k; 0, x^{(0)} + \bar{s}\right) + \\
&D_t\Phi\left(T(x^{(0)}) + \sum_{|k|=1}^{m} \tau_k s^k; 0, x^{(0)} + \bar{s}\right) \sum_{|k|=m+1} \tau_k s^k \\
&= x^{(1)} + \sum_{|k|=1}^{m+1} a_k s^k + f(x^{(1)}) \sum_{|k|=m+1} \tau_k s^k.
\end{aligned}$$

To obtain the last equality note that, as $D_t\Phi$ is multiplying $\sum_{|k|=m+1} \tau_k s^k$ which is already of order $m + 1$, we have to use the terms of degree 0 of $D_t\Phi$, that is, $D_t\Phi(T(x^{(0)}; 0, x^{(0)})$ which is $f(x^{(1)})$. Therefore, for $|k| = m+1$, imposing condition eq. (1.8) leads to the same expression as before,

$$\tau_k = -\frac{\langle a_k, \vec{n}\rangle}{\langle f(x^{(1)}), \vec{n}\rangle}.$$

Let us summarise how to apply these formulas. We first integrate for a time $T(x^{(0)})$ such that the orbit starting at the initial condition $x^{(0)}$ lands on the Poincaré section Σ. This integration can be done with jet transport so that we obtain $\Phi(T(x^{(0)}); 0, x^{(0)} + \bar{s})$. Then, to compute the return time eq. (1.7) such that the power expansion of the flow lays inside Σ up to degree m, we proceed degree by degree in eq. (1.7): for degree 1, we use first the formulas above to compute the numbers τ_k and then we perform a step of numerical integration with step

$$h = \sum_{|k|=1} \tau_k s^k,$$

starting at $\Phi(T(x^{(0)}); 0, x^{(0)} + \bar{s})$ to obtain $\Phi(T(x^{(0)}) + \sum_{|k|=1} \tau_k s^k; 0, x^{(0)} + \bar{s})$ which is a power expansion with its first order terms inside Σ. Next, using the second order terms w.r.t s in $\Phi(T(x^{(0)}) + \sum_{|k|=1} \tau_k s^k; 0, x^{(0)} + \bar{s})$ (the coefficients of these terms are the values a_k above) we compute the values τ_k for $|k| = 2$ and we perform another numerical integration step,

$$h = \sum_{|k|=2} \tau_k s^k,$$

starting at $\Phi(T(x^{(0)}) + \sum_{|k|=1} \tau_k s^k; 0, x^{(0)} + \bar{s})$ to obtain the expression $\Phi(T(x^{(0)}) + \sum_{|k|=1}^{2} \tau_k s^k; 0, x^{(0)} + \bar{s})$ with its second order terms inside Σ. This process is continued up to the desired order.

1.4.2 The parametrisation method

This method was already used for numerical computations in the 80's by C. Simó (see also [FR81]), but it is remarkable that is also an excellent tool to prove the existence of invariant manifolds, as shown by X. Cabré, E. Fontich, and R. de la Llave [CFdlL05]. Here we simply summarise the method from an algorithmic point of view. A very good exposition of the method can be found in the book [HCF+16].

Let us start with the case of a 1D invariant manifold. Let us denote by P the Poincaré map and assume that the fixed point is at z_0. Let λ be a real eigenvalue of $DP(z_0)$ and let $s \mapsto z(s)$ be a parametrisation of the manifold associated to λ. We assume that P is analytic and that a suitable nonresonance condition between λ and $\operatorname{Spec} DP(z_0)$ is satisfied, so that the manifold can be written (locally) as a convergent power series,

$$z(s) = \sum_{k \geqslant 0} a_k s^k.$$

The invariance condition is

$$P(z(s)) = z(\lambda s).$$

We will solve the invariance equation recursively, order by order. It is immediate to check that order 0 is given by the coordinates of the fixed point, $a_0 = z_0$ and order 1 is given by the eigenvector related to the eigenvalue λ, $DP(z_0)a_1 = \lambda a_1$. To proceed recursively, assume we have computed the manifold up to order m. We denote by $z_{\leqslant m}(s)$ the power expansion $z(s)$ truncated to order m, $z_{\leqslant m}(s) = \sum_{k \leqslant m} a_k s^k$. Then, the coefficient a_{m+1} satisfies

$$(DP(z_0) - \lambda^{m+1} I) a_{m+1} = -b_{m+1},$$

where b_{m+1} denotes the coefficient of order $m+1$ in the evaluation of the manifold up to order m, $z_{\leqslant m}(s)$, by the Poincaré map P:

$$P_{\leqslant m+1}(z_{\leqslant m}(s)) = \sum_{k=0}^{m} b_k s^k + b_{m+1} s^{m+1}.$$

To compute $P_{\leqslant m+1}(z_{\leqslant m}(s))$ we need to evaluate the Poincaré map P on the (truncated) formal series $z_{\leqslant m}(s)$. This is done by means of jet transport. From a computational point of view, this is by far the most expensive operation.

This method can easily extended to compute power expansions of higher dimensional manifolds. For instance, for a 2D manifold related to two real eigenvalues λ_1 and λ_2, we look for a parametrisation $(s_1, s_2) \mapsto z(s_1, s_2)$ and we assume that the needed conditions for the existence of an analytic manifold are satisfied. Then, the manifold can be written (locally) as a convergent power series,

$$z(s_1, s_2) = \sum_{m \geqslant 0} \sum_{|k|=m} a_k s_1^{k_1} s_2^{k_2}, \qquad \text{where } k = (k_1, k_2) \text{ and } |k| = k_1 + k_2.$$

The invariance equation is

$$P(z(s_1, s_2)) = z(\lambda_1 s_1, \lambda_2 s_2),$$

that is solved recursively. As before, orders 0 and 1 are given by the coordinates of the fixed point and the two eigenvectors. Assuming that we have computed the manifold up to order m, the coefficients for order $m+1$ are given by

$$(DP(z_0) - \lambda_1^{k_1} \lambda_2^{k_2} Id) a_k = -b_k,$$

for each k such that $k_1 + k_2 = m+1$ and b_k are the coefficients of the terms of order $m+1$ of the evaluation of the manifold up to order m by the Poincaré map:

$$P_{\leqslant m+1}(z_{\leqslant m}(s_1, s_2)) = \sum_{|k|=0}^{m} b_k s_1^{k_1} s_2^{k_2} + \sum_{|k|=m+1} b_k s_1^{k_1} s_2^{k_2}.$$

1.5 Examples

In order to illustrate the theory, let us consider two examples whose models can find in [JC19]. The first one illustrates the computation of the unstable manifold of a model in celestial mechanics. And the second one the manifold computation of a chemistry model which involves eigenvalues of with large opposite values.

1.5.1 The unstable manifold of L_4 in the Bicircular Problem

The (Earth-Moon) Bicircular Problem (BCP) is a restricted version of the Four Body Problem [Hua60, CRR64]. This model assumes that (while Earth and Moon move as in the RTBP) Sun and the Earth-Moon barycentre move along a circular orbit around the centre of mass of the Sun-Earth-Moon system, everything in the same plane. The BCP can be regarded as a (periodic) time dependent perturbation of the RTBP. The associated Hamiltonian function can be written as

$$H_{BCP} = \frac{1}{2}(p_x^2 + p_y^2 + p_z^2) + yp_x - xp_y \\ - \frac{1-\mu}{r_{PE}} - \frac{\mu}{r_{PM}} - \frac{m_S}{r_{PS}} - \frac{m_S}{a_S^2}\big(y\sin\theta - x\cos\theta\big). \quad (1.9)$$

where the units are taken as in the Earth-Moon RTBP, m_S is the mass of Sun, a_S the semimajor axis of Sun, $r_{PE}^2 = (x-\mu)^2 + y^2 + z^2$, $r_{PM}^2 = (x-\mu+1)^2 + y^2 + z^2$, $r_{PS}^2 = (x-x_S)^2 + (y-y_S)^2 + z^2$, $x_S = a_S\cos\theta$, $y_S = -a_S\sin\theta$, $\theta = \omega_S t$ and ω_S is the mean angular velocity of Sun in these synodic coordinates.

In the BCP the Lagrangian points are no longer equilibria, they are replaced by periodic orbits with the same period as the perturbation. In particular, the triangular point L_4 is replaced by three periodic orbits with the same period as Sun, see [SGJM95, CJ00]. One of these orbits is slightly unstable, of linear type saddle×centre×centre. The unstable eigenvalue of the orbit, regarded as a fixed point of the stroboscopic map, is close to 1.098. Notice that the instability is remarkably mild, that is, an initial condition on the manifold near to the fixed point needs a large number of iterates to get far from it. Therefore, to grow numerically the manifold from the linear approximation is numerically expensive. We can, however, produce a high order approximation of the manifolds and produce large pieces of the manifolds that can be mapped a few times to get even larger pieces of the manifold, see Figure **1.2**. Let us explain how to produce Figure **1.2**: The first thing is to build a Runge-Kutta-Fehlberg 7-8 with arithmetic of polynomials of one dimension. Then we apply the parametrisation method to obtain, order by order, a Taylor expansion of the manifolds. At each step, after we compute the coefficient of order k, we use the root criterion to estimate the radius of convergence. We denote by U^+ and U^- the two pieces of the unstable manifold, which have been expanded up to order 54. On the other hand, the stable pieces, denoted by S^+ and U^-, are expanded up to order 46. Then, all those Taylor expansions are evaluated to obtain the curves in Figure **1.2**.

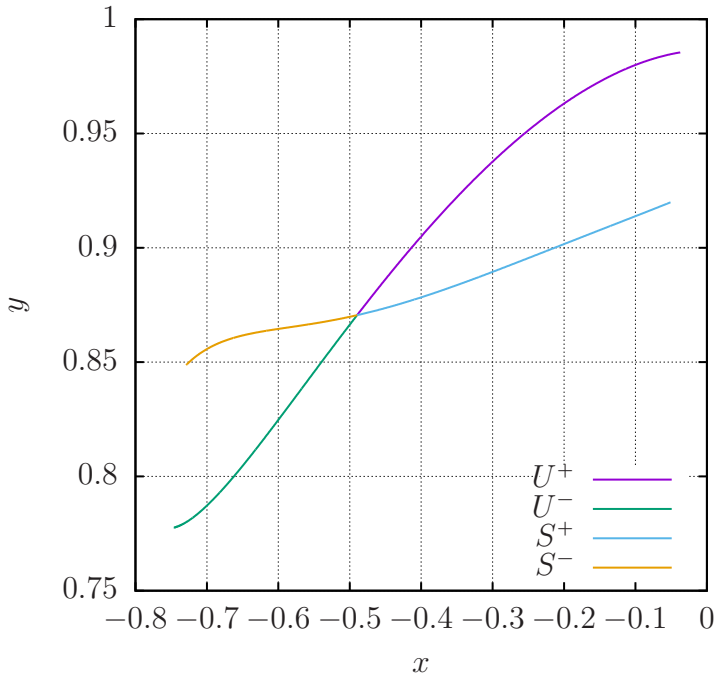

Figure 1.2. High order approximations of the stable (S^+, S^-) and unstable (U^+, U^-) manifolds attached to the dynamical equivalent of L_4 in the Earth-Moon BCP.

1.5.2 A chemistry problem

Consider an atom that, by some mechanism, ionises i.e. an electron abandons the atomic core. Depending on some conditions, the electron may be recaptured by the atom following the Coulomb's laws. When this happens, we say that the electron **recollides** with its parent ion, see [Cor93, Cor14]. See also [MCU10, MKCU12, KCUM14, KMCU14, NCUW15] for works approaching this problem from the point of view of the dynamical systems.

Usually the electron is expelled out the core by the action of a laser field. The effect of the laser is modelled by means of a periodic function. Near the core, the laser acts as a perturbation of the central problem induced by the (soft) Coulomb potential

$$H = \frac{1}{2}(p_x^2 + p_y^2) - \frac{1}{\sqrt{x^2 + y^2 + a^2}} + E_c x \cos \omega t + E_s y \sin \omega t, \qquad (1.10)$$

with $a = 1$, $\omega = 0.0584$, $E_c = 0.1$, and $E_s = 0$. The dynamical mechanism that leads to most of the recolliding trajectories is well understood when the electrons are allowed to move in a one dimensional space (the dynamics restricted to the invariant subspace $\{y = 0, p_y = 0\}$ of system eq. (1.10). The stable and unstable manifolds of some key hyperbolic periodic orbit drive these trajectories to recollide many times, see [KCUM14].

The hyperbolic periodic orbit studied in [KCUM14] has period $\frac{2\pi}{\omega}$ and in system eq. (1.10) is located near $x = 30.5$, $y = p_x = p_y = 0$. This orbit is easily found by means of a Newton method on the map defined by the time-period ($\frac{2\pi}{\omega}$) map. The eigenvalues of the monodromy matrix are

```
1.0598923797401292e+03
2.1924563502992269e+00
4.5610942259513210e-01
9.4349201788190840e-04
```

so it has a 2D unstable manifold and a 2D stable manifold. There is a strong unstable direction and a weak unstable direction. The weak one is the direction contained in the invariant subspace, the one whose related invariant manifold drive most of the recolliding orbits in the 1D case. The strongly unstable direction appears as cause of adding the transversal (to the polarisation laser) direction. Therefore, the dynamics near the periodic orbit is dominated by the strongly unstable direction which is transversal to $\{y = 0, p_y = 0\}$. Because of the magnitude of the strong eigenvalue, most of the trajectories nearby the fixed point get expelled away from the atom and do not return back, at least, in a few laser cycles. It is possible, however to find thin strips close to the invariant subspace $\{y = 0, p_y = 0\}$ with a lot of recolliding trajectories. However, numerically, it is challenging to compute the 2D unstable (stable) manifold due to a remarkable propagation of error.

To illustrate this fact, let us first focus the 1D manifold related to the "weakly" unstable eigenvalue $\lambda = 2.1924563502992269$. Here we have to pay attention to the fact that this manifold is not attracting (recall that there is another eigenvalue at the point close to 1059.89). To deal with this error amplification, at each iteration of the Poincaré map we compute (and accumulate) the norm of the differential so that we have an estimate of the growth of the error at each step.

As example, we select an initial point on this manifold at 1 unit of distance from the fixed point. We estimate the error on the manifold (we can use, for instance, the last terms of its power expansion). Then, using multiple accuracy, we can monitor the growth of the (estimated) error during the iterations:

```
iter:  0  err: 0.000000e+00
iter:  1  err: 8.466197e-43  dist: 2.199796e+00
iter:  2  err: 8.928646e-40  dist: 4.848533e+00
iter:  3  err: 9.240140e-37  dist: 1.081419e+01
iter:  4  err: 8.411957e-34  dist: 2.553592e+01
iter:  5  err: 2.083436e-32  dist: 1.745048e+01
iter:  6  err: 1.966030e-29  dist: 1.976583e+01
iter:  7  err: 1.310301e-27  dist: 7.533221e+01
iter:  8  err: 1.615796e-27  dist: 1.267686e+02
iter:  9  err: 1.771004e-27  dist: 1.773365e+02
iter: 10  err: 1.873796e-27  dist: 2.275002e+02
```

The first column is the iterate of a point obtained from the parametrisation of the manifold, the second column is the accumulated product of the norms of the differential of the Poincaré map at each point and the third is the distance to the fixed point. As it happens in many situations, the instability of this weakly unstable manifold decreases as the move away from the fixed point. This simplifies the approximation of the manifold up to long distances.

A conclusion of this experiment is that the propagation of error tends to soften at some distance of the periodic orbit. This vindicates the computation of a high order approximation of a parametrisation of the 2D unstable manifold. This allows us to grow the manifold numerically far away from the fixed point, avoiding this pathological propagation of error. Let

$$W\colon \Lambda_1 \times \Lambda_2 \to \mathbb{R}^4,$$

(with Λ_1 and Λ_2 intervals containing the origin) a parametrisation of the unstable invariant manifold related to $\mathcal{O}_1$. This parametrisation verifies the following invariance equation:

$$f(W(s_1, s_2)) = W(\lambda_1 s_1, \lambda_2 s_2).$$

Recall that the unstable eigenvalues are $\lambda_1 \approx 2.1924563502992269$ and $\lambda_2 \approx 1059.8923797401292$. Computing this 2D manifold (double precision) up to order 8 takes 0.5s. Using MPFR with mantissa of 128 bits (39 decimal digits) it takes 1m 19s. Computing up to order 16 requires 15m 26s. Finally, to compute it up to order 30 using extended precision arithmetic (MPFR with 192 bits mantissa $\approx$ 57 decimal digits) takes 8h 50m. As in the 1D case, we use these different approximations to estimate the error on the coefficients of the expansion. Figure **1.3** shows a representation of this manifold.

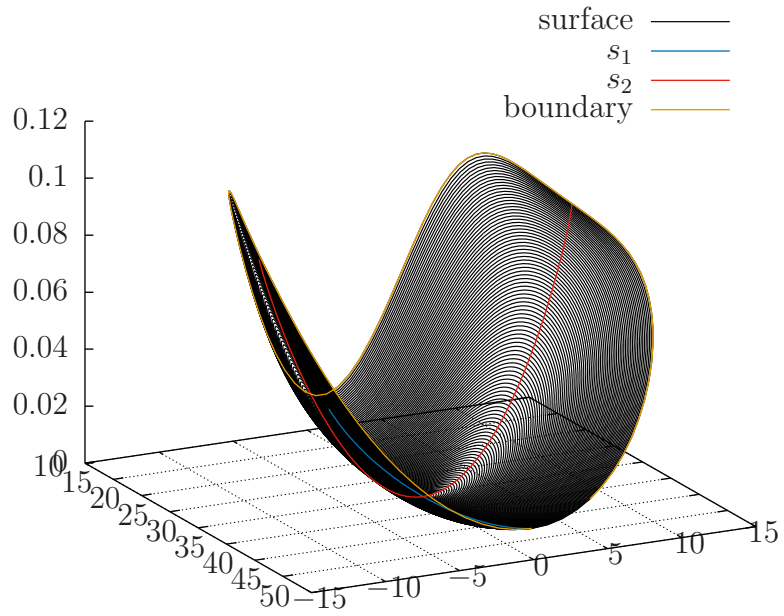

Figure 1.3. The 2D manifold drawn from the expansion obtained in the parametrisation method.

Chapter 2

Jet transport in delay numerical integrators

ACK: This work is a collaboration with Prof. Àngel Jorba and partially with Dr. Josep Sardanyés.

2.1 Introduction – Splicing condition

To pose the problems, and fix notations let us start considering a constant delay differential equation (DDE) expressed by

$$\frac{d}{dt}x(t) = f(x(t), x(\alpha(t))), \qquad \alpha(t) = t - \tau \tag{2.1}$$

with f smooth, and τ a fixed and positive real number. Clearly the case of $\tau = 0$ leads to an ordinary differential equation (ODE). After a time scaling, $t = \tau s$, we can always assume that $\tau = 1$.

In the case of a finite number of constant delays we can re-scale the time in such a way that all the delays involved in the DDE are in $(0, 1]$.

The delay term implies that the initial condition needs to live in the space of mappings defined in the interval $[-1, 0]$. These functions are going to be assumed to be at least continuous but in practice the assumption will involve as many regularity as was needed.

If x is a map defined in an interval $[t_a, t_b]$, $x_t(s) = x(t + s)$ is a map with s in $[-1, 0]$ and t in $[t_a - 1, t_b]$. Therefore an initial value problem for a delay differential equation (IVP-DDE) consists in finding a solution through an initial condition u at time 0, denoted by $x(0, u)$, and verifying

$$\begin{cases} \frac{d}{dt}x(t) = f(x(t), \varphi(t)) \\ x_0(s) = u(s) \end{cases} \qquad \text{with } \varphi(t) = x(\alpha(t)). \tag{2.2}$$

Due to the fact that an arbitrary mapping is represented by a table of value in a computer, the strategy for a numerical computation is clear; a standard ordinary differential integrator will used in intervals multiple of $[-1, 0]$.

Whenever an evaluation of the function φ is required for an unknown value in its discresation, an interpolation is going to be perform. On the other hand, an IVP-DDE may also involve discontinuities in the orbit. These are the two main drawbacks in the numerical integration of a DDE which are, in general, harder to figure out in the state delay differential equations (SDDE).

Indeed, since the initial condition lives now in the space of mappings, but the orbit is shown as a trajectory in the real line, it may happen the derivative at $t = 0$ does not coincide with the value of the initial condition. That is, the solution has a jump in the first derivative, $\frac{d}{ds}u(0) \neq \frac{d}{dt}x(0,u)(0)$. If $x^{\pm}(t)$ denotes the value at time t of the solution from the left $x^{-}(t)$ and from the right $x^{+}(t)$, then

$$\ddot{x}^{\pm} = D_x f(x, \varphi)\dot{x} + D_\varphi f(x, \varphi)\dot{\varphi}^{\pm}$$

with $\dot{\varphi}^{\pm} = (\dot{x} \circ \alpha)^{\pm}\dot{\alpha}$. For all time value ξ such that it is a simple root of $\alpha(t)$, then the orbit $x(0, u)$ has a jump discontinuity in its second derivative at ξ because $\dot{\varphi}^{-}(\xi) \neq \dot{\varphi}^{+}(\xi)$.

The repetition of the process leads to the fact that if a jth splicing condition happens, i.e. $\frac{d^i}{ds^i}u(0) = \frac{d^i}{dt^i}x(0,u)(0)$ for $0 \leqslant i < j$, we can ensure that no jump discontinuities in the jth first derivatives are going to be, and a standard ODE integration of order j can be used without any trouble.

On the other hand, if no splicing condition is assumed or with not enough j-range, we are going to have different levels of discontinuities. To be more precise, fixed $j > 1$ and the initial condition u defined in $[-1, 0]$ so that $\frac{d^{j-1}}{ds^{j-1}}u(0) \neq \frac{d^{j-1}}{dt^{j-1}}x(0,u)(0)$ but there is equality for the previous derivatives. Then the set

$$\mathcal{Z}^0 = \{\xi > 0 \colon \xi \text{ is a simple root for } \alpha(t) = 0\}$$

consists in all the jump discontinuities in the jth derivative of the solution through u propagated by the one at time $t = 0$. In general, the kth level of jump discontinuities is defined recurrently by

$$\mathcal{Z}^k = \{\xi > 0 \colon \xi \text{ is simple root for } \alpha(t) = \zeta \text{ for some } \zeta \in \mathcal{Z}^l \text{ with } 0 \leqslant l < k\}$$

which are the jump discontinuities in the $(j + k)$th solution derivative.

These regularity obstructions can be accumulated in an infinite number of points and assumptions on α are commonly imposed. For instance,

- $\alpha(t) \leqslant t$ for all t. Otherwise we required values in the future.
- $\alpha(t) \neq t$. That is, it is always required to need to take values in the past.
- $t - \alpha(t) \leqslant M$ for some $M > 0$. It means to have a fading memory which allows us to have a finite segment of past history to store.

In the case of constant delays, $\alpha(t) = t - 1$, the jump discontinuities are perfectly located before any integration step. Indeed, if the splicing condition is not verified, the kth level of jump discontinuities will happen in $\{k\}$ therefore at each time value $t = k$ the orbit becomes smoother.

There are invariant objects where the splicing condition is always true. Examples of these kind of objects are equilibria, periodic orbits, and tori whose proofs are done by contradiction.

THEOREM 2.1. *The splicing condition is satisfied to all orders for equilibria, periodic orbits and tori if the flying time is bigger than* 1.

Proof. Let us argue for each of the three objects involve in the statement:

Equilibria: If u is an equilibrium, it is a constant function on $[-1, 0]$.

Periodic orbits: Given an initial condition u defined in $[-1, 0]$, and a period $T > 1$ such that $x(0, u)_T = u$. If u did not verify the splicing condition, $x(0, u)_T$ would not do, and neither $x(0, u)_{T\mathbb{N}}$ which contradicts the fact that the orbit becomes smoother as the time goes far.

Tori: Let K be a mapping defined in $\mathbb{T}^d$, and ω be a frequency vector in $\mathbb{T}^d$. After a scaling, we can consider P to be the time 1-map. The invariance equation for a torus is $K(\theta + \omega) = P \circ K(\theta)$. If there is θ_0 so that $K(\theta_0)$ does not satisfy the splicing condition, it contradicts the fact that $K(\theta_0) = P \circ K(\theta_0 - \omega)$, and that each composition with P the regularity goes up. □

Theorem **2.1** tells us that in a neighbourhood of those invariant objects the splicing condition will be satisfied as well. This fact allows us to consider standard ODE methods to compute them under the suitable adaptations in the context of DDE.

2.2 Interpolation

As it has been pointed out, the initial conditions of a DDE live in the space of mappings defined in $[-1, 0]$. In order to deal with initial conditions in a

computer, they are going to be discretised in a finite number of points, see Figure **2.1**.

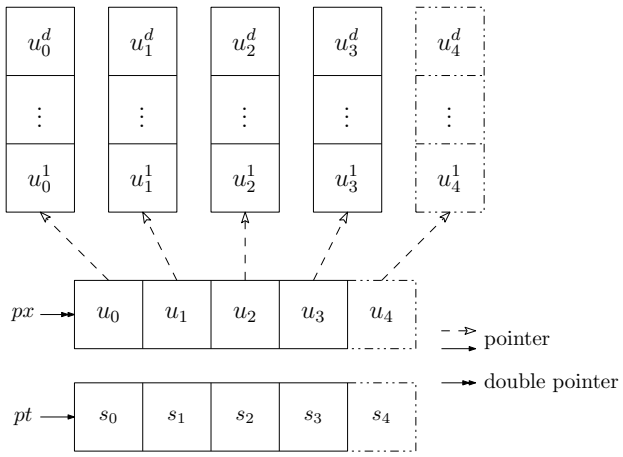

Figure 2.1. Table of values $(s_i, u_i)_{i=0}^{5-1}$ of an initial condition $u\colon [-1, 0] \to \mathbb{R}^d$.

On the other hand, the standard ODE integrators compute an approximation of the orbit with increments in the time by fixed or controlled stepsize.

If we consider an IVP-DDE like in eq. (2.2), and to exemplify an explicit Euler method is used, then its iterative scheme with fixed stepsize $h = \frac{1}{N}$ is given by

$$\begin{aligned} x_{n+1} &= x_n + hf(x_n, \varphi(t_n)), \\ t_{n+1} &= t_n + h. \end{aligned} \tag{2.3}$$

The value x_n denotes an approximation of the solution at time t_n, that is, $x_n \approx x(0, u)(t_n)$.

In the case of only one constant delay, the stepsize $h = \frac{1}{N}$ stops exactly at all the jump discontinuity points in case that the initial condition does not satisfy the splicing condition, and then whenever $\varphi(t_n)$ lies in these discontinuities we can take the left or right value.

The values $\varphi(t_n)$ are always known if the stepsize is fixed in the scheme given in eq. (2.3). However, for other strategies when the stepsize is not fixed or even when to compute each step requires the use of unknown values. The latter one is common for Runge-Kutta methods. To illustrate it, let us consider a popular explicit Runge-Kutta method with 4 stages and order 4 whose Butcher's Tableau is in table **2.1**.

0				
$\frac{1}{2}$	$\frac{1}{2}$			
$\frac{1}{2}$	0	$\frac{1}{2}$		
1	0	0	1	
	$\frac{1}{6}$	$\frac{1}{3}$	$\frac{1}{3}$	$\frac{1}{6}$

$$\begin{aligned}
\kappa_1 &= f(x_0, \varphi(t_0)) \\
\kappa_2 &= f(x_0 + \tfrac{h}{2}\kappa_1, \varphi(t_0 + \tfrac{h}{2})) \\
\kappa_3 &= f(x_0 + \tfrac{h}{2}\kappa_2, \varphi(t_0 + \tfrac{h}{2})) \\
\kappa_4 &= f(x_0 + h\kappa_3, \varphi(t_0 + h)) \\
x_1 &= x_0 + \tfrac{h}{6}(\kappa_1 + 2\kappa_2 + 2\kappa_3 + \kappa_4) \\
t_1 &= t_0 + h.
\end{aligned}$$

Table 2.1. RK4 equations..

Therefore even if the stepsize is fixed, to compute the κ's may require to know some values in the history of its trajectory that are in fact not known in the table of values, like Figure **2.2** illustrates.

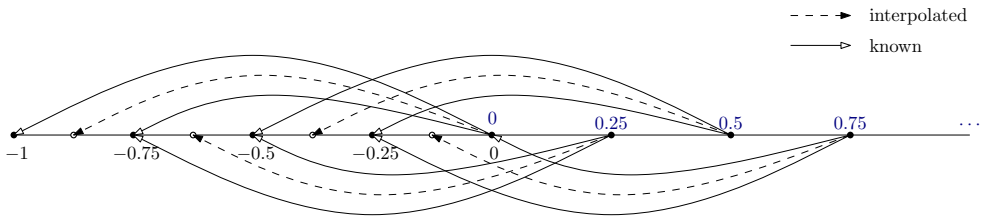

Figure 2.2. Points needed to known for 4 steps of a Runge-Kutta 4 with fixed stepsize..

The general interpolation problem states as follows: Given a table of values $(t_i, \varphi_i)_{i=0}^{n-1}$ of a real continuous mapping φ defined in a close real interval. The goal is to give the value $\varphi(t)$. Without loss of generality we can always assume $t_0 < \cdots < t_{n-1}$.

In a numerical implementation is required to keep the history of the orbit in order to evaluate $\varphi(t)$ of eq. (2.2) in potentially unknown values but at the same time the new steps must be saved to provide values of $\varphi(t)$ for further times. Figure **2.3** illustrates the fact that a previous history given by a table of values (pt_i, px_i) and the current history with an incomplete table of values, (ct_i, cx_i).

In the following sections we describe several, though standard, interpolation techniques, and we show that in all of them the spatial jet transport applies. That will imply that the automatic differentiation provides a jet transport such that at each step the spatial jet will coincide with the extended system involving all the derivatives.

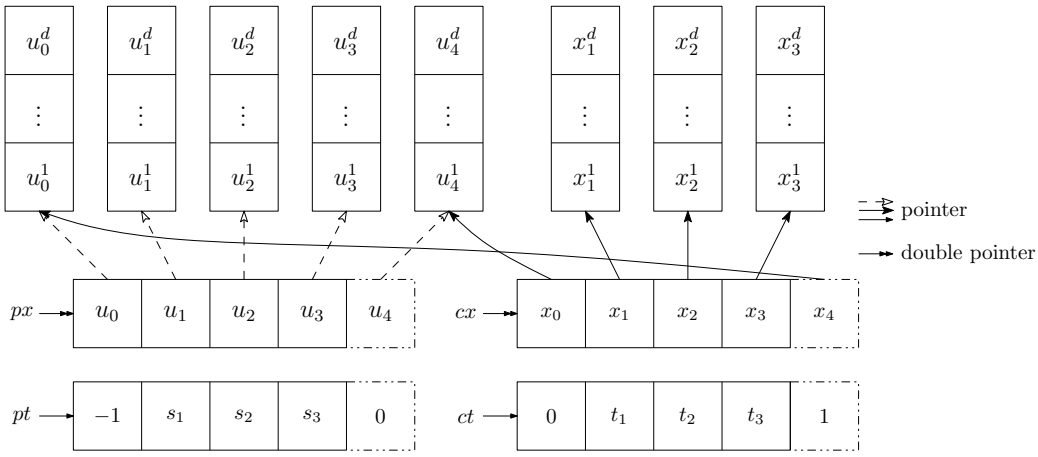

Figure 2.3. Previous (pt, px) and current (ct, cx) history with distinction in jump discontinuities..

2.2.1 Polynomial interpolation

Let $(t_i, \varphi_i)_{i=0}^{n-1}$ be a table of values of a smooth mapping φ. The polynomial interpolation consists in finding a polynomial, let us say p, of degree at most n that interpolates φ at the nodes t_i, i.e.,

$$p(t_i) = \varphi_i, \qquad 0 \leqslant i < n.$$

The problem is well-posed in the sense that it has a unique solution that depends continuously on the data. The solution can be written in the well-known Lagrange form

$$p(t) = \sum_{j=0}^{n-1} \varphi_j \ell_j(t), \qquad \ell_j(t) \coloneqq \frac{\prod\limits_{k \neq j} (t - t_k)}{\prod\limits_{k \neq j} (t_j - t_k)}. \tag{2.4}$$

The polynomial ℓ_j is called Lagrange polynomial corresponding to the node t_j, and it satisfies that $\ell_j(t_k) = \delta_{jk}$ where δ_{jk} denotes the Kronecker delta.

The Lagrange interpolant acts as a linear mapping w.r.t. the φ_i's. Therefore the spatial jet transport will apply, i.e. the operations performs by the automatic differentiation in the Lagrange interpolant will be exactly the same as perform the Lagrange interpolant in each order of the jet independently.

PROPOSITION 2.2. *The spatial jet transport applies to the polynomial interpolation.*

Proof. If $\varphi_j + \overline{\varphi}_j s$, then

$$\sum_{j=0}^{n-1}(\varphi_j + \overline{\varphi}_j s)\ell_j(t) = \sum_{j=0}^{n-1}\varphi_j\ell_j(t) + \sum_{j=0}^{n-1}\overline{\varphi}_j\ell_j(t)s = p(t) + \overline{p}(t)s. \qquad \square$$

Polynomial interpolation is sensitive to the Runge phenomenon which means that adding more nodes may give a worst approximation of the real mapping φ. It has other shortcomings that must be pointed out such as its computation is numerically unstable or each evaluation of $p(t)$ has a computational cost $\Theta(n^2)$ additions, and multiplications. Although other approaches to get the same polynomial $p(t)$, expressed in a different manner, can provide a linear cost. For instance, the Newton's approach, and its Newton tableau of divided differences [DB08]. But if we have several mappings in the same nodes, it might get a slightly better performance because ℓ_j's in eq. (2.4) are the same.

In the case of the IVP-DDE, the jump discontinuity points constraints the number of nodes that are allowed to use in a neighbourhood of those points. Thus, the polynomial interpolation may give bad approximations close to the jump discontinuities at the beginning of the orbit.

2.2.2 Rational barycentric interpolation

Let $(t_i, \varphi_i)_{i=0}^{n-1}$ be a table of values, and $\ell(t) \coloneqq \prod_{j=0}^{n-1}(t - t_j)$. If we define the barycentric weights

$$w_j \coloneqq \frac{1}{\ell'(t_j)} = \frac{1}{\prod_{k\neq j}(t_j - t_k)}, \qquad 0 \leqslant j < n, \tag{2.5}$$

then the Lagrange polynomials in eq. (2.4) can be rewritten as

$$p(t) = \ell(t)\sum_{j=0}^{n-1}\frac{w_j}{t - t_j}\varphi_j, \qquad \text{with } \ell_j(t) = \ell(t)\frac{w_j}{t - t_j}.$$

Due to the fact that $1 = \sum_{j=0}^{n-1}\ell_j(t)$, the rational barycentric interpolation is expressed by

$$p(t) = \frac{\sum_{j=0}^{n-1}\frac{w_j}{t - t_j}\varphi_j}{\sum_{j=0}^{n-1}\frac{w_j}{t - t_j}}. \tag{2.6}$$

Similarly to Proposition **2.2**, we also prove Proposition **2.3**.

PROPOSITION 2.3. *The spatial jet transport applies to the rational barycentric interpolation.*

To implement the rational barycentric interpolation, the barycentric weights must be chosen. The first attempt is to consider the ones corresponding to equidistant nodes that according to [BT04] they are

$$w_j = 2^{n-1}(b-a)^{1-n}(-1)^j \binom{n-1}{j}$$

when φ is defined in the general interval $[a,b]$. These choice is ill-conditioned in the sense that changes in the input may generate big changes [TW91].

One of the easiest nodes that gives easy weights are the Chebyshev points of the second kind

$$\mathtt{II}_k = \mathtt{II}_k^n = \cos(k\pi/(n-1)), \qquad 0 \leqslant k < n \tag{2.7}$$

Notice that $\mathtt{II}_0 > \cdots > \mathtt{II}_{n-1}$, and $\mathtt{II}_k = -\mathtt{II}_{n-1-k}$ for any $0 \leqslant k < \lceil \frac{n-1}{2} \rceil$. And then it is enough to store $\lceil \frac{n+1}{2} \rceil$ Chebyshev nodes and the n values by φ.

Since $\mathtt{II}_k$ are in $[-1,1]$, the affinity defined by

$$\phi\colon [-1,1] \to [a,b], \qquad s \mapsto \frac{1}{2}((a-b)s + a + b) \tag{2.8}$$

allows to get the values in the t-range solving $t_k = \phi(s_k)$. In other words, the interpolation is done for the mapping $\varphi \circ \phi^{-1}$. Then eq. (2.6) becomes

$$p(t) = \frac{\dfrac{\varphi_0}{2(s-\mathtt{II}_0)} + \displaystyle\sum_{1\leqslant j\leqslant \frac{n-1}{2}} \frac{(-1)^j\varphi_j}{s-\mathtt{II}_j} + \sum_{\frac{n-1}{2}<j<n} \frac{(-1)^j\varphi_j}{s-\mathtt{II}_{n-1-j}} + \dfrac{(-1)^{n-1}\varphi_{n-1}}{2(s-\mathtt{II}_0)}}{\dfrac{1}{2(s-\mathtt{II}_0)} + \displaystyle\sum_{1\leqslant j\leqslant \frac{n-1}{2}} \frac{(-1)^j}{s-\mathtt{II}_j} + \sum_{\frac{n-1}{2}<j<n} \frac{(-1)^j}{s-\mathtt{II}_{n-1-j}} + \dfrac{(-1)^{n-1}}{2(s-\mathtt{II}_0)}}, \tag{2.9}$$

with $t = \phi(s)$. It has linear computational complexity, $\Theta(n)$, and linear space complexity, $\Omega(n)$, due to the Chebyshev nodes. Other well-known nodes are the Chebyshev of first type defined by

$$\mathtt{I}_k = \mathtt{I}_k^n = \cos(\pi(k+1/2)/n), \qquad 0 \leqslant k < n.$$

In this case, $\mathtt{I}_0 > \cdots > \mathtt{I}_{n-1}$, and $\mathtt{I}_k = -\mathtt{I}_{n-1-k}$ for all $0 \leqslant k < \lceil n/2 \rceil$. In this case it is enough to store $\lceil n/2 \rceil$ Chebyshev points, and its n values by φ.

If N is even, eq. (2.6) becomes

$$p(t) = \frac{\displaystyle\sum_{0\leqslant j<n/2} (-1)^j \frac{\mathtt{I}_{n/2-1-j}}{s-\mathtt{I}_j}\varphi_j + \sum_{n/2\leqslant j<n} (-1)^j \frac{\mathtt{I}_{j-n/2}}{s+\mathtt{I}_{n-1-j}}\varphi_j}{\displaystyle\sum_{0\leqslant j<n/2} (-1)^j \frac{\mathtt{I}_{n/2-1-j}}{s-\mathtt{I}_j} + \sum_{n/2\leqslant j<n} (-1)^j \frac{\mathtt{I}_{j-n/2}}{s+\mathtt{I}_{n-1-j}}},$$

with $t = \phi(s)$.

In both cases, it was proved in [BBN99] that eq. (2.9) they do not have any pole in the interval $[-1, 1]$ as well as it has exponential convergence on an ellipse with foci ± 1 and sum of its major and minor axes equal to 2ρ with $\rho > 1$.

2.2.3 Chebyshev interpolation

It consists in express a function φ defined on an arbitrary interval $[a, b]$ as a linear combination of Chebyshev polynomials. Those polynomials are defined, in the real case, recurrently by

$$\begin{aligned} T_0(s) &= 1, \\ T_1(s) &= s, \\ T_{n+1}(s) &= 2sT_n(s) - T_{n-1}(s), \quad n \geqslant 1. \end{aligned}$$

Then φ is approximated by

$$\varphi(t) \approx \frac{c_0}{2} + \sum_{j=1}^{n-1} c_j T_j(s), \quad \text{with } t = \phi(s), \tag{2.10}$$

where ϕ is defined in eq. (2.8). The coefficients c_j's are obtained for the evaluation of $\varphi_k = \varphi \circ \phi^{-1}(s_k)$ with $s_k = \cos(\pi(k+\frac{1}{2})/n)$ nodes for $0 \leqslant k < n$. More precisely,

$$c_j = \frac{2}{n} \sum_{k=0}^{n-1} \varphi_k \cos\left(\frac{\pi j(k+\frac{1}{2})}{n}\right). \tag{2.11}$$

The coefficients c_j's in eq. (2.11) can be compute quickly using the discrete cosinus transform of type III, known as DCT-III, and its corresponding inverse DCT-II whose computational complexities can be in $\Theta(n \log n)$.

To evaluate eq. (2.10) in an arbitrary t inside the interval of definition of φ, one can use Clenshaw's recurrence formula [Cle62] whose complexity is linear, $\Theta(n)$.

Proposition **2.4** tells us that the spatial jet transport (the one w.r.t. φ_k's) can be used in the Chebyshev interpolation. Its proof is immediate because, in terms of points φ_k, the Chebyshev interpolation is just a (linear) change of variables.

PROPOSITION 2.4. *The spatial jet transport applies to the Chebyshev interpolation.*

2.2.4 Choosing the interpolation strategy

The previous interpolation methods are well-known in the community of numerical analysts. Lagrange interpolant requires $\Theta(n^2)$ for each evaluation of the polynomial $p(t)$, its computation is numerically unstable which implies the use of small number of nodes, and well-balance nodes around the unknown time value to approximate. However, in the case of a non-splicing condition for an IVP-DDE, it may happen that its interpolation for values close to the jump discontinuities are either non-accurate or does not have well-balanced nodes.

The other two methods; rational barycentric, and Chebyshev, are defined in a closed real interval which allows us to have under control the jump discontinuities whenever they become known. In terms of computational and space complexities, rational barycentric interpolation is better. In fact the proof of the rational barycentric interpolation in [BBN99] uses convergence result of the Chebyshev interpolation. Another issue to point out is the choice of the nodes. The Chebyshev of second kind, eq. (2.7), contains the extreme of the interval which allows to do a special treatment in case that some of the those were a jump discontinuity.

2.3 Runge-Kutta methods with delay

Among all the Runge-Kutta methods, those admitting an automatic stepsize control have become popular. Several versions with slight changes can be found in the literature. Here, we are going to show a simple example which computes two different RK with different order and uses the one with higher order to give a prediction of the stepsize for the next step. We want to identify in which steps the jet transport plays an important role or not.

ALGORITHM 2.5 (RK $p < q$ with controlled stepsize).

- ⋆ `Inputs:` tolerance tol, $h_{min} \leqslant |h| \leqslant h_{max}$, matrix $(b_{ij}) \in \mathbb{R}(\sigma, \sigma)$, vectors $(a_1, \ldots, a_\sigma)$, $(c_1, \ldots, c_{\sigma_1})$ and $(d_1, \ldots, d_{\sigma_2})$, and an initial value (t_0, x_0).

1. Compute

$$\kappa_i = f\big(x_0 + h\sum_{j=1}^{i-1} b_{ij}\kappa_j, \varphi(t_0 + a_i h)\big), \quad 1 \leqslant i \leqslant \sigma,$$

   where the values $\varphi(t_0 + a_i h)$ are interpolated by the history.

2. Compute approximations with respective order p and q by

$$x_1^{(1)} = \sum_{i=1}^{\sigma_1} c_i\kappa_i, \qquad \text{and} \qquad x_1^{(2)} = \sum_{i=1}^{\sigma_2} d_i\kappa_i.$$

3. Assign $\delta \leftarrow \|x_1^{(1)} - x_1^{(2)}\|$.

4. If $tol < \delta$, then $h \leftarrow 0.9h(tol/\delta)^{1/q}$.

   4.1. If $|h| \leqslant h_{min}$, error message and exit.

   4.2. Iterate the process with the new value h.

5. If $\delta < tol$, then

$$\begin{aligned} x_0 &\leftarrow x_0 + x_1^{(2)}, \\ t_0 &\leftarrow t_0 + h, \\ h &\leftarrow 0.9h\min\{1.2, (tol/\delta)^{1/q}\}. \end{aligned}$$

   5.1. If $h_{max} \leqslant |h|$, then $h \leftarrow h_{max}h/|h|$.

Algorithm **2.5** needs some remarks:

- Some of the coefficients of the Butcher's tableau can be found extensively in the literature like [Ver78, HNrW93].
- The values $\varphi(t_0 + a_i h)$ in item **1** are approximated by, for instance, some of the interpolation methods in section **2.2**.
- The norm in item **3** must be adapted in case of jet transport.
- The value 0.9 in items **4** and **5** are safety factor.
- Formally, in item **5** the approximation $x_1^{(1)}$ should be used instead of $x_1^{(2)}$ since we are using an approximation of order q to check the approximation of order $p < q$.

Algorithm **2.5** is just a sketch of the steps for an explicit RK with controlled stepsize and slightly modifications are possible depending on the specific IVP-DDE to solve. There are other strategies to solve an IVP-DDE such as the RETARD in [HNrW93, II.17]. In that case, the integrator is based on a modification DOPRI5 with dense output [DP86]. A dense output consists in a σ-stage RK with $\sigma' - \sigma$ extra stages to get the expression of the polynomials $b_i(\theta)$ so that the polynomial

$$p(\theta) = x_0 + h \sum_{i=0}^{\sigma'} b_i(\theta)\kappa_i \tag{2.12}$$

verifies $|p(\theta) - x(x_0 + \theta h)| = O(h^{\sigma'+1})$. In other words, points nearby x_0 can be approximated by polynomials and an error depending on the stepsize. The polynomials $b_i(\theta)$ are independent of the points of the orbit. That implies that the linear combination in eq. (2.12) applies for the jet transport as well.

More sophisticated integrators explained in [BZ13] seems to be candidates for jet transport, although we did not check them in detail all of them. A special attention needs RADAR explained in [GH01, GH08]. It is an implicit RK method based in Radau IIA, [HW10], with control in jump discontinuities by extending the Newton needed in each of the iterations.

2.4 Taylor method

The splicing condition in an IVP-DDE like eq. (2.2) depends on the initial condition. The interpolation may be required, and in such a case, it must be done in the space of temporal jets. That is, the output of the interpolation must a Taylor expansion at the time that is requested.

A first observation is that there are some situations where the interpolation may not be needed. For instance, when there is only a constant delay and the step size is fixed.

However, in general, interpolation will be required. Similar to Figure **2.3**, now we need to be able to keep the history (pt, px) at the same time that the current history (ct, cx) must be prepared for further time steps.

Now, before the jet transport, the values in px and cx are vectors of temporal jets of order p in an arbitrary d-dimensional space. Depending on the interpolation nodes, some values in px and cx may coincide. Following the notation in Figure **2.4** let us give a pseudo-code to deal with the potential jump discontinuities.

ALGORITHM 2.6.

⋆ Given a past history (pt, px) with length $plen < njets$, and a current history (ct, cx) with length $clen < njets$.

1. Interpolate order-by-order, $px^{[j]}$ for $0 \leqslant j \leqslant p$.
2. Once the boundary time is reached,
   2.1. $pt \leftrightarrow ct$ and $px \leftrightarrow cx$ (swapping the pointers).
   2.2. Force $ct_1 \leftarrow pt_{clen}$.
   2.3. $plen \leftarrow clen$ and $clen \leftarrow 0$.
3. If at some moment the $clen$ is equal to $njets$, reallocate the memory.

The item **1** in Algorithm **2.6** deserves a special attention. The first attempts were to differentiate as many times as were needed the Lagrange or Newton polynomial or even the Hermite polynomial, [DB08], but we realised, using interval arithmetic, that the numerical error is, in general, really bad for the higher order terms of the temporal jet. That is related with the fact that differentiation is a notoriously ill-posed problem due to of the lack of information in the discretesed problem. The solution was to use the interpolation order-by-order as independent functions.

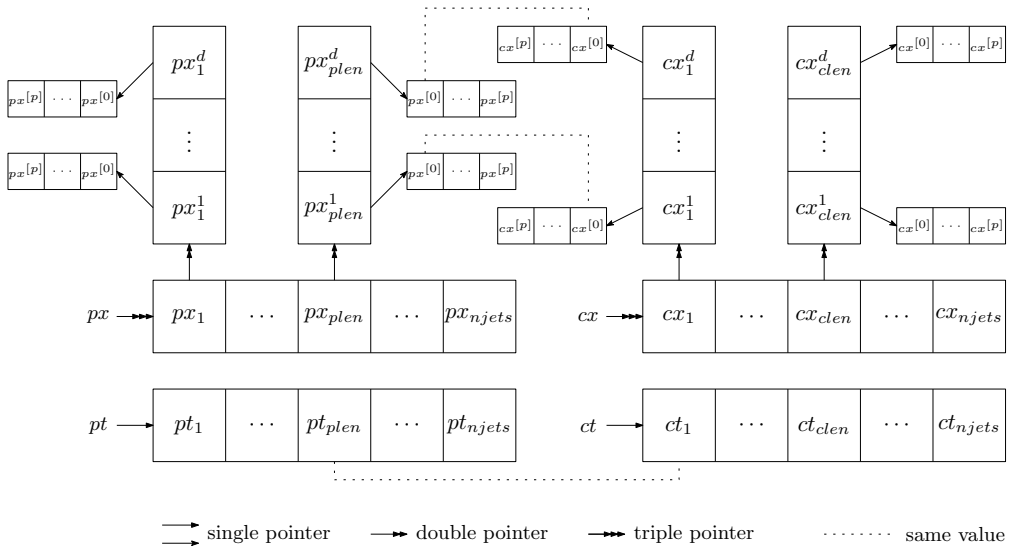

Figure 2.4. Previous history (pt, px) and current history (ct, cx) with their normalised p-order Taylor coefficients $px^{[j]}$ and $cx^{[j]}$ for $0 \leqslant j \leqslant p$.

If the splicing condition of the initial condition was not satisfied up to the order used by the Taylor integrator, the jump discontinuity points must

be detected and use their left or right values of the temporal jet since the radius of convergence is defined respective for negative or right values as it illustrates Figure **2.5**.

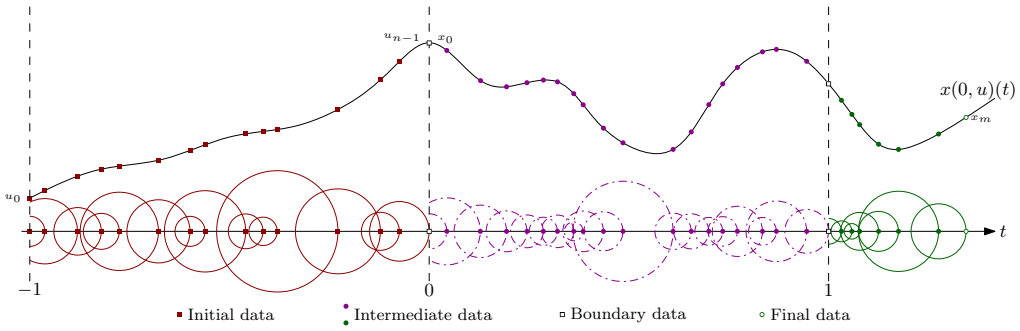

Figure 2.5. Illustrations of a Taylor integration with half of the convergence disk at the jump discontinuity points.

2.5 An application – time lags in saddle-node remnant

An equilibrium point of a DDE like eq. (2.1) is a map $x^\star$ defined in $[-1, 0]$ such that there is solution for the IVP-DDE like eq. (2.2) through $x^\star$ and $\frac{d}{dt}x(0, x^\star)(t) = 0$ for all t. In other words, $x^\star$ must be a constant function so that

$$f(x^\star, x^\star) = 0.$$

In the constant delay case, the fixed points of the ODE obtained with no lags (those assigned to zero) will still be in the DDE one.

The stability is given, in the case of constant delay, by the study of the characteristic equation

$$\det(\lambda Id - D_x f(x^\star, x^\star) - e^{-\lambda} D_\varphi f(x^\star, x^\star)) = 0, \qquad \lambda \in \mathbb{C}. \tag{2.13}$$

Different phenomena can happen. For instance, the stability may change depending on the delay values. It was showed in [GJS18] that a system describing the density-dependent reproduction of a single specie with time lags preserves exactly the same equilibria with the same stability but with a different quantity values.

PROPOSITION 2.7. *The model with parameters $k > 0$ and $\varepsilon > 0$ given by*

$$\frac{dx}{dt}(t) = kx(t-\tau)^2(1-x(t)) - \varepsilon x(t) \tag{2.14}$$

has constant functions $x_\pm = (1 \pm \sqrt{1-4\varepsilon/k})/2$, and $x_0 = 0$ defined in $[-\tau, 0]$. They are the only equilibrium points of eq. (2.14) whose stabilities are independent of the delay τ. For $0 < \varepsilon/k < 1/4$, x_0 is exponentially stable, x_+ is stable, and x_- is unstable, due to a real eigenvalue. At $\varepsilon/k = 1/4$, the equilibria x_- and x_+ merge to $x = 1/2$ in a saddle-node bifurcation, and become complex for $\varepsilon/k > 1/4$.

Proof. The equilibrium points are the constants functions that are roots of the right hand side of eq. (2.14). That is, the same points x_* discussed in the previous Section, but its stability must be analyzed studying the transcendental eigenvalue problem for λ [HVL93],

$$-kx_*^2 - \varepsilon + 2k(1-x_*)x_* e^{-\lambda\tau} - \lambda = 0,$$

which is equivalent to

$$(-kx_*^2 - \varepsilon)\tau e^{\lambda\tau} + 2k(1-x_*)x_*\tau - \lambda\tau e^{\lambda\tau} = 0. \tag{2.15}$$

Defining the values $p = (-kx_*^2 - \varepsilon)\tau$, $q = 2k(1-x_*)x_*\tau$, and $z = \lambda\tau$, then the Theorem 1 in [Hay50] says that if $0 < \varepsilon/k < 1/4$ the stability of x_0 is subjected to the conditions $-\varepsilon < \min\{1/\tau, 0\}$, and $0 < ((\tan a_1)^2 + 1)^{1/2}$ while the stability of $x_\pm$ is subjected to $-kx_\pm < \min\{1/\tau, -2\varepsilon\}$, and $-2\varepsilon < ((a_1/\tau)^2 + (kx_\pm)^2)^{1/2}$ where in these conditions a_1 denotes the root of $a = p\tan a$ such that $0 < a < \pi$.

In particular, the stability of the real point x_* does not depend on the delay $\tau > 0$ and the conditions of being stable or unstable are the same as for the model without time lags. That is, $x_0 = 0$ is exponentially stable if, and only if, $-\varepsilon < 0$, and $x_\pm$ is exponentially stable if, and only if, $2\varepsilon - kx_\pm < 0$.

We have only shown whether the equilibrium points $x_0, x_\pm$ are stable or not but we did not quantify their stability. However, we can apply Lemma 1 in [Hay50] to transform eq. (2.15) into $s = ce^s$, where $s = -(\lambda + kx_\pm)\tau$, and $c = -2\varepsilon\tau e^{kx_\pm\tau}$, whenever $0 < \varepsilon/k < 1/4$. Since $c < 0$ we conclude that the stability of $x_\pm$ is governed by a real eigenvalue such that x_+ is stable and x_- is unstable. In other words, the bifurcation at $\varepsilon/k = 1/4$ is also a saddle–node (s-n) bifurcation for the delayed model. The difference arises in how strong is the (un)stability at $(x_-)x_+$ depending on τ. When $0 < \varepsilon/k < 1/4$, it is quantified by the real number $\lambda = -kx_\pm - s/\tau$ being s the real solution of $c^2e^{2s} = s^2, s < 0$. After the bifurcation, i.e. $\varepsilon/k > 1/4$, the stability of

$x_\pm$ is determined by the eigenvalue with maximum real part of eq. (2.15). According to Theorem 1.2 in [Nis16] $x_\pm$ are unstable regardless of the value of $\tau > 0$. □

While Proposition **2.7** shows that the equilibria, and their stability coincide with those when $\tau = 0$, it does not say anything about how much stable or unstable are those equilibria. Preliminary simulations shows that there is a difference in the time needed before the extinction depending on the delay τ. Indeed, for larger τ more time is needed to extinct the specie as Figure **2.6** shows. The dynamics near $x = 1/2$ after the saddle-node is slow and it can be seen as a passage near a saddle equilibrium point with complex coordinates. It depends on the size of the real part of the eigenvalue in the saddle.

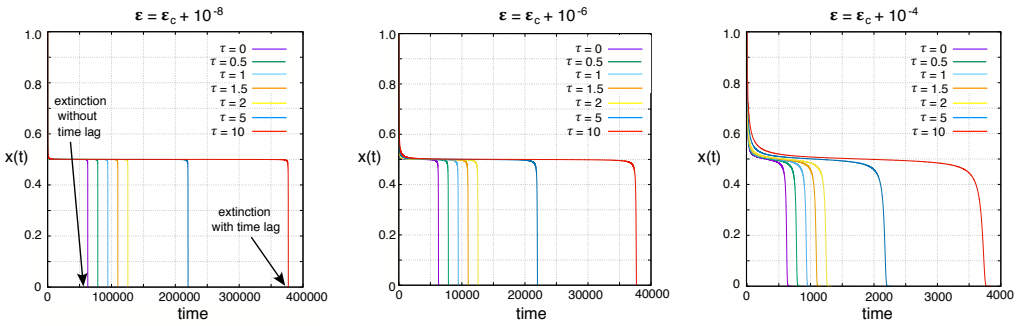

Figure 2.6. Extinction times near the saddle-node remnant for different delay time in eq. (2.14). As large delay is longer, more transient time is needed.

To study the dominant eigenvalue when $x_\pm$ become complex, we must study the characteristic equation in a neighbourhood of $(x, \tau) = (1/2, 0)$. Let us fix a small value $\delta > 0$ so that $\varepsilon/k = (1 + \delta)/4$. Then $x_\pm = (1 \pm \mathtt{i}\sqrt{\delta})/2$ are complex numbers and eq. (2.13) in eq. (2.14) at the points $x_\pm$ becomes

$$1 \pm \sqrt{\delta} - (1 + \delta)e^{-\lambda\tau} + 2\lambda/k = 0. \tag{2.16}$$

The values $(\tau, \lambda) = (0, 2\varepsilon - kx_\pm)$ verifies eq. (2.16). The derivative w.r.t. λ at that point is $2/k$, which is always a non-zero value. Then there exists a unique analytic mapping $\tau \mapsto \lambda(\tau; \delta)$ satisfying eq. (2.16) and an explicit

computation leads to

$$\begin{aligned}\operatorname{Re}\lambda(\tau;\delta) =& k\frac{\delta}{2} - k^2\left(\frac{\delta^2}{4}+\frac{\delta}{4}\right)\tau + k^3\left(\frac{3\delta^3}{2}+\frac{\delta^2}{2}+\frac{\delta}{8}\right)\frac{\tau^2}{2!}\\ &- k^4\left(\delta^4+\frac{25\delta^3}{16}+\frac{3\delta^2}{8}-\frac{3\delta}{16}\right)\frac{\tau^3}{3!}\\ &+ k^5\left(\frac{125\delta^5}{32}+\frac{207\delta^4}{32}-\frac{\delta^3}{32}-\frac{131\delta^2}{32}-\frac{3\delta}{2}\right)\frac{\tau^4}{4!} \qquad +O(\tau^5).\end{aligned}$$

These approximations leads to the following result proved in [GJS18].

PROPOSITION 2.8. *In fact,* $\operatorname{Re}\lambda(\tau;\delta) = k\delta g(\tau;\delta)$ *for some analytic mapping* g *with* $g(0;0)\neq 0$.

Proof. It is enough to prove it in a neighbourhood of $\delta = 0$. As the mapping $\lambda(\tau;\delta)$ is analytic, let us proceed by induction on the order of the derivative. Indeed, $\operatorname{Re}\lambda(0;\delta) = k\delta/2$ and if now we assume that $\operatorname{Re}\frac{\partial^i\lambda}{\partial\tau^i}(\tau;\delta)$ can be factorised by $k\delta$ for all $i<j$, then $\operatorname{Re}\frac{\partial^j\lambda}{\partial\tau^j}(\tau;\delta)$ is the sum of a combination of $\operatorname{Re}\frac{\partial^i\lambda}{\partial\tau^i}(\tau;\delta)$ with $i<j$, and the jth partial derivative of eq. (2.16) with respect τ that always has $k\delta$ as a factor. □

τ	ε_c+10^{-4}	ε_c+10^{-6}	ε_c+10^{-8}
0	2.000000e−04	2.000000e−06	2.000000e−08
0.05	1.950620e−04	1.950639e−06	1.950642e−08
0.1	1.902566e−04	1.902602e−06	1.902602e−08
1	1.259111e−04	1.259258e−06	1.259259e−08
1.5	1.037753e−04	1.037899e−06	1.037901e−08
2	8.748623e−05	8.749986e−07	8.750000e−09
5	4.255738e−05	4.256552e−07	4.256559e−09
10	2.175476e−05	2.175921e−07	2.175926e−09

Table 2.2. The greatest real part of eigenvalues of $x_\pm$ when $\varepsilon_c = 1/4$ and $k = 1$.

Table 2.2 shows the values of $\operatorname{Re}\lambda(\delta,\tau)$ for different values of δ and τ, computed by solving numerically eq. (2.16), that is, integrate τ units of time the constant DDE, propagate the first variational equation and look for the eigenvalue with larger real part.

Note the similarity between columns of this table, which is due to the form of $\operatorname{Re}\lambda(\delta,\tau)$, Proposition **2.8**. Moreover, as the derivative of $\operatorname{Re}\lambda(\delta,\tau)$ at $\tau = 0$ is negative, we have that the real part of the eigenvalue becomes

smaller as τ increases. Hence, we expect a longer transition time when a small delay is added.

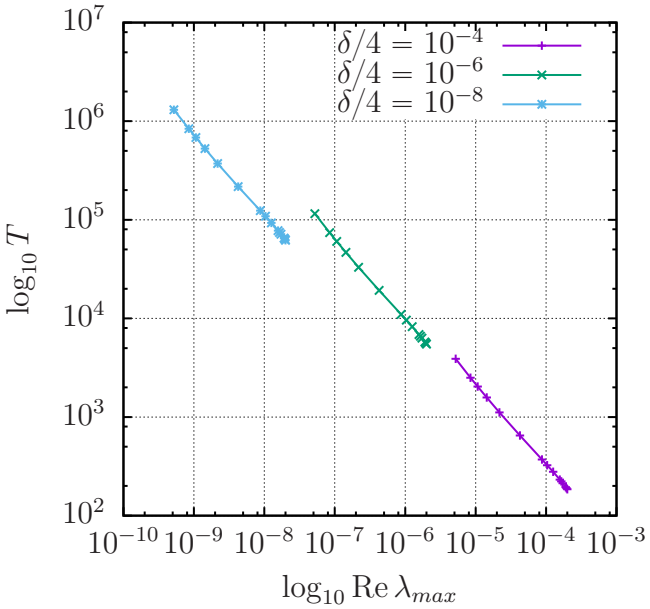

Figure 2.7. The values $\mathrm{Re}\,\lambda(\delta,\tau)$ vs. the time spent near $x = 1/2$ for three values of δ: $\delta/4 = 10^{-4}$ (cyan), $\delta/4 = 10^{-6}$ (green), and $\delta/4 = 10^{-8}$ (violet).

By means of a numerical integration, we quantify the time that a trajectory is close to $x = 1/2$ for several values of τ. More concretely, we compute the time needed to go through $x = 1/2$ as the difference between the first time t that verifies $|\frac{dx}{dt}(t)| < 10^{-4}$ and $|x(t) - 1/2| < 0.005$, and the first one that does not verify it. Figure **2.7** displays, in log scale, the relation between the values $\mathrm{Re}\,\lambda(\delta,\tau)$ and the time taken to go through $x = 1/2$. Note that the plot shows the expected result for a linear system, in which the passage time near a saddle is proportional to the inverse of the largest real part of the eigenvalues of the saddle. As we are close to an equilibrium point, it is clear that the linear part dominates the dynamics, and this implies a longer transition through $x = 1/2$.

Hence, this justifies the results displayed in Figure **2.6** in the sense that τ involves a longer delayed transition near to the saddle-node remnant. In this figure three different values of ε are studied beyond, but close to the bifurcation. Specifically, we plot, for each case, a time series for the model given by the associated ODE in eq. (2.14) (violet trajectory $\tau = 0$), and

six other trajectories applying increased time lags. For example, using $\varepsilon = \varepsilon_c + 10^{-8}$ the time delay with $\tau = 0$ is $t \approx 6 \times 10^3$, while for $\tau = 10$ this time becomes $t \approx 3.75 \times 10^5$. The dependence between the time delays and the distance to the bifurcation value for different time lags (including $\tau = 0$) is displayed in Figure **2.8**. Panel (a) displays the results in a linear-linear scale while (b) shows the same results in a log-log plot. Note that the time lag does not modify the inverse square-root law. Indeed, the increase of $\tau > 0$ in delaying times with respect to the model without time lags is linear. This relation is represented in Figure **2.9**, where the time differences for the model with $\tau = 0$ is plotted as a function of τ.

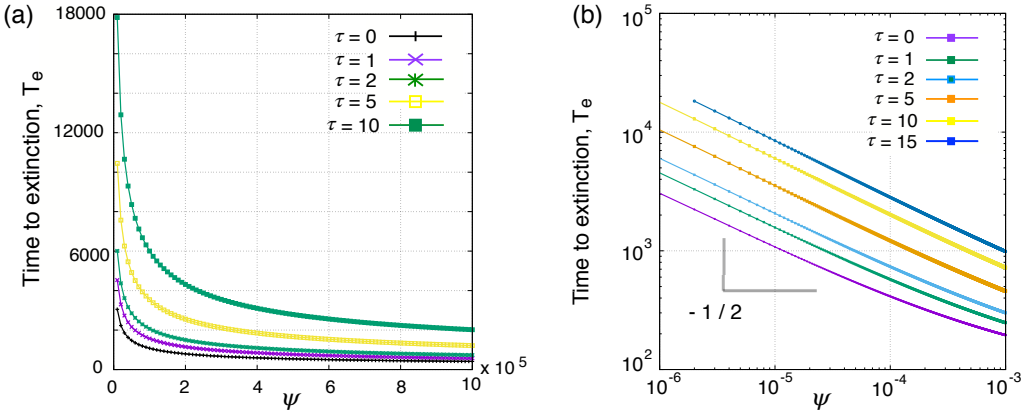

Figure 2.8. Dependence of extinction times (T_e) on the distance to bifurcation threshold, $\psi = \varepsilon - \varepsilon_c$. (a) Time to extinction, T_e at increasing parameter ε above the bifurcation value ε_c. Notice that this extinction time diverges near the bifurcation value (results shown in a linear-linear plot). (b) Inverse square-root law also found in the system with no time lags (violet curve). Notice that the same power-law is found by including time lags. Here for all of the values of τ analysed the time to extinction scales accordingly to $T_e \sim \psi^{-1/2}$.

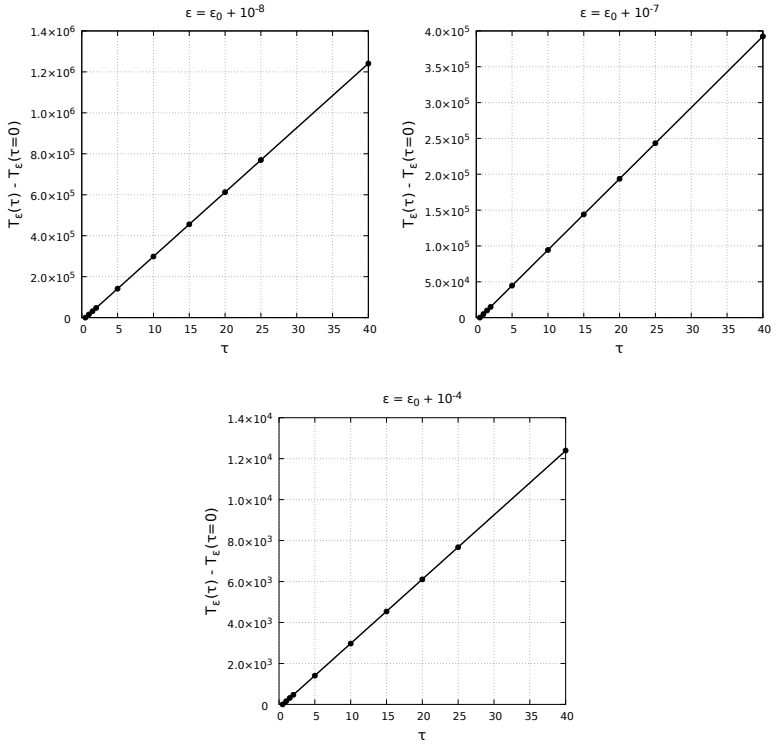

Figure 2.9. Linear dependence between the time that trajectories spend in the slow passage near the saddle-node remnant and the time lag τ. The points indicate the difference between the delayed transition for the system with no time lag and with different time lags, computed as $T_e(\tau) - T_e(\tau = 0)$, while the solid line is the linear regression. We display these results for three different values of the bifurcation parameter ε beyond the bifurcation value ε_c, plotting this difference between times at increasing lag times, τ.

Chapter 3

Numerical methods for periodic and quasi-periodic motions

ACK: This work is a collaboration with Prof. Àngel Jorba and partially with Prof. Ken Hayami at National Institute of Informatics (NII) of Japan.

3.1 Introduction

Once we have the numerical integrators which provide the first order flow, we can use it to compute invariant objects by the use of the Poincaré mapping in its delay version. In the constant case the phase space of a delay differential equation (DDE) is an infinite space. Hence, from a numerical point of view, the Poincaré needs to be discrete. As consequence, the size of the linear system to solve in a Newton approach may be quite large. However, the Poincaré mapping will be, in general, a compact operator, which implies that its spectrum will be clustered and we can use iterative methods to solve the linear system.

3.2 Iterative solver for linear systems

Iterative methods for the solution of linear systems of equations have become famous in the last decades. In particular, the methods based on Krylov projection. They include popular methods such as Conjugate Gradients, MINRES, QMR, CGS, LSQR, Bi-CGSTAB, GMRES, ... [Saa03] We are going to focus on GMRES which has demonstrated to be quite robust for a variety of problems. However, we tested some of the other ones, such as Bi-CGSTAB, with worst performance and accuracy.

The classical iterative methods, such as Jacobi or Gauss-Seidel, require to have access to specific parts of the matrix. If for instance, the matrix is

generated by some recurrence expression, or it has a specific structure, the classical iterative solvers are good in terms of performance and resources. However, there are plenty of situations where to know a specific part of the matrix is not feasible. This is the case for the kind of problems we are interested; the computation of periodic orbits and tori for an arbitrary constant DDE.

3.2.1 Krylov subspace

Let $A\boldsymbol{x} = \boldsymbol{b}$ be a linear of equations. Assume that we are able to solve a simpler system of the form $K\boldsymbol{x}_0 = \boldsymbol{b}$ and we take $\boldsymbol{x}_0$ as an approximation for $\boldsymbol{x}$. The goal is to perform an iteration procedure. Hence, let $\boldsymbol{z}$ be the correction of the original system so that

$$A(\boldsymbol{x}_0 + \boldsymbol{z}) = \boldsymbol{b}.$$

This leads to a new linear system $A\boldsymbol{z} = \boldsymbol{b} - A\boldsymbol{x}_0$ where we can apply again the same simpler solver to figure out the linear system

$$K\boldsymbol{z}_0 = \boldsymbol{b} - A\boldsymbol{x}_0.$$

Now the new approximation becomes $\boldsymbol{x}_1 = \boldsymbol{x}_0 + \boldsymbol{z}_0$. The correction procedure can be applied for $\boldsymbol{x}_1$ again, leading to an iterative method of the form

$$\boldsymbol{x}_{i+1} = \boldsymbol{x}_i + \boldsymbol{z}_i = \boldsymbol{x}_i + K^{-1}(\boldsymbol{b} - A\boldsymbol{x}_i). \tag{3.1}$$

The basic idea behind this process is that we are considering the simpler matrix K as a preconditioner of the original one. That is, the linear system we are trying to solve is

$$(K^{-1}A)\boldsymbol{x} = K^{-1}\boldsymbol{b}.$$

By eq. (3.1), we can consider the iteration as

$$\boldsymbol{x}_{i+1} = \boldsymbol{b} + (I - \alpha_i A)\boldsymbol{x}_i = \boldsymbol{x}_i + \boldsymbol{r}_i \tag{3.2}$$

with $\boldsymbol{r}_i = \boldsymbol{b} - \alpha_i A\boldsymbol{x}_i$ is the weighted residual. The latter expression contains $\boldsymbol{x}_i$ as well as $\boldsymbol{r}_i$, and it hinders its study. Let us focus on the residuals, which should be small in case of that the iteration tends to the solution.

$$\boldsymbol{b} - \alpha_{i+1}A\boldsymbol{x}_{i+1} = \boldsymbol{b} - \alpha_{i+1}A\boldsymbol{x}_i - \alpha_{i+1}A\boldsymbol{r}_i$$

whose expression leads to

$$\boldsymbol{r}_{i+1} = (I - \alpha_{i+1}A)\boldsymbol{r}_i = \prod_{j=1}^{i+1}(I - \alpha_j A)\boldsymbol{r}_0 = P_{i+1}(A; \boldsymbol{\alpha})\boldsymbol{r}_0.$$

P_{i+1} is a polynomial of degree $i+1$ that verifies $P_{i+1}(0) = 1$. If we want to have guaranteed the convergence for all initial residual $\boldsymbol{r}_0$, we should require $\|I - \alpha_j A\| < 1$ for all j.

Going back to eq. (3.2), we have

$$\boldsymbol{x}_{i+1} = \boldsymbol{r}_0 + \cdots + \boldsymbol{r}_i = \boldsymbol{r}_0 + \sum_{j=1}^{i} \prod_{k=1}^{j} (I - \alpha_k A)\boldsymbol{r}_0 \in \mathcal{K}^{i+1}(A; \boldsymbol{r}_0) \tag{3.3}$$

where, by definition, $\mathcal{K}^{i+1}(A; \boldsymbol{r}_0) = \text{span}\{\boldsymbol{r}_0, A\boldsymbol{r}_0, \ldots, A^i\boldsymbol{r}_0\}$ is a $(i+1)$-dimensional vectorial space called Krylov subspace. In general, we are going to consider $\alpha_j = 1$ for all j. But the weighted residual with some extra considerations provides the first machinery to consider rational Krylov subspace [BG15]. However, it seems to require a more computational effort and to make some decisions in the implementation such as the choice of the poles which may strongly depend on the equation to study.

Due to eq. (3.3), all the vectors $\boldsymbol{x}_i$ lives in a Krylov subspace with the same base vector $\boldsymbol{r}_0$. We want to generate a projection to these Krylov subspaces and solve the projected linear system, which is going to be an approximation of the real solution. There are different kind of projections that leads to different iterative solvers such as FOM, GMRES, MINRES, CG, ... [Saa03].

Ritz-Galerkin: Find $\boldsymbol{x}_k$ so that $\boldsymbol{r}_k \perp \boldsymbol{x}_0 + \mathcal{K}^k(A; \boldsymbol{r}_0)$.

Petrov-Galerkin: Find $\boldsymbol{x}_k$ so that $\boldsymbol{r}_k \perp \boldsymbol{x}_0 + \mathcal{L}$ with $\mathcal{L}$ a k-dimensional space.

Minimum norm residual: Find $\boldsymbol{x}_k$ so that $\|\boldsymbol{r}_k\|_2$ is minimal over the space $\boldsymbol{x}_0 + \mathcal{K}^k(A; \boldsymbol{r}_0)$.

Minimum norm error: Find $\boldsymbol{x}_k$ in $A^T(\boldsymbol{x}_0 + \mathcal{K}^k(A^T; \boldsymbol{r}_0))$ so that $\|\boldsymbol{x}_k - \boldsymbol{x}\|_2$ is minimal.

The Generalised Minimum RESidual, GMRES, consists in the minimisation of the residual (in Euclidian norm) over the space $\boldsymbol{x}_0 + \mathcal{K}^k(A; \boldsymbol{r}_0)$. It generates, at each iteration, a new unit vector orthogonal to the previous ones and join with the previous generated vector give a base for the new Krylov subspace.

3.2.2 The GMRES and the Arnoldi process

The Arnoldi process provides a systematic orthonormal basis of the Krylov subspace in such a way that the basis increases the dimension at each new iteration. Algorithm **3.1** summarises all this process.

ALGORITHM 3.1 (Arnoldi process).

⋆ `Notation:` To solve an n-by-n linear system $A\boldsymbol{x} = \boldsymbol{b}$. Let V_k be an n-by-k matrix and $H_{k+1,k}$ be a $(k+1)$-by-k matrix such that

(a) $AV_k = V_{k+1}H_{k+1,k}$.

(b) $V_{k+1} = \begin{bmatrix} V_k & \boldsymbol{v}_{k+1} \end{bmatrix}$ and $V_k = \begin{bmatrix} \boldsymbol{v}_1 & \cdots & \boldsymbol{v}_k \end{bmatrix}$ is an n-by-k matrix.

(c) $V_k^T V_k = I_k$ but, in general, $V_k V_k^T \neq I_n$.

(d) $H_k = \begin{bmatrix} I_k & 0 \end{bmatrix} H_{k+1,k}$ and H_k is a k-by-k upper Hessenberg.

(e) $H_k = V_k^T A V_k$ but, in general, $V_k H_k V_k^T \neq A$.

⋆ `Input:` $1 \leqslant j < k$, V_j and $H_{j+1,j}$.

⋆ `Output:` V_{j+1} and $H_{j+2,j+1}$.

1. If $j = 1$, then $\boldsymbol{v}_1 \leftarrow \boldsymbol{v}_1/\|\boldsymbol{v}_1\|$.
2. $\boldsymbol{v}_{j+1} \leftarrow A\boldsymbol{v}_j$.
3. $\tau_1 \leftarrow \|\boldsymbol{v}_{j+1}\|$.
4. $\boldsymbol{h}_j \leftarrow V_j^T \boldsymbol{v}_{j+1}$.
5. $\boldsymbol{v}_{j+1} \leftarrow \boldsymbol{v}_{j+1} - V_j \boldsymbol{h}_j$.
6. $\tau_2 \leftarrow \|\boldsymbol{v}_{j+1}\|$.
7. If $\tau_2 \leqslant 0.717\tau_1$, then
   - 7.1. $\boldsymbol{h}_{j+1} \leftarrow V_j^T \boldsymbol{v}_{j+1}$.
   - 7.2. $\boldsymbol{v}_{j+1} \leftarrow \boldsymbol{v}_{j+1} - V_j \boldsymbol{h}_{j+1}$.
   - 7.3. $\boldsymbol{h}_j \leftarrow \boldsymbol{h}_j + \boldsymbol{h}_{j+1}$.
8. $h_{j+1,j} \leftarrow \|\boldsymbol{v}_{j+1}\|$.
9. If $h_{j+1,j} = 0$, return.
10. $\boldsymbol{v}_{j+1} \leftarrow \boldsymbol{v}_{j+1}/h_{j+1,j}$.

Algorithm **3.1** needs some remarks to be pointed out:

- The initial vector $\boldsymbol{v}_1$ should be the residual $\boldsymbol{r}_0 = \boldsymbol{b} - A\boldsymbol{x}_0$ except when we consider a restarting iterative method.

- The item **7** tries to prevent the loss of orthogonality due to round-off as it has been suggested in, for instance, [DGKS76].
- All the operations that requires the use of the matrix A are just matrix times a vector and it can be obtained by the use of jet transport.
- The columns of the matrix V_k contains an orthonormal basis of the Krylov $\mathcal{K}^{k-1}(A; \boldsymbol{v}_1)$.
- In case of exit by item **9**, the solution is exactly in $\mathcal{K}^j(A; \boldsymbol{v}_1)$.

The Arnoldi process provides an orthonormal basis of the Krylov subspace and a factorisation of the matrix A. In order to minimise the residual vector, we can use such a factorisation as follows:

$$\begin{aligned} \|\boldsymbol{b} - A\boldsymbol{x}\|_2 &= \|\boldsymbol{b} - A(\boldsymbol{x}_0 + V_k\boldsymbol{y})\|_2 \\ &= \|\boldsymbol{r}_0 - AV_k\boldsymbol{y}\|_2 \\ &= \|\boldsymbol{r}_0 - V_{k+1}H_{k+1,k}\boldsymbol{y}\|_2 \\ &= \|V_{k+1}^T(\|\boldsymbol{r}_0\|\boldsymbol{v}_1 - V_{k+1}H_{k+1,k}\boldsymbol{y})\|_2 \qquad (3.4) \\ &= \|\|\boldsymbol{r}_0\|\boldsymbol{e}_1 - H_{k+1,k}\boldsymbol{y}\|_2. \end{aligned}$$

where in eq. (3.4) we use that a left orthonormal matrices are invariant under the Euclidian norm. Hence,

$$\inf_{\boldsymbol{x}\in\boldsymbol{x}_0+\mathcal{K}(A;\boldsymbol{r}_0)} \|\boldsymbol{b} - A\boldsymbol{x}\|_2 = \inf_{\boldsymbol{y}\in\mathbb{R}^k} \|\|\boldsymbol{r}_0\|\boldsymbol{e}_1 - H_{k+1,k}\boldsymbol{y}\|_2. \qquad (3.5)$$

The matrix $H_k = \begin{bmatrix} I_k & 0 \end{bmatrix} H_{k+1,k}$ is upper Hessenberg and a new column and row are added in each new iteration independently of the previous values of the matrix. Therefore, just a Givens rotation of the new information and a forward substitution are needed to compute the infimum in eq. (3.5).

3.2.3 Restarting GMRES

GMRES always convergence and, in fact, the sequence of residual $(\boldsymbol{r}_i)$ is always decreasing. But while the maximum number of iterations are upper bounded by the dimension of A, let us say n. Typically n is really large and we do not want to reach a lot of iterations. Because of that, the restarted GMRES, denoted by GMRES(m), consists in perform m iterations and restart the process by an initial vector $\boldsymbol{v}_1$ which is a linear combination of the previous ones. When the restarted GMRES is applied, the convergence is not guaranteed and the residual may stagnate.

3.2.4 Preconditioners

It has been shown that empirically the GMRES and many other iterative solvers, convergence faster if the spectrum of A is clustered and A is well-conditioned. The preconditioning process consists in providing a matrix M such that it approximates the matrix A and it is easy to solve linear systems. There are two kind of preconditioning:

Left: Solve $M^{-1}A\boldsymbol{x} = M^{-1}\boldsymbol{b}$ whose solution is also of $A\boldsymbol{x} = \boldsymbol{b}$.

Right: Solve $AM^{-1}\boldsymbol{y} = \boldsymbol{b}$ whose solution provides the solution of $A\boldsymbol{x} = \boldsymbol{b}$ by $\boldsymbol{x} = M^{-1}\boldsymbol{y}$.

3.2.5 Iterative solvers in recurrence solutions

A direct solver, such as those based in LU or QR, has no the features to have control of the residual or error values to solve the linear system accordingly to a prescribed tolerance. But iterative solvers have, in general, that feature because at each step they try to provide a better approximation of the linear system of equations.

In a recurrence method, such as Newton method or fixed point method, a finite sequence of linear systems must be solved. Not all of these linear system require the same accuracy for the recurrence method. That needs a specific stopping criterion. For instance, in a Newton method, we can try to force the quadratic convergence by the stopping criterion

$$\|\boldsymbol{b} - A\boldsymbol{x}_k\|_2 \leqslant \max(tol/2, \|\boldsymbol{b}\|_2^2 10^{-2}),$$

being *tol* the Newton tolerance.

3.3 Periodic motions in constant delay differential equations

The theory of existence and uniqueness is well established for IVP-DDE, like eq. (2.2), with constant delays. A periodic orbit in the DDE setting is an initial condition u defined in $[-1, 0]$ so that the solution of the IVP-DDE through u verifies that after a finite time bigger than 1, it returns exactly to u. That is, there is $t^\star \geqslant 1$ such that $x(0, u)_{t^\star} = u$.

The mapping, denoted by P, that takes an initial condition in $[-1, 0]$ and provides its integration up to a time bigger than 1 has been proved to be compact [HVL93]. Such those mappings are commonly called time-maps or

Poincaré maps. The Theorem **2.1** tells us that locally to the periodic orbits the splicing condition is going to be satisfied.

As in the ODE case, we can distinguish two situations. When a temporal section is involved in the definition of P, or when it involves a spatial section. We have already proved that the jet transport applies to the delay integrators, and in particular to the interpolation steps. Hence there are only few things that make a difference w.r.t. the ODE case.

Firstly, the condition to ensure the fixed point in the Poincaré map must be done in the space of mappings defined in $[-1, 0]$. That implies that a numerical simulation will need a discretisation of those mappings and the equality will be imposed in terms of their table of values. In other words, if $(s_i, u_i)_{i=0}^{n-1}$ is a table of values of the initial condition, and $v = P(u)$ so that $(s_i, v_i)_{i=0}^{n-1}$ is its table of values (in the same nodes s_i), then we require $u_i = v_i$ for all $0 \leqslant i < n$. As consequence the number of unknowns will be increased by a factor n.

Secondly, the fact that the fixed point in the time-map must done between table of values will generate an extra effort (specially for the spatial section) to adjust the tables in the same nodes.

Finally, the linear a approximation of the time-map will also be compact so its spectrum is going to be clustered and iterative solvers to generate a matrix-free Newton scheme will improve the performance and it is going to be the problem numerically feasible.

3.3.1 Poincaré sections

As in the ODE there are essentially two kind of Poincaré sections. The temporal ones and the spatial ones. Each of those need a special attention.

Temporal section

This is the standard section for systems having a dependency on time that is periodic with a known period, let us say ρ. Then, periodic orbits must have a period $t^\star$ multiple of ρ. In such a case, the Poincaré section is given by $t \equiv 0 \pmod{\rho}$ and the Poincaré mapping consists in the time-ρ map.

Depending on the interpolation strategy of the DDE integrator, it may happen that one needs to integrate further more to ensure to get enough information to interpolate at the nodes required for the time-ρ map.

In terms of the jet transport, there is no any extra step to make into account. Indeed, because the interpolation applies to jet transport and the DDE integrators are based on the ODE ones which has been proved that

they works correctly with the jet transport. If the section is temporal, the time-ρ map allows us to get the spatial jet during the integration.

Spatial section

This is the situation when the period is not known. A smooth manifold will be considered as a section, for instance continuous affine mappings or even just fixing a coordinate. These manifolds will be defined in the set of mappings defined in $[-1, 0]$ and assuming extra hypothesis, one proves that the Poincaré mapping defining in such manifolds is compact [SZ18].

As in the ODE the process is as follows:

1. Integrate the IVP until the number of crossing to the spatial section have been reached.
2. Look for the time (after the crossings) in such a way the orbit lie in the section.
3. Fit function defined in $[-1, 0]$ in the same nodes as the initial condition.
4. In case of jet transport, project the values in the section as well.

3.3.2 Stability, continuation and bifurcation detection

The eigenvalues of the Poincaré map says information about the stability of the periodic orbit and allows to perform a continuation and bifurcation detection in a similar manner as it has been done in ODE context like those explained in [IJ90].

Since a matrix-free Newton method is available, the study of the stability can be matrix-free as well. Among all the packages to compute eigenvalues of a matrix one of the most commonly used is the ARnoldi PACKage [LSY98]. It allows to solve large-scale Hermitian, non-Hermitian, standard or generalised eigenvalues problems computing a few, eigenvalues with user-specified features. Due to the compactness of the operator, only the ones with higher modulus are needed to study the stability.

At the same time it works also for bifurcation detection since, in general, a finite number of eigenvalues are needed to detect them.

3.3.3 Numerical experiments

Spatial section

The next example illustrates that the method is independent of the model if an integrator compatible with jet transport is available. In particular, it can

be applied for several delays as well. Let us consider the equation studied by [Nus78] and more recently in [KL12] where the existence of the periodic orbit has been proved for some values of the parameters.

$$\frac{dx}{dt}(t) = -\big(\lambda_1 x(t-\tau_1) + \lambda_2 x(t-\tau_2) + \lambda_3 x(t-\tau_3)\big)(1+x(t)) \tag{3.6}$$

Let us take the values $\lambda_1 = \lambda_2 = 2.5$, $\lambda_3 = 0.25$, $\tau_1 = 1.65$, $\tau_2 = 0.35$, and $\tau_3 = 1$ where the existence of a periodic orbit is guaranteed.

The initial condition u at time $t_0 = 0$ is the integration of the orbit through $\cos(t)$ at t_0 up to a final time 4. The initial condition is discretesed in a table of values $(s_i, u_i)_{i=0}^{65-1}$. The spatial section consists in fixing the last coordinate after four crosses. The Hairer integrator RETARD has been used with a relative and absolute tolerance 10^{-14}. A speed-up factor of 5.5 of the matrix-free version w.r.t. the full matrix.

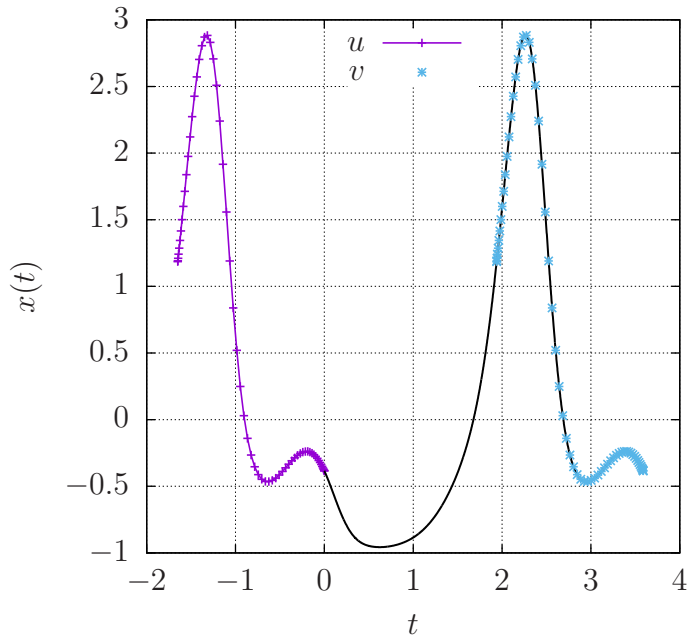

Figure 3.1. Stable periodic orbit of eq. (3.6) with $\lambda_1 = \lambda_2 = 2.5$, $\lambda_3 = 0.25$, $\tau_1 = 1.65$, $\tau_2 = 0.35$ and $\tau_3 = 1$. The final period is around 3.5894.

Spatial section and continuation

Let us consider the DDE

$$\frac{dx}{dt}(t) = -\alpha x(t-1)\frac{1+x(t-1)^2}{1+x(t-1)^4}. \tag{3.7}$$

It has an equilibrium point $x_0 = 0$. It has a Hopf bifurcation for $\alpha = \pi/2$, [LELR97]. That means that a family of periodic orbits rise nearby to that bifurcations. Since these periodic orbits have an unknown period, a temporal section is unfeasible.

Let Σ be the spacial section defined by

$$\Sigma = \{u \in C([-1,0],\mathbb{R})\colon u(-1) = 0\}$$

Taking an initial guess $u \in \Sigma$ near to the equilibrium point and with α close to $\pi/2$, let us say, $\alpha = 1.57$. The matrix-free Newton approach allows to compute a period 4 periodic orbit, Figure **3.2**, via an integrator based on a RK78F method.

Now, the standard pseudo-arc-length continuation method w.r.t. α leads to a continuation method of the initial periodic orbit previously computed. Notice that in this scheme the derivatives obtained by jet transport must be project to the section but not the part corresponding to the new equation that refers to the condition for α. Figure **3.3** shows the result of the continuation and the branch detection of several bifurcations.

Temporal section and continuation

Let us consider a periodic perturbation of period $2\pi/\tau$ of a DDE.

$$\tau\frac{dx}{dt}(t) = -\alpha x(t-1)\frac{1+x(t-1)^2}{1+x(t-1)^4} + \varepsilon(\sin(\tau t) + \cos(\tau t)). \tag{3.8}$$

It has a periodic orbit of period $2\pi/\tau$ close to $\varepsilon = 0$ and $x = 0$ which can be continuated as Figures **3.4** and **3.5** illustrate.

3.4 Quasi-periodic motions in constant delay differential equations

Let P be a smooth discrete system defined in the $\mathbb{T}^m \times C$ with C denotes the space of continuous mappings in $[-1,0]$. A quasi-periodic motion associated

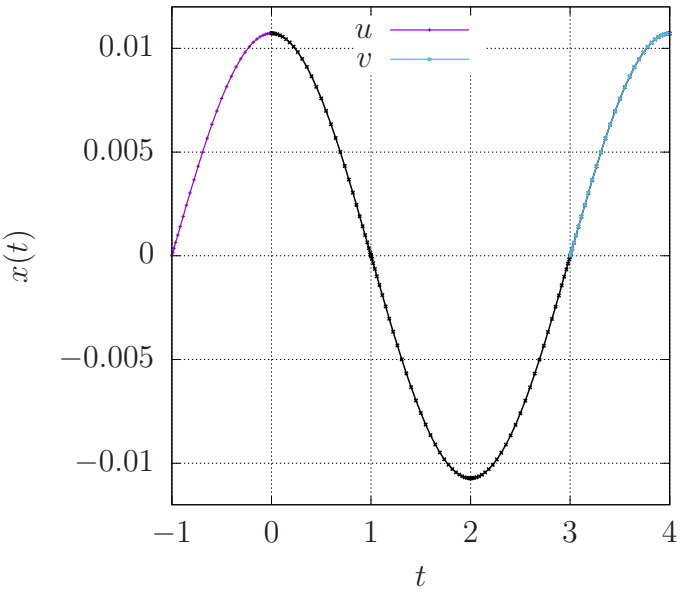

Figure 3.2. Periodic orbit close to the Hopf bifurcation ($\alpha = 1.57$) of the equilibrium $x_0 = 0$ of eq. (3.7).

to this system with a $\mathbb{Q}$-linearly independent vector ω in $\mathbb{T}^m$ is a periodic mapping $K\colon \mathbb{T}^m \to C$ verifying the invariance equation

$$P \circ K = T_\omega \circ K, \tag{3.9}$$

where T_ω is a linear operator defined in C by $T_\omega(K(\theta)) = K(\theta + \omega)$. In fact, it is a linear homeomorphism with inverse $T_{-\omega}$.

The stability of the invariant object associated to K, that is an m-dimensional torus, is given by the study of the spectrum $T_{-\omega} \circ DP \circ K$. It always has 1 as eigenvalue and if λ is an eigenvalue, then $\lambda \exp(2\pi \mathtt{i} k\omega)$ is also an eigenvalue for all $k \in \mathbb{Z}$, see [Jor01].

In the case of constant delay differential equation we are going to focus on the case $m = 1$. The discrete system P is obtained by the use of the Poincaré mapping (via temporal or spatial section). Since the Poincaré mapping for DDE is a compact mapping, its differential is clustered and the operator $T_{-\omega} \circ DP \circ K$ will also have a clustered spectrum in circles around the origin. There are three situations where the quasi-motions appears:

1. Quasi-perturbation of an equilibrium point.

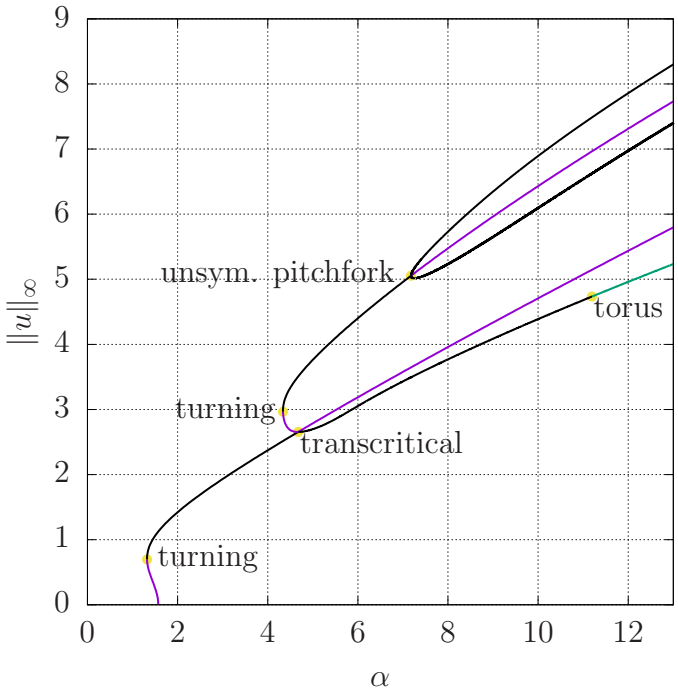

Figure 3.3. Continuation w.r.t. α of eq. (3.7).

2. Non-resonant periodic perturbation of a periodic orbit.

3. Neimark-Sacker bifurcation.

In each of the different case, slightly modifications in the methods are required. To explain each of these changes, let us start from the easiest one to the hardest.

3.4.1 Quasi-perturbation of an equilibrium point

Let us consider a smooth constant DDE like

$$\begin{aligned} \frac{dx}{dt}(t) &= f(x(t), x(t-1), \theta_1(t), \theta_2(t), \varepsilon), \\ \theta_i(t) &= \theta_i^{(0)} + \omega_i t, \qquad i = 1, 2, \end{aligned} \tag{3.10}$$

where f depends periodically on $\theta_1(t)$ and $\theta_2(t)$ for $0 < \varepsilon \ll 1$, $\theta_1^{(0)}, \theta_2^{(0)} \in [0, 2\pi)$, ω_1/ω_2 is an irrational number and it has a zero for $\varepsilon = 0$. Then by fixing the section $\theta_2^{(0)} = 0$, the return map P is defined as follows: Given

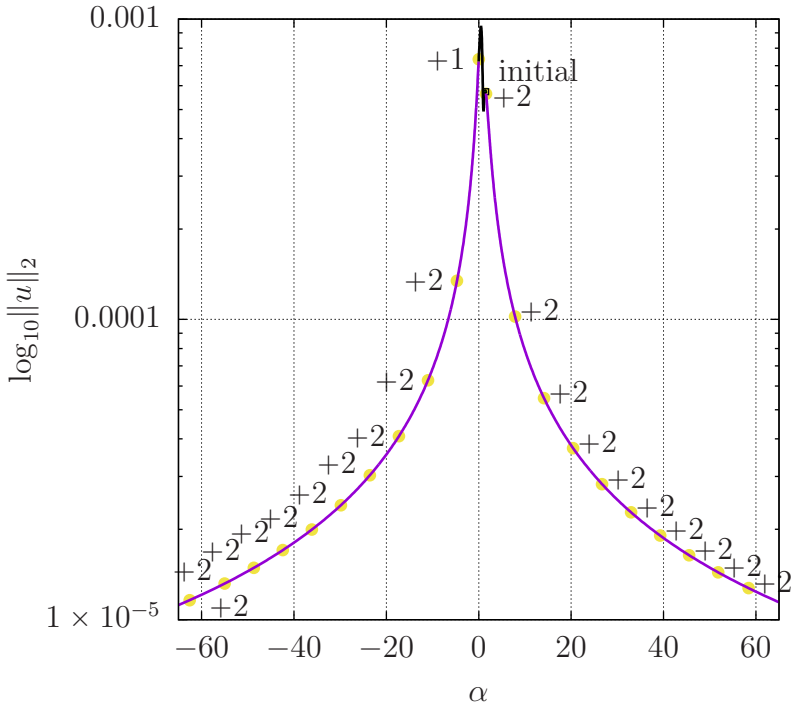

Figure 3.4. Continuation w.r.t. α in eq. (3.8).

an initial condition u defined in $[-1, 0]$ and θ in $[0, 2\pi)$ we apply the time $2\pi/\omega_2$ map over the data $(x_0, \theta_1^{(0)}, \theta_2^{(0)}) = (u, \theta, 0)$. Thus, $(v, \theta + \omega, 1)$ with $\omega = 2\pi\omega_1/\omega_2$ is obtained and we can write all the process simply by

$$\begin{aligned} \bar{x} &= P(\theta, x), \\ \bar{\theta} &= \theta + \omega. \end{aligned}$$

Matrix-free Newton approach

The function to find a zero K is

$$F(K(\theta)) = P(\theta, K(\theta)) - T_\omega(K(\theta)), \qquad \text{for all } \theta. \tag{3.11}$$

To apply the Newton method to the equation eq. (3.11) we need to decide the computer representation of the unknown to be able to operate with the differential matrix and to solve the linear system.

We are going to use the discrete Fourier transform to represent the unknown K. That is an extra layer of discretisation; the first one is for the table of values in the segment $[-1, 0]$ and the second one, for each of those values, we associate a discrete Fourier series.

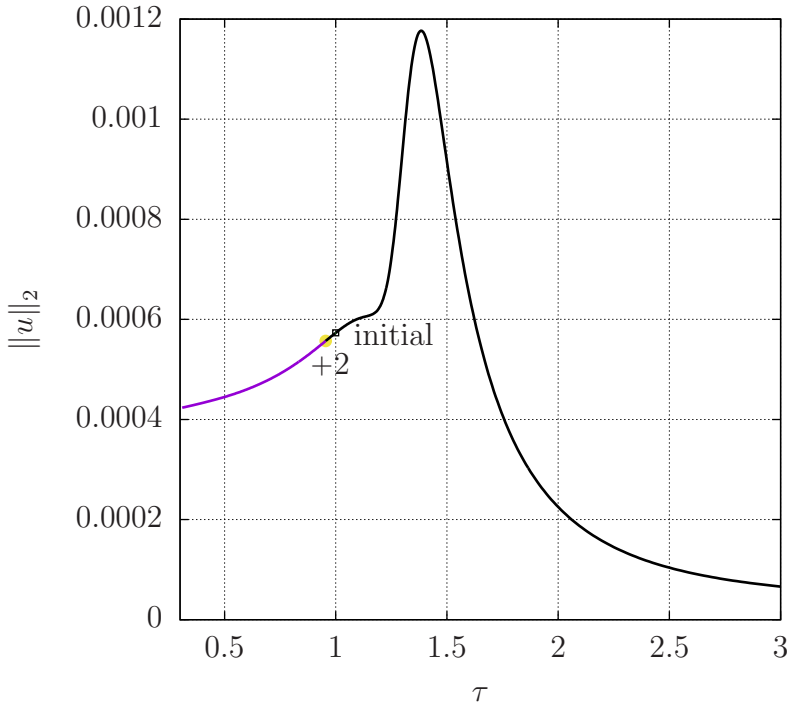

Figure 3.5. Continuation w.r.t. ε in eq. (3.8).

The use of discrete Fourier series admits two representations; one as a mesh points and the other one as Fourier coefficients. Depending on the operation to perform is better to have the object in one or the other representation. For instance, in eq. (3.11) is easier to perform the evaluation by P with K as a mesh points because, in general, the DDE is expressed in points. On the other hand, the shift by ω, that is the evaluation of T_ω, is easy to have it in Fourier coefficients.

The two different representations are just a change of basis, i.e. a linear isomorphism. The Fast Fourier Transform is a well-known algorithm to apply that linear mapping (or its inverse), with a computational complexity in $\Theta(n \log n)$. Therefore the unknowns will be either in values or in coefficients. That gives 4 versions of eq. (3.11), each of them with an equivalent solution (just changing the basis). Indeed, let us assume that P is evaluated in points, T_ω in coefficients and FFT means to take coefficients and to give its

representation in points. Then,

$$\begin{aligned} F_{p2p} &= P - \mathrm{FFT} \circ T_\omega \circ \mathrm{FFT}^{-1} && \text{(from points to points)}, \\ F_{p2c} &= \mathrm{FFT}^{-1} \circ P - T_\omega \circ \mathrm{FFT}^{-1} && \text{(from points to coeffs.)}, \\ F_{c2p} &= P \circ \mathrm{FFT} - \mathrm{FFT} \circ T_\omega && \text{(from coeffs. to points)}, \\ F_{c2c} &= \mathrm{FFT}^{-1} \circ P \circ \mathrm{FFT} - T_\omega && \text{(from coeffs. to coeffs.)}. \end{aligned} \tag{3.12}$$

Notice that their differentials are just affected by matrix multiplications, and the different versions differs in the condition number. Intuitively, the version $c2c$ may give a differential matrix with worst condition number because it involves values possibly smaller due to the decaying Fourier coefficients in smooth mappings. In any of the cases, we are able to arrive to a matrix-free Newton approach using the jet transport in P since all the other mappings involved in F are linear mappings w.r.t. the representation of the unknown K.

It is important to remark that the study of the stability must be done in the same basis, that is, the one for F_{p2p} or F_{c2c}.

Preconditioning

A discrete system like eq. (3.11) coming from a DDE has the operator $T_{-\omega} \circ DF \circ K(\theta)$ spectrum in circles centred at the origin and accumulated to it. Therefore we are going to consider the following left preconditioners to eq. (3.12) for a restarted GMRES linear iterative solver

$$\begin{aligned} M_{p2p} &= \mathrm{FFT} \circ T_\omega \circ \mathrm{FFT}^{-1}, & M_{c2p} &= \mathrm{FFT} \circ T_\omega, \\ M_{p2c} &= T_\omega \circ \mathrm{FFT}^{-1}, & M_{c2c} &= T_\omega. \end{aligned}$$

They lead respectively to

$$\begin{aligned} M_{p2p}^{-1} F_{p2p} &= \mathrm{FFT} \circ T_{-\omega} \circ \mathrm{FFT}^{-1} \circ P - I, \\ M_{p2c}^{-1} F_{p2c} &= \mathrm{FFT} \circ T_{-\omega} \circ \mathrm{FFT}^{-1} \circ P - I, \\ M_{c2p}^{-1} F_{c2p} &= T_{-\omega} \circ \mathrm{FFT}^{-1} \circ P \circ \mathrm{FFT} - I, \\ M_{c2c}^{-1} F_{c2c} &= T_{-\omega} \circ \mathrm{FFT}^{-1} \circ P \circ \mathrm{FFT} - I, \end{aligned} \tag{3.13}$$

whose differentials are the same just changing P by $D_2 P$.

3.4.2 Periodic perturbation of a periodic orbit

Let us consider the constant DDE

$$\begin{aligned} \frac{dx}{dt}(t) &= f(x(t), x(t-1), \theta_2(t), \varepsilon), \\ \theta_2(t) &= \theta_2^{(0)} + \omega_2 t, \end{aligned} \tag{3.14}$$

where f depends periodically on $\theta_2(t)$ for $0 < \varepsilon \ll 1$, $\theta_2^{(0)} \in [0, 2\pi)$, it has a (known) periodic orbit with period ω_1 for $\varepsilon = 0$ and ω_1/ω_2 is an irrational number.

Assume that the known periodic orbit for $\varepsilon = 0$ has frequency ω_1 and it has been obtained by a Poincaré mapping P_0 via a temporal or a spatial section Σ_0. To give a discrete system for the invariance equation like eq. (3.9) be distinguish two cases for $0 < \varepsilon \ll 1$.

Temporal section

In this case the discrete system is exactly like in eq. (3.10), P is given by the $2\pi/\omega_1$ integration of eq. (3.14). But the initial guess for the Newton will be the known periodic orbit for $\varepsilon = 0$ instead of the equilibrium point.

Spatial section

Now the frequency ω is also an unknown. So there is the freedom to impose an extra equation to ensure the convergence of the invariance equation eq. (3.9). That extra equation must be a constraint that it has to be able to be satisfied. We know that for $\varepsilon = 0$, $P_0 \colon \Sigma_0 \to \Sigma_0$ has a fixed point in the space of function defined in $[-1, 0]$. Then the unknowns K and ω are obtained finding a zero of the mapping

$$F(K(\theta), \omega) = \begin{bmatrix} P(\theta, K(\theta)) - T_\omega(K(\theta)) \\ g(K(\theta), \omega) \end{bmatrix} \tag{3.15}$$

where, P is defined by similarly the $2\pi/\omega_2$ integration of eq. (3.14) with $0 < \varepsilon \ll 1$. The condition for ω is given by g which can be, for instance, a condition the $K(0) \in \Sigma_0$.

The differential matrix of eq. (3.15) has the form

$$DF = \begin{bmatrix} \overbrace{\frac{\partial P}{\partial K(\theta)} - T_\omega}^{m = n_c \cdot n_d} & \overbrace{-\frac{\partial T_\omega}{\partial \omega}}^{1} \\ \frac{\partial g}{\partial K(\theta)} & \frac{\partial g}{\partial \omega} \end{bmatrix} \begin{matrix} \} m \\ \} 1 \end{matrix}$$

with n_c being the mesh size for θ and n_d being the mesh size for the interval $[-1, 0]$. Notice that by the use of jet transport in the block m-by-m is still feasible to consider a matrix-free Newton method and the preconditioning of section **3.4.1** in that sub-block will work as well.

3.4.3 Experiments

In order to quantify how good are the preconditioning of the matrix-free Newton method, let us a consider a quasi-periodic time-dependent perturbation of a constant DDE like in eq. (3.10)

$$\frac{dx}{dt}(t) = -3.6x(t-1)\frac{x(t-1)^2+1}{x(t-1)^4+1} + \frac{\varepsilon}{\sin(\theta_1)+\sin(\theta_2)+3}, \qquad \varepsilon = 10^{-2},$$
$$\frac{d\theta_1}{dt}(t) = \omega_1 = 1, \qquad \frac{d\theta_2}{dt}(t) = \omega_2 = \frac{\sqrt{5}-1}{2},$$

We use the discrete system eq. (3.11) and the 4 different expressions to find the zeros of eq. (3.12). Moreover, we want to show if the preconditioning versions eq. (3.13) give a better performance. To this end, tables **3.1** to **3.3** reports speed-factor between the preconditioning matrix-free iterative solver, and a direct solver for different number of Fourier coefficients. This means the quotient of the CPU time between the an LU solver of the linear systems and the preconditioned GMRES. Also the speed-factor between the preconditioned and the non-preconditioned solvers. In table **3.2** shows the CPU-time of the direct and preconditioned linear solvers.

		direct/precond				noprecond/precond			
nc	M	p2p	p2c	c2p	c2c	p2p	p2c	c2p	c2c
64	1088	1.22	1.08	0.94	0.92	–	–	13.19	–
128	2176	1.92	1.27	1.37	1.01	1.14	3.74	1.87	4.49
256	4352	2.12	1.45	1.47	1.08	0.96	3.20	2.00	5.15
512	4352	3.99	2.71	1.11	1.14	0.96	2.53	2.55	6.16
1024	17408	4.54	3.32	1.72	1.26	1.40	2.50	1.77	16.80

Table 3.1. Speed factor with number of Fourier coefficients nc and matrix size M.

3D visualisation

Inspired in the hyper-cycle model [GJS18] and references therein let us consider the eq. (3.16).

$$\begin{aligned}
\dot{x}(t) &= 10^{-4}z(t)y(t-1)/1 - x(t)/1 + 10^{-3}\sin(\theta_2),\\
\dot{y}(t) &= 10^{-4}x(t)z(t-1)/2 - y(t)/2 + 10^{-3}\cos(\theta_2),\\
\dot{z}(t) &= 10^{-4}y(t)x(t-1)/3 - y(t)/3 + 10^{-3}(\sin(\theta_1)+\sin(2\theta_2)),\\
\dot{\theta}_1(t) &= \omega_1 = 1, \qquad \dot{\theta}_2(t) = \omega_2 = \frac{\sqrt{5}-1}{2}.
\end{aligned} \tag{3.16}$$

		direct				precond			
nc	M	p2p	p2c	c2p	c2c	p2p	p2c	c2p	c2c
64	1088	0.31	0.32	0.36	0.36	0.31	0.20	0.39	0.25
128	2176	1.84	1.37	2.06	1.52	1.10	0.66	1.50	1.00
256	4352	7.80	5.82	8.73	6.52	4.22	2.29	5.99	3.98
512	4352	32.28	24.09	36.48	27.09	16.41	8.71	23.93	16.12
1024	17408	150.25	112.31	163.67	124.54	66.15	33.72	95.98	72.41

Table 3.2. CPU-time in minutes number of Fourier coefficients nc and matrix size M.

		direct				noprecond/precond			
nc	M	p2p	p2c	c2p	c2c	p2p	p2c	c2p	c2c
64	1088	2	2	2	2	3/3	3/2	3/3	3/2
128	2176	3	2	3	2	3/3	3/2	3/3	3/2
256	4352	3	2	3	2	3/3	3/2	3/3	3/2
512	4352	3	2	3	2	3/3	3/2	4/3	3/2
1024	17408	3	2	3	2	4/3	3/2	4/3	3/2

Table 3.3. Number of Newton iterations number of Fourier coefficients nc and matrix size M.

It has a torus nearby the equilibrium point. Once $K\colon \mathbb{T} \to C([-1,0],\mathbb{R}^3)$ has been computed imposing the invariance equation of the discrete system like eq. (3.9), we can go back to the continuous DDE and represent the invariant object T defined in $\mathbb{T}^2$. We want to represent T in a mesh, that is, $T(\theta_1^i,\theta_2^j) \in \mathbb{R}^3$ with $\theta_1^i = 2\pi i/n_1$, $0 \leqslant i < n_1$, and $\theta_2^j = 2\pi j/n_2$, $0 \leqslant j < n_2$. We have obtained $T(\theta_1^i,0) = K(\theta_1^i)(0)$. If we follow the flow t units of time, the angles θ_1, and θ_2, then we obtain $T(\theta_1^i+\omega_1 t,\omega_2 t)$. Therefore, solving the linear system for (φ,t)

$$\begin{cases} \theta_1^i + \omega_1 t = \varphi, \\ \theta_2^j = \omega_2 t. \end{cases}$$

We can get the initial condition $K(\varphi)$ and solve the IVP-DDE of eq. (3.16) integrating t units of time, and obtaining $T(\theta_1^i,\theta_2^j)$.

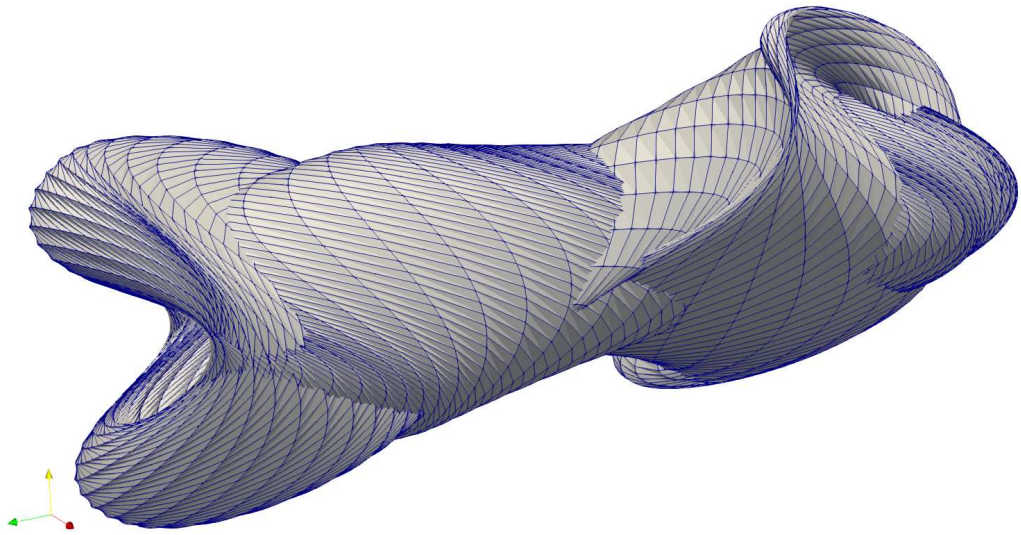

Figure 3.6. (x, y, z) torus visualisation of eq. (3.16).

Chapter 4

State-dependent perturbation of an ODE

ACK: This work is a collaboration with Ms. Jiaqi Yang and Prof. Rafael de la Llave during my stays at School of Mathematics in Georgia Institute of Technology, Atlanta GA, USA.

4.1 Introduction

We are going to consider simple models, that is planar Ordinary Differential Equations (ODEs) and we will assume the existence of a limit cycle. We are going to show that all the solutions present in the undelayed model persists when we add a state-dependent delayed perturbation.

We notice that adding that kind of perturbation, which is a very singular one, the nature of the differential equations changes; the unperturbed ODE is always finite dimensional while the perturbed one is always an infinite dimensional problem since it becomes a State-dependent Delay Differential Equation (SDDE).

Such kind of models appear in several concrete problems in natural science such as circuits, neuroscience, and population dynamics. However, we still have to look into it more carefully.

The main idea of this chapter is that we bypass the general theory of existence for solutions of the SDDE by establishing the existence of some finite dimensional families of solutions, which resemble the solutions of the original system.

Although we are not going to give details here, preliminary results show that the method explained here can be extended to higher dimensional problems with a more careful study.

4.1.1 Overview and comments on the results

In order to summarise the main results of this chapter, let us give an informal overview of the method and let us provide some useful comments.

It is known that in a neighbourhood of a limit cycle of a planar ODE, let us say $\dot{x} = X(x)$, we can find a mapping $K\colon \mathbb{T} \times [-1,1] \to \mathbb{R}^2$, a frequency $\omega_0 \neq 0$, and a speed rate λ_0 in such a way that for all θ and s, the function

$$x(t) = K(\theta + \omega_0 t, se^{\lambda_0 t}) \tag{4.1}$$

solves the ODE. The fact that All the solution of the form eq. (4.1) are solutions of the original ODE is equivalent to the solve a functional equation (also called invariance equation) for K, ω_0, and λ_0. Efficient methods to study the resulting functional equation were presented in detail in [HdlL13].

After a state-dependent perturbation of the initial planar ODE, we impose solution of the SDDE are of the form

$$x(t) = K \circ W(\theta + \omega t, se^{\lambda t}). \tag{4.2}$$

It leads to a functional equation for W, ω, and λ, which is also called invariance equation.

The goal will so be to solve such an invariance equation using techniques of functional analysis to get the unknown embedding W, the unknown new frequency ω and the unknown new speed rate λ. Initially the unknowns are expected to be close to the identity, to ω_0 and to λ_0 respectively.

The equation is rather degenerate and its treatment needs several steps. Firstly, we will express $W(\theta, s)$ as an asymptotic expansion in power of s to a finite order, and then, we will formulate a fixed point problem for the remainder. Some technical problems are going to arise, such as, the matching between the domains of definitions. Nevertheless, similar problems have appeared in the theory of centre manifolds [Car81].

The main results of the chapter is Theorem **4.12** which establish that if the perturbation is small enough and given an approximate solution of the invariance equations with some non-degeneracy conditions, then there is a true solution nearby. Sometimes this kind of Theorem formulation is referred as *a posteriori* format and it allows to provide an approximate enough solution to validate the real solution even if it has been obtained by a non-rigorous method. To this end, we are going to specify a numerical algorithm in order to compute the perturbed limit cycles and its 2D manifold.

It is important to point out that by solving the invariance equation, one actually obtains a parametrisation of the limit cycle and its isochrons (the 2D manifold of the limit cycle for the unperturbed case). In other words,

$K \circ W(\theta, 0)$ parametrises the limit cycle and for a fixed θ, $K \circ W(\theta, s)$ parametrises the manifold of the point $K \circ W(\theta, 0)$ on the limit cycle.

We remark the existence of previous related work [HVL93, chapter 10] to the persistence of limit cycles but they were studied with a different methods. They have also studied stable manifolds of periodic orbits of SDDEs, however, what they obtained is an infinite dimensional manifold, while we study the submanifold of such a infinite dimensional manifolds which corresponds to the slowest contraction rate. We did not find any reference describing the computation of that stable submanifold, whereas the unstable (and finite dimensional) manifold has been occasionally studied [GMJ17].

The notions of approximate solutions and that of solutions close to the approximate ones, requires to specify a norm in the space of functions. In works like [HdlL13], it was natural to specify analytic norms. However, we are going to use finitely differentiable functions due to the fact that we conjecture that the solutions we are producing are not more than finitely differentiable when we have a non-constant SDDE.

A rather subtle point is that we do not obtain local uniqueness of the solution. The reason is that the proof for the remainder of the invariance equation involves cutting off the perturbation and the solution may depend on the cut-off function. Both the finite regularity and the lack of uniqueness due to the introduction of cut-off functions are reminiscent to the effects found in the study of centre manifolds [Car81, Lan73].

4.2 Unperturbed case

Following the results in [HdlL13] we establish and fix the notation for the unperturbed case which is going to use later on for the SDDE case. Let so be an analytic planar ODE $\dot{x} = X(x)$ having a hyperbolic limit cycle. In other words, if $\Phi(t; x_0)$ denotes its flow of the through the initial condition x_0 in $\mathbb{R}^2$, then we are assuming that there is $K_0 \colon \mathbb{T} \to \mathbb{R}^2$, and a frequency $\omega_0 \neq 0$ such that $\Phi(t; K_0(0)) = K_0(\omega_0 t)$. Furthermore $\mathcal{K} = K_0(\mathbb{T})$ is an exponentially attracting set with speed rate λ_0, that is,

$$d(\Phi(t; y), \mathcal{K}) \leqslant Ce^{-\lambda_0 t}$$

for some $C > 0$ and y close enough to $\mathcal{K}$.

Under the previous assumptions it was proved in [HdlL13, Theorem 3.2] the existence of an analytic local diffeomorphism $K \colon \mathbb{T} \times [-1, 1] \to \mathbb{R}^2$ such that

$$(\omega_0 \partial_\theta + \lambda_0 s \partial_s) K(\theta, s) = X \circ K(\theta, s). \tag{4.3}$$

They provided an effective method to compute such frequency ω_0, speed rate λ_0, and K.

4.2.1 Numerical computation

The next Algorithm **4.1** from [HdlL13] reproduces the steps to get, by a quasi-Newton method with still a quadratic convergence, the frequency ω_0, the contraction rate λ_0 and the analytic parametrisation $K\colon \mathbb{T}\times[-1,1]\to\mathbb{R}^2$ of an arbitrary analytic planar ODE with a hyperbolic limit cycle. Since the resulting parametrisation K will be locally analytic, we can express K as a power series of the form $K(\theta,s)=\sum_j K_j(\theta)s^j$ and then look for all the coefficients in s so that the invariance equation, eq. (4.3), is satisfied.

Algorithm 4.1. Quasi-Newton method

- ⋆ `Input:` $\dot{x}=X(x)$ in $\mathbb{R}^2$, $K(\theta,s)=K_0(\theta)+K_1(\theta)b_0 s$, $\omega_0>0$, $\lambda_0\in\mathbb{R}$ and scaling factor $b_0>0$.
- ⋆ `Output:` $K(\theta,s)=\sum_{j=0}^{m-1}K_j(\theta)(b_0 s)^j$, ω_0 and λ_0 such that $\|E\|\ll 1$.

1. $E\leftarrow X\circ K-(\omega_0\partial_\theta+\lambda_0 s\partial_s)K$.
2. Solve $DK\tilde{E}=E$ and denote $\tilde{E}\equiv(\tilde{E}_1,\tilde{E}_2)$.
3. $\sigma\leftarrow\int_0^1\tilde{E}_1(\theta,0)\,d\theta$ and $\eta\leftarrow\int_0^1\partial_s\tilde{E}_2(\theta,0)\,d\theta$.
4. $E_1\leftarrow\tilde{E}_1-\sigma$ and $E_2\leftarrow\tilde{E}_2-\eta s$.
5. Solve $(\omega_0\partial_\theta+\lambda_0 s\partial_s)W_1=E_1$ imposing $\int_0^1 W_1(\theta,0)\,d\theta=0$.
6. Solve $(\omega_0\partial_\theta+\lambda_0 s\partial_s)W_2-\lambda_0 W_2=E_2$ imposing $\int_0^1\partial_s W_2(\theta,0)\,d\theta=0$.
7. $W\equiv(W_1,W_2)$.
8. Update: $K\leftarrow K+DKW$, $\omega_0\leftarrow\omega_0+\sigma$ and $\lambda_0\leftarrow\lambda_0+\eta$.
9. Iterate (1) until convergence in K, ω and λ. Then undo the scaling b_0.

Algorithm 4.1 requires some practical remarks to be pointed out:

i. Initial guess. $K_0\colon\tilde{\mathbb{T}}\to\mathbb{R}^2$ will be the periodic orbit of the ODE with frequency ω_0. It can be obtained by a Poincaré section method or any

other standard technique. An approximation for $K_1\colon \tilde{\mathbb{T}} \to \mathbb{R}^2$ and λ can be obtained when one solves the variational equation

$$DX \circ K_0(\theta)U(\theta) = \omega_0 \frac{d}{d\theta}U(\theta),$$
$$U(0) = Id_2.$$

Hence if $(e^{\lambda_0/\omega_0}, K_1(0))$ is the eigenpair of $U(1)$ such that $\lambda_0 < 0$, then $K_1(\theta) = U(\theta)K_1(0)e^{-\lambda_0\theta/\omega_0}$.

ii. Stopping criterion. As any Newton method a possible stopping could be when either $\|E\|$ or $\max\{\|DKW\|, |\sigma|, |\eta|\}$ is smaller than a given tolerance.

iii. Uniqueness. If $K(\theta, s)$ is a solution, then $K(\theta+\theta_0, b_0 s)$ is also a solution for fixed $\theta_0, b_0 \in \mathbb{R}$. The value of θ_0 can be chosen in such a way that $\sup_\theta \|K_0(\theta+\theta_0)\|$ is reached and then give $K_0(\theta+\theta_0)$ as part of the input. The value b_0 is used as a scaling factor to be sure that the mappings K_j are comparable. Heuristically a good chosen of b_0 can be done as follows: 1^{st}) Run the simulation with $b_0 = b_0^{(0)}$ the inverse of a power of the radix of the arithmetic and a not too small tolerance to get a first approximation of $K(\theta, s)$. 2^{nd}) Take $b_0 \approx 0.9 b_0^{(0)} \|K_{m-1}\|_\infty^{-1/(m-1)}$ and run it again with a smaller tolerance. Here, $\|\cdot\|_\infty$ is computed through a mesh for θ and 0.9 is a security factor.

iv. Convergence. It has been proved in [HdlL13] that even to be a quasi-Newton method, it still has quadratic convergence.

To solve the namely cohomological equations (5) and (6) in Algorithm 4.1 strongly depends on the numerical representation of periodic functions. In [HdlL13, §4.3.1] there are two results to solve them, whose integral version is not efficient from a numerical point of view but useful for theoretical purpose. For completeness, let us quote the result without proof.

PROPOSITION 4.2 (Fourier version, [HdlL13]). *Let* $E(\theta, s) = \sum_{j,k} E_{jk} e^{2\pi \mathrm{i} k\theta} s^j$.

- *If* $E_{00} = 0$, *then* $(\omega\partial_\theta + \lambda s\partial_s)u(\theta, s) = E(\theta, s)$ *has solution* $u(\theta, s) = \sum_{j,k} u_{jk} e^{2\pi \mathrm{i} k\theta} s^j$ *and*

$$u_{jk} = \begin{cases} \frac{E_{jk}}{\lambda j + 2\pi \mathrm{i}\omega k} & \text{if } (j,k) \neq (0,0) \\ \alpha & \text{otherwise.} \end{cases}$$

for all real α. *Imposing* $\int_0^1 u(\theta, 0)\, d\theta = 0$, *then* $\alpha = 0$.

- *If* $E_{10} = 0$, *then* $(\omega\partial_\theta + \lambda s\partial_s - \lambda)u(\theta, s) = E(\theta, s)$ *has solution* $u(\theta, s) = \sum_{j,k} u_{jk} e^{2\pi \mathtt{i} k\theta} s^j$ *and*

$$u_{jk} = \begin{cases} \frac{E_{jk}}{\lambda(j-1)+2\pi \mathtt{i}\omega k} & \text{if } (j,k) \neq (1,0) \\ \alpha & \text{otherwise.} \end{cases}$$

for all real α. *Imposing* $\int_0^1 \partial_s u(\theta, 0)\, d\theta = 0$, *then* $\alpha = 0$.

PROPOSITION 4.3 (Integral version, [HdlL13]). *Let* $E(\theta, s) = \sum_j E_j(\theta) s^j$ *and* $\lambda\omega < 0$.

- *If* $\int_0^1 E_0(\theta)\, d\theta = 0$, *then* $(\omega\partial_\theta + \lambda s\partial_s)u(\theta, s) = E(\theta, s)$ *has solution*

$$u(\theta, s) = \alpha + \frac{1}{\omega}\int_0^\theta E_0(\sigma)\, d\sigma - \int_0^\infty \big(E_j(\theta + \omega t, se^{\lambda t}) - E_0(\theta + \omega t)\big)\, dt$$

or, equivalently,

$$u(\theta, s) = \alpha + \frac{1}{\omega}\int_0^\theta E_0(\sigma)\, d\sigma - \frac{1}{\omega}\sum_{j\geqslant 1} \frac{s^j}{1 - e^{j\lambda/\omega}} \int_0^1 E_j(\theta + z) e^{zj\lambda/\omega}\, dz$$

for all real α. *Imposing* $\int_0^1 u(\theta, 0)\, d\theta = 0$, *then* $\alpha = \frac{1}{\omega}\int_0^1 \theta E_0(\theta)\, d\theta$. *And it is the only solution in* $C^0(\mathbb{T} \times [-1, 1])$.

- *If* $\int_0^1 E_1(\theta)\, d\theta = 0$, *then* $(\omega\partial_\theta + \lambda s\partial_s - \lambda)u(\theta, s) = E(\theta, s)$ *has solution*

$$\begin{aligned} u(\theta, s) = &\int_0^\infty e^{\lambda t} E_0(\theta - \omega t)\, dt + \left[\alpha + \frac{1}{\omega}\int_0^\theta E_1(\sigma)\, d\sigma\right] s \\ &- \int_0^\infty e^{-\lambda t}\big(E(\theta + \omega t, se^{\lambda t}) - E_0(\theta + \omega t) - se^{\lambda t} E_1(\theta + \omega t)\big)\, dt \end{aligned}$$

or, equivalently,

$$\begin{aligned} u(\theta, s) = &\frac{1}{\omega(1 - e^{\lambda/\omega})} \int_0^1 E_0(\theta - z) e^{z\lambda/\omega}\, dz + \left[\alpha + \frac{1}{\omega}\int_0^\theta E_1(\sigma)\, d\sigma\right] s \\ &- \frac{1}{\omega}\sum_{j\geqslant 2} \frac{s^j}{1 - e^{(j-1)\lambda/\omega}} \int_0^1 E_j(\theta + z) e^{z(j-1)\lambda/\omega}\, dz \end{aligned}$$

for all real α. *Imposing* $\int_0^1 \partial_s u(\theta, 0)\, d\theta = 0$, *then* $\alpha = \frac{1}{\omega}\int_0^1 \theta E_1(\theta)\, d\theta$. *And it is the only solution in* $C^2(\mathbb{T} \times [-1, 1])$.

The solution of the linear system in item **2** of Algorithm **4.1** can be done by power matching.

LEMMA 4.4. *Let $A(\theta, s)x(\theta, s) = b(\theta, s)$ be a linear system. Assume that it is equivalent to*

$$\left(\sum_{k\geqslant 0} A_k(\theta)s^k\right)\sum_{k\geqslant 0}\boldsymbol{x}_k(\theta)s^k = \sum_{k\geqslant 0}\boldsymbol{b}_k(\theta)s^k.$$

Then $\boldsymbol{x}_k(\theta)$ is obtained recurrently by solving the linear system

$$A_0(\theta)\boldsymbol{x}_k(\theta) = \boldsymbol{b}_k(\theta) - \sum_{j=1}^{k} A_j(\theta)\boldsymbol{x}_{k-j}(\theta).$$

4.3 Formulation of the perturbed problem

Let us consider a planar SDDE like

$$\dot{x}(t) = X(x(t), \varepsilon\widetilde{x}(t)), \qquad \widetilde{x}(t) \coloneqq x(t - r(x(t))), \tag{4.4}$$

where X is analytic, $x(t)$ is in $\mathbb{R}$, $0 \leqslant \varepsilon \ll 1$, and r is real-valued, positive, and analytic mapping called delay map.

Formally, eq. (4.4) is a state-dependent perturbation of the ODE for $\varepsilon = 0$. Thus, it can be rewritten like

$$\dot{x}(t) = X(x(t), 0) + \varepsilon P(x(t), \widetilde{x}(t), \varepsilon). \tag{4.5}$$

where, by definition, $\varepsilon P(x, \widetilde{x}, \varepsilon) = X(x, \varepsilon\widetilde{x}) - X(x, 0)$.

Let us assume that the ODE, the one for $\varepsilon = 0$, has a hyperbolic limit cycle in the finite dimensional phase space. We want to find the 2D family of solutions of eq. (4.4) which resembles the 2D dimensional family of the ODE. More concretely, we are going to provide the slowest invariant manifold.

Note that this is a much simpler problem than developing a general theory of existence and solutions of SDDE, which is a rather difficult problem. Although we are facing a very singular perturbation.

4.3.1 Limit cycle and its isochrons

Under the assumption that for $\varepsilon = 0$, the ODE eq. (4.5) has a stable limit cycle. There will so be a stable manifold for such a limit cycle. Moreover, in a neighbourhood of the limit cycle, points have asymptotic phases. Thus, points sharing the same asymptotic phase as p on the limit cycle gives the stable manifold for the point p. Therefore, the stable manifold of the limit cycle is foliated by the stable manifolds for points on the limit cycle, which is sometimes referred as stable foliations.

In other fields [Guc75], such a stable manifold for points on the limit cycle are called isochrons. In order to distinguish from the infinite dimensional stable manifolds in [HVL93], we are going to use the term isochrons.

As we have already discussed, there is a local parametrisation (K, ω_0, λ_0), for $\varepsilon = 0$ in eq. (4.5), which can be computed by Algorithm **4.1**. It verifies the invariance equation eq. (4.3). In particular, K is periodic in θ, i.e. $K(\theta + 1, s) = K(\theta, s)$. Thus if $\widetilde{\mathbb{T}}$ denotes the universal cover of $\mathbb{T} \cong [0, 1)$, we can extend K and rename it again as $K\colon \widetilde{\mathbb{T}} \times [-1, 1] \to \mathbb{R}^2$. It also verifies that fixed $(\theta, s) \in \widetilde{\mathbb{T}} \times [-1, 1]$, eq. (4.2) is a solution of the ODE.

For a geometric point of view, K can be interpreted as a change of coordinates, under which the original vector fields is equivalent to the vector field given by $(\omega_0, \lambda_0 s)$ in the space $\widetilde{\mathbb{T}} \times [-1, 1]$. Hence, we could have started with this vector field and then added some perturbation to it. Hence eq. (4.5) can be seen as

$$\begin{pmatrix} \xi \\ \eta \end{pmatrix}' = \begin{pmatrix} \omega_0 \\ \lambda_0 \eta \end{pmatrix} + \varepsilon Q((\xi, \eta), \widetilde{(\xi, \eta)}, \varepsilon).$$

However, for a numerical implementation we need to keep the change of coordinates given by the local diffeomorphism K so we will keep the model eq. (4.5).

In order to show if the limit cycle and its isochrons persist when $0 < \varepsilon \ll 1$, we look for a parametrisation of eq. (4.5) using the knowledge when $\varepsilon = 0$. More precisely, we look for a new frequency $\omega \neq 0$, close to ω_0, a new speed rate $\lambda < 0$, close to λ_0, and an embedding W which is a mapping from a subset of $\widetilde{\mathbb{T}} \times \mathbb{R}$ to a subset of $\widetilde{\mathbb{T}} \times \mathbb{R}$ such that eq. (4.2) is now a solution of eq. (4.5). Hence $K \circ W(\theta, s)$ gives us a parametrisation of the limit cycle as well as of the stable foliations in a neighbourhood of the limit cycle. The embedding W must verify a periodicity condition

$$W(\theta + 1, s) = W(\theta, s) + \left(\begin{smallmatrix} 1 \\ 0 \end{smallmatrix}\right), \tag{4.6}$$

and it must be define in a subset of $\widetilde{\mathbb{T}} \times \mathbb{R}$ so that its composition with K is always well-defined.

4.4 The well-defined invariance equation

Let us substitute the potential solution eq. (4.2) into eq. (4.5), let us take $t = 0$, and let us use the fact that DK is invertible. Then eq. (4.2) is a solution if, and only if, W, ω, and λ satisfy

$$(\omega \partial_\theta + \lambda s \partial_s) W(\theta, s) = \begin{pmatrix} \omega_0 \\ \lambda_0 W_2(\theta, s) \end{pmatrix} + \varepsilon Y(W(\theta, s), \widetilde{W}(\theta, s), \varepsilon). \tag{4.7}$$

Where $W_2(\theta, s)$ denotes the second component of $W(\theta, s)$, $\widetilde{W}$ is the term affected by the delay whose expression is

$$\widetilde{W}(\theta, s) = W(\theta - \omega r \circ K \circ W(\theta, s), se^{-\lambda r \circ K \circ W(\theta, s)}), \tag{4.8}$$

and

$$Y(W(\theta, s), \widetilde{W}(\theta, s), \varepsilon) = (DK \circ W(\theta, s))^{-1} P(K \circ W(\theta, s), K \circ \widetilde{W}(\theta, s), \varepsilon).$$

Notice that eq. (4.7) assumes (K, ω_0, λ_0) to be known and only (W, ω, λ) are unknowns.

In order to match the domain of W with the composition by K, it cannot be defined on $\widetilde{\mathbb{T}} \times [-1, 1]$ (or an arbitrary interval like $[-a, a]$ due to the scaling factor b_0). Indeed, the second component of $\widetilde{W}$ leads to

$$|se^{-\lambda r \circ K \circ W(\theta, s)}| > |s|$$

because λ is supposed to be close to $\lambda_0 < 0$ and $r(x)$ only gives positive values for all x. Therefore, W, and consequently $\widetilde{W}$, cannot have s belonging to a finite interval. To figure it out s must be defined on the whole real line. That is, we look for the function $W \colon \widetilde{\mathbb{T}} \times \mathbb{R} \to \widetilde{\mathbb{T}} \times \mathbb{R}$.

The collateral downside of s being in the whole real line is that now eq. (4.7) may not always be well-defined. Similar drawbacks arises in the study of centre manifolds [Car81]. It needs a special care, and thanks to the discussions with R. de la Llave and J. Yang, we decided to use cut-off functions which allows to consider extensions of functions.

Let us consider, momentously, a well-defined invariance equation (by extensions) similar to eq. (4.7).

$$(\omega \partial_\theta + \lambda s \partial_s) W(\theta, s) = \begin{pmatrix} \omega_0 \\ \lambda_0 W_2(\theta, s) \end{pmatrix} + \varepsilon \overline{Y}(W(\theta, s), \widetilde{W}(\theta, s), \varepsilon). \tag{4.9}$$

where now $\overline{Y}$ is defined on $(\widetilde{\mathbb{T}} \times \mathbb{R})^2 \times \mathbb{R}_+$ into $\mathbb{R}^2$ and $\widetilde{W}$ defined in eq. (4.8) is now renamed by

$$\widetilde{W}(\theta, s) = W(\theta - \omega \overline{r \circ K} \circ W(\theta, s), se^{-\lambda \overline{r \circ K} \circ W(\theta, s)}), \tag{4.10}$$

where $\overline{r \circ K}$ is defined on $\widetilde{\mathbb{T}} \times \mathbb{R}$ into $\mathbb{R}_+$.

The use of the cut-off functions leads to a dependency of the unknowns (W, ω, λ) to such a cut-off. However, we are going to see that W has the same asymptotic expansion in s. On the other hand, these cut-off functions will not be needed to use for a numerical simulations, as we are going to point out later.

4.4.1 Extensions of functions

Following the standard practise in theory of centre manifolds for ODEs [Car81]. Let us detail the extensions in eqs. (4.9) and (4.10).

- For $r \circ K$ defined on $\widetilde{\mathbb{T}} \times [-1,1]$ into $\mathbb{R}_+$, we define the mapping $\overline{r \circ K}$ on $\widetilde{\mathbb{T}} \times \mathbb{R}$ which agrees with $r \circ K$ on $\widetilde{\mathbb{T}} \times [-\frac{1}{2}, \frac{1}{2}]$, and is zero outside of $\widetilde{\mathbb{T}} \times [-1,1]$.

- Similarly, for Y defined on $(\widetilde{\mathbb{T}} \times [-1,1])^2 \times \mathbb{R}_+$, we define $\overline{Y}$ on $(\widetilde{\mathbb{T}} \times \mathbb{R})^2 \times \mathbb{R}_+$ which match with Y on $(\widetilde{\mathbb{T}} \times [-\frac{1}{2}, \frac{1}{2}])^2 \times \mathbb{R}_+$, and is zero outside $(\widetilde{\mathbb{T}} \times [-1,1])^2 \times \mathbb{R}_+$.

More precisely, let $\phi \colon \mathbb{R} \to [0,1]$ be a C^∞ cut-off function defined by

$$\phi(x) = \begin{cases} 1 & \text{if } |x| \leqslant \frac{1}{2}, \\ 0 & \text{if } |x| > 1. \end{cases} \tag{4.11}$$

Then

$$\overline{r \circ K}(\theta, s) = r \circ K(\theta, s)\phi(s),$$

and

$$\overline{Y}(W(\theta,s), \widetilde{W}(\theta,s), \varepsilon) = Y(W(\theta,s), \widetilde{W}(\theta,s), \varepsilon)\phi(W_2(\theta,s))\phi(\widetilde{W}_2(\theta,s)).$$

4.4.2 Finite system of invariance equations

To study the solution of the invariance equation eq. (4.9), let us consider the unknown W admits a formal form like

$$W(\theta, s) = W^0(\theta) + W^1(\theta)s + \sum_{j=2}^{n-1} W^j(\theta)s^j + W^>(\theta, s). \tag{4.12}$$

Where $W^j \colon \widetilde{\mathbb{T}} \to \widetilde{\mathbb{T}} \times \mathbb{R}$ for $0 \leqslant j < n$, and $W^> \colon \widetilde{\mathbb{T}} \times \mathbb{R} \to \widetilde{\mathbb{T}} \times \mathbb{R}$. Then by power matching in eq. (4.9) we obtain a finite sequence of invariance equations. Due to the fact that ω and λ are also unknowns we have the freedom to impose some extra conditions. These conditions will be a periodicity condition to fix ω and a normalisation to fix λ. The former will be imposed at the same time W^0 is being computed and the latter with W^1. Inductively, W^j can be obtained and finally $W^>$ will require a special attention since it has (θ, s) instead of only θ and the cut-off will play an important role.

At this point, we can point out that eq. (4.6) leads to

$$\begin{aligned} W^0(\theta+1) &= W^0(\theta) + \left(\begin{smallmatrix}1\\0\end{smallmatrix}\right), \\ W^j(\theta+1) &= W^j(\theta), \qquad\qquad 1 \leqslant j < n, \\ W^{>}(\theta,s) &= W^{>}(\theta,s). \end{aligned} \tag{4.13}$$

which justify the use fact that W^0 needs to be treated separately. However, it is not a problem for $\overline{Y}$ in eq. (4.9). Indeed, for all θ and s,

$$\begin{aligned} \overline{Y}(W(\theta,s) + \left(\begin{smallmatrix}1\\0\end{smallmatrix}\right), \widetilde{W}(\theta,s), \varepsilon) &= \overline{Y}(W(\theta,s), \widetilde{W}(\theta,s) + \left(\begin{smallmatrix}1\\0\end{smallmatrix}\right), \varepsilon) \\ &= \overline{Y}(W(\theta,s), \widetilde{W}(\theta,s), \varepsilon). \end{aligned}$$

0th invariance equation and the periodicity condition

Solving the next nonlinear invariance equation eq. (4.14) gives a condition for W^0,

$$\left[\omega\partial_\theta - \begin{pmatrix} 0 & 0 \\ 0 & \lambda_0 \end{pmatrix}\right] W^0(\theta) = \begin{pmatrix} \omega_0 \\ 0 \end{pmatrix} + \varepsilon\overline{Y}(W^0(\theta), \widetilde{W}^0(\theta;\omega), \varepsilon), \tag{4.14}$$

where

$$\widetilde{W}^0(\theta;\omega) = W^0(\theta - \omega\overline{r \circ K} \circ W^0(\theta)).$$

On the other hand, the periodicity condition of $W(\theta, s)$ in eq. (4.13) leads to a condition for other unknown ω. Concretely, because of Proposition **4.3**,

$$\omega = \omega_0 + \varepsilon \int_0^1 \overline{Y}_1(W^0(\theta), \widetilde{W}^0(\theta;\omega), \varepsilon)\, d\theta. \tag{4.15}$$

1st invariance equation and the normalisation

At this step W^1 and λ want to be obtained. The invariance equation is now a relative eigenvector problem.

$$\left[\omega\partial_\theta + \begin{pmatrix} \lambda & 0 \\ 0 & \lambda - \lambda_0 \end{pmatrix}\right] W^1(\theta) = \varepsilon\overline{Y}^1(\theta, \lambda, W^1, \varepsilon), \tag{4.16}$$

where $\overline{Y}^1(\theta, \lambda, W^1, \varepsilon)$ is the coefficient of s in $\overline{Y}$ and it is linear in the unknown W^1. That is,

$$\overline{Y}^1(\theta, \lambda, W^1, \varepsilon) = A(\theta)W^1(\theta) + B(\theta;\lambda)\widetilde{W}^1(\theta), \tag{4.17}$$

where

$$\begin{aligned} A(\theta) &= -\omega D_2\overline{Y}(W^0(\theta),\widetilde{W}^0(\theta),\varepsilon)D\widetilde{W}^0(\theta)D(\overline{r\circ K})\circ W^0(\theta) \\ &\quad + D_1\overline{Y}(W^0(\theta),\widetilde{W}^0(\theta),\varepsilon), \\ B(\theta;\lambda) &= e^{-\lambda\overline{r\circ K}\circ W^0(\theta)}D_2\overline{Y}(W^0(\theta),\widetilde{W}^0(\theta),\varepsilon), \\ \widetilde{W}^1(\theta) &= W^1(\theta-\omega\overline{r\circ K}\circ W^0(\theta)). \end{aligned} \tag{4.18}$$

Among all the possible conditions for λ, we want that one that is close enough to λ_0 but $\lambda \neq \lambda_0$.

$$\int_0^1 W_2^1(\theta)\,d\theta = \rho, \qquad \rho \neq 0. \tag{4.19}$$

Due to the scaling factor for W, we can always choose $\rho = 1$.

jth invariance equation, the inductive step

If now $2 \leqslant j < n$, the only unknown is W^j and its invariance equation is

$$\left[\omega\partial_\theta + \begin{pmatrix} \lambda j & 0 \\ 0 & \lambda j - \lambda_0 \end{pmatrix}\right] W^j(\theta) = \varepsilon\overline{Y}^j(\theta, W^0, W^j, \varepsilon) + R^j(\theta;\lambda), \tag{4.20}$$

where R^j is a function of θ which depends only on W^0, $W^1,\ldots,W^{j-1}$, and $\overline{Y}^j(\theta, W^0, W^j, \varepsilon)$ is the coefficient of s^j in $\overline{Y}$ which is linear in W^j. That is,

$$\overline{Y}^j(\theta, W^0, W^j, \varepsilon) = A(\theta)W^j(\theta), \tag{4.21}$$

where $A(\theta)$ is given in eq. (4.18).

Remainder invariance equation and the extensions

To get the invariance equation for the unknown $W^>(\theta, s)$ in eq. (4.12), we are going to use a cut-off function. That is, the invariance equation is

$$\left[\omega\partial_\theta + \begin{pmatrix} \lambda s & 0 \\ 0 & \lambda s - \lambda_0 \end{pmatrix}\right] W^>(\theta, s) = \varepsilon\overline{Y}^>(W^>, \theta, s, \varepsilon), \tag{4.22}$$

where $\overline{Y}^>$ extends a function $Y^>$ which is defined like

$$\begin{aligned} \overline{Y}^>(W^>,\theta,s,\varepsilon) &= Y^>(W^>,\theta,s,\varepsilon)\phi(s), \\ Y^>(W^>,\theta,s,\varepsilon) &= \overline{Y}(W(\theta,s),\widetilde{W}(\theta,s),\varepsilon) - \sum_{i=0}^{n-1}\overline{Y}^i(\theta)s^i, \\ \overline{Y}^i(\theta) &= \frac{1}{i!}\frac{\partial^i}{\partial s^i}(\overline{Y}(W(\theta,s),\widetilde{W}(\theta,s),\varepsilon))|_{s=0}, \end{aligned} \tag{4.23}$$

with ϕ being a cut-off like in eq. (4.11).

4.4.3 The need of the extensions for finite orders

Let us emphasise that to find the low order terms, $W^0, \ldots, W^j$, the extensions were not needed if ε is chosen to be small enough. Indeed we take the initial guess for zero order term as $W^{0,0}(\theta) = \binom{\theta}{0}$, the error for this initial guess is of order ε. Then by Theorem **4.11**, the true solution W^0 is within a distance of order ε from $W^{0,0}(\theta)$. Therefore, we can assume that $\sup_{\theta\in\widetilde{\mathbb{T}}} |W_2^0(\theta)| < \frac{1}{2}$, by taking ε small enough.

Recall the invariance equation for W^0, eq. (4.14), with above assumption, we are reduced to the case without extension, since

$$\begin{aligned}
&\overline{r \circ K}(W^0(\theta)) = r \circ K(W^0(\theta)),\\
&\overline{Y}(W^0(\theta), \widetilde{W}^0(\theta;\omega), \varepsilon) = Y(W^0(\theta), \widetilde{W}^0(\theta;\omega), \varepsilon).
\end{aligned}$$

where,

$$\widetilde{W}^0(\theta;\omega) = W^0(\theta - \omega r \circ K(W^0(\theta))).$$

Then we can rewrite eq. (4.14) as:

$$\left[\omega\partial_\theta - \begin{pmatrix} 0 & 0 \\ 0 & \lambda_0 \end{pmatrix}\right] W^0(\theta) = \begin{pmatrix} \omega_0 \\ 0 \end{pmatrix} + \varepsilon Y(W^0(\theta), \widetilde{W}^0(\theta;\omega), \varepsilon). \tag{4.24}$$

Similar argument will work for the equations for W^1 and W^j's if we look at expressions of $\overline{Y}^1$ in eq. (4.17), $\overline{Y}^j$ in eq. (4.21), and form of R^j.

4.5 The strategy

The formulation of a system of invariance equations in section **4.4.2** allows to obtain recurrently the expression of $W(\theta, s)$ in eq. (4.12) and also the frequency ω fixed by the periodicity condition in eq. (4.15) and the speed rate λ which is fixed by a normalisation like eq. (4.19) among all the other possible λ choices.

We have then all the ingredients to provide a proof of the existence and uniqueness of $W(\theta, s)$ of the form eq. (4.12) so that eq. (4.2) will give a parametrisation of the slowest manifold of the limit cycle for the SDDE in eq. (4.5). Moreover, we can also specify the steps for a numerical computation.

Firstly, we are going to address the specifications for the numerical computation via Algorithms **4.5** and **4.6** as well as the difficulties therein. We advance that the main problem will be the computation of $\widetilde{W}$, its composition with K and the getting, via jet transport, of the right hand side of

eq. (4.16) and (4.20). In particular, for the numerical simulation we can avoid to consider the remainder invariance equation, eq. (4.22), as well as the extensions.

Finally, the formal proofs are going to be detailed in section **4.7**. Basically, we will see that we can always choose ε in eq. (4.5) small enough such that all the invariance equations in section **4.4.2** can be expressed as a contractive mapping. Thus, it justifies the fixed-point approach in Algorithms **4.5** and **4.6**.

4.6 Numerical computation – perturbed case

We compute all the coefficients in s of the truncated expression $W(\theta, s)$ order by order. The zero and first orders require a special attention due to the fact that the values ω and λ are obtained in respectively in s^0 and s^1. The condition that allows to obtain ω comes from the periodicity condition eq. (4.15). However, the periodicity condition tells us that W^0 will not be a periodic function. It can be figured out if one define the periodic mapping $\hat{W}^0(\theta) \coloneqq W^0(\theta) - \left(\begin{smallmatrix}\theta\\0\end{smallmatrix}\right)$. The condition for λ is given by the normalisation condition eq. (4.19). As in the unperturbed case, we are allowed to use a scaling factor. Because of that the value of ρ can be taken equal to 1.

Algorithm **4.5** sketches the fixed-point procedure to get W^0 and ω. In this case the initial condition will be ω_0 (the value for $\varepsilon = 0$) for ω and $\left(\begin{smallmatrix}\theta\\0\end{smallmatrix}\right)$ for $W^0(\theta)$ since $W(\theta, s)$ is closed to the identity.

Algorithm 4.5 (s^0 case). Let $\widetilde{W^0}(\theta) \coloneqq W^0\big(\theta - \omega r \circ K(W^0(\theta))\big)$.

- ⋆ `Input:` $\dot{x} = X(x) + \varepsilon P(x, \tilde{x}, \varepsilon)$, $0 < \varepsilon \ll 1$, $K(\theta, s) = \sum_{j=0}^{m-1} K_j(\theta)(b_0 s)^j$, $b_0 > 0$, $\omega_0 > 0$, and $\lambda_0 < 0$.
- ⋆ `Output:` $\hat{W}^0 \colon \mathbb{T} \to \mathbb{R}^2$ and $\omega > 0$.

1. $\hat{W}^0(\theta) \leftarrow 0$ and $\omega \leftarrow \omega_0$.
2. $W^0(\theta) \leftarrow \begin{pmatrix}\theta\\0\end{pmatrix} + \hat{W}^0(\theta)$.
3. Solve $DK \circ W^0(\theta)\eta(\theta) = \varepsilon P(K \circ W^0(\theta), K \circ \widetilde{W^0}(\theta), \varepsilon)$. Let $\eta \equiv (\eta_1, \eta_2)$.
4. $\alpha \leftarrow \int_0^1 \eta_1(\theta)\, d\theta$ and $\omega \leftarrow \omega_0 + \alpha$.
5. Solve $\omega \partial_\theta \hat{W}_1^0(\theta) = \eta_1(\theta) - \alpha$ imposing $\int_0^1 \hat{W}_1^0(\theta)\, d\theta = 0$.

6. Solve $(\omega\partial_\theta - \lambda_0)\hat{W}_2^0(\theta) = \eta_2(\theta)$.

7. Iterate item **2** until convergence in W^0 and ω.

Assuming that we have obtained the W^0 and the ω, we are able to compute the higher orders whenever ε was small enough to ensure the contraction. Algorithm **4.6** sketches the steps to compute (W^1, λ) and W^n for $n \geqslant 2$. The initial guesses are λ_0 for λ, $\binom{0}{1}$ for W^1 and $\binom{0}{0}$ for W^n. In both cases it is required to solve a linear system of the form of the Lemma **4.4** as well as similar cohomological equation like in the unperturbed case.

ALGORITHM 4.6 (s^1 case and s^n case with $n \geqslant 2$).
Let $\widetilde{W}(\theta, s) \coloneqq W\big(\theta - \omega r \circ K(W(\theta, s)), se^{-\lambda r \circ K(W(\theta,s))}\big)$.

- ⋆ `Input:` $\dot{x} = X(x) + \varepsilon P(x, \widetilde{x}, \varepsilon)$, $0 < \varepsilon \ll 1$, $K(\theta, s) = \sum_{j=0}^{m-1} K_j(\theta)(b_0 s)^j$, $b_0 > 0$, $\omega_0 > 0$, $\lambda_0 < 0$, $W(\theta, s) = \sum_{j=0}^{n-1} W^j(\theta)(bs)^j$, $b > 0$, and $\omega > 0$.
- ⋆ `Output:` either $W^1 \colon \mathbb{T} \to \mathbb{R}^2$ and $\lambda < 0$ or $W^n \colon \mathbb{T} \to \mathbb{R}^2$.

1. $W^n(\theta) \leftarrow 0$.

s^1 If $n = 1$, $W^1(\theta) \leftarrow (0, 1)$ and $\lambda \leftarrow \lambda_0$.

2. $W(\theta, s) \leftarrow \begin{pmatrix}\theta \\ 0\end{pmatrix} + \hat{W}^0(\theta) + \sum_{j=1}^{n} W^j(\theta)(bs)^j$.

3. $Y(W(\theta, s)) \leftarrow DK \circ W(\theta, s)^{-1} P(K \circ W(\theta, s), K \circ \widetilde{W}(\theta, s), \varepsilon)$.

4. $\eta(\theta) \leftarrow \varepsilon \frac{\partial^n Y}{\partial s^n}(W(\theta, s))_{|s=0}$. Let $\eta \equiv (\eta_1, \eta_2)$.

s^1 If $n = 1$, then $\lambda \leftarrow \lambda_0 + \int_0^1 \eta_2(\theta)\, d\theta$.

5. Solve $(\omega\partial_\theta + n\lambda)W_1^n(\theta) = \eta_1(\theta)$.

6. Solve $(\omega\partial_\theta + n\lambda - \lambda_0)W_2^n(\theta) = \eta_2(\theta)$.

7. Iterate item **2** until convergence. Then undo the scaling b.

Both Algorithms **4.5** and **4.6** need explanations about different nontrivial parts, such as, the effective computation of $\widetilde{W}$, the numerical composition of K with W, and also with $\widetilde{W}$, the effective computation of the step in item **4** in Algorithm **4.6**, the stopping criterion and the choice of the scaling factor. On the other hand, there are steps that we can use the same methods in the unperturbed case, such as, the solution of linear systems like item **3** in Algorithm **4.6** or the solution of the cohomological equations.

4.6.1 Stopping criterion

Algorithms **4.5** and **4.6** require to stop the iterations until their convergences have been reached. Since we are in a fixed-point scheme, namely $x_{l+1} = \phi(x_l)$ with ϕ having a contraction rate $0 < q < 1$. Let us define

$$q_l \coloneqq \frac{\|x_{l+1} - x_l\|}{\|x_l - x_{l-1}\|}, \qquad l \geqslant 2.$$

Clearly $q_l \to q$ as $l \to \infty$. Thus, if $q_l > 0.5$, we stop when $\|x_l - x_{l-1}\| < \epsilon$. Otherwise, $\frac{q_l}{1-q_l}\|x_l - x_{l-1}\| < \epsilon$.

4.6.2 Scaling factor

As in the unperturbed case if $W(\theta, s)$ is a solution, then $W(\theta + \theta_0, bs)$ will be a solution too. A difference from $\varepsilon = 0$ case is that now $K \circ W$ and $K \circ \widetilde{W}$ are required to be well-defined. That means the second component of W and $\widetilde{W}$ must lie in $[-1, 1]$ in norm. Stronger conditions are

$$\sum_{j\geqslant 0} \|W_2^j(\theta)\||s|^j \leqslant 1, \qquad \text{and} \qquad \sum_{j\geqslant 0} \|\widetilde{W_2^j}(\theta)\||s|^j \leqslant 1.$$

In the iterative scheme of Algorithm **4.6**, these series become finite sums and a condition for the value $b > 0$ is led by the upper-bound $\min\{s^*, \widetilde{s}^*\}$ where s^* is the value so that $p(s) = 1$ with $p(s)$ the polynomial in s with positive coefficients given by $\|W_2^j(\theta)\|$. And similarly for $\widetilde{s}^*$ with $\|\widetilde{W_2^j}(\theta)\|$. Notice that if s^0 has been computed, the solution of s^* and $\widetilde{s}^*$ exist because $\|W_2^0(\theta)\| < 1$, $\|\widetilde{W_2^0}(\theta)\| < 1$ and the polynomials are strictly positive for $s \geqslant 0$.

4.6.3 Numerical composition of periodic maps

One of the hardest part of Algorithms **4.5** and **4.6** are the compositions between K with W and with $\widetilde{W}$. Due to the step item **4** of the Algorithm **4.6** the composition should be done so that the output is still a polynomial in s. To this end, we suggest to use an Automatic Differentiation (AD) approach [HCF+16, GW08]. If $W \equiv (W_1, W_2)$ are the components in $\mathbb{R}^2$, then

$$K \circ W(\theta, s) = \sum_{j=0}^{m-1} K_j(W_1(\theta, s))\big(b_0 W_2(\theta, s)\big)^j. \tag{4.25}$$

It can be evaluated with $m - 1$ polynomial products and $m - 1$ polynomial sums. The hard part is to compute $K_j \circ W_1(\theta, s)$, in fact $K_j(\theta + \hat{W}_1(\theta, s))$.

That is, fixed θ the problem is reduced to compute the composition of a periodic mapping K_j with a polynomial in s of order $0 \leqslant k \leqslant n$. We are going to see that such a composition can be done with a complexity $\Theta(k^4)$. Hence, for a fixed θ, the computational complexity to compute eq. (4.25) will be $\Theta(mk^4)$.

Let $K(\theta)$ be an arbitrary function and let $q(s) = \sum_{j=0}^{k} q_j s^j$ be polynomial of a fixed order $k \geqslant 0$. We want to compute the polynomial $p \coloneqq K \circ q$ up to order k. Assume that we are able to compute $g(q_0)$ with a bounded computational cost for a finite collection function g of the same type of K. The chain rule gives us a procedure to compute the coefficients of $p(s)$. Indeed, one can build a table like Table **4.1** following the generation rule in Figure **4.1**. That is, given (as input) the first row, the first column and the entry $a_{22} \coloneqq \frac{d}{ds}q(s)$. The entries a_{ij} with $2 \leqslant j \leqslant i \leqslant k+1$ are given by

$$a_{ij} = \frac{1}{j}\big(\frac{d}{ds}(a_{i-1,j})_{|s=0} + \frac{d}{ds}q(0)a_{i-1,j-1}\big). \tag{4.26}$$

Then the coefficients of $p(s)$ are $p_j = \sum_{l=0}^{k} a_{jl}\frac{d^l}{d\theta^l}K(q_0)$ for $0 \leqslant j \leqslant k$.

	$K(q_0)$	$\frac{d}{d\theta}K(q_0)$	$\frac{d^2}{d\theta^2}K(q_0)$	$\cdots$	$\frac{d^{k-1}}{d\theta^{k-1}}K(q_0)$	$\frac{d^k}{d\theta^k}K(q_0)$
p_0	1	0				
p_1	0	$\frac{d}{ds}q(s)$	0			
p_2	0	$\frac{1}{2}\square$	$\frac{1}{2}\square$			
$\vdots$	$\vdots$	$\vdots$	$\vdots$	$\ddots$	0	
p_{k-1}	0	$\frac{1}{k-1}\square$	$\frac{1}{k-1}\square$	$\cdots$	$\frac{1}{k-1}\square$	0
p_k	0	$\frac{1}{k}\square$	$\frac{1}{k}\square$	$\cdots$	$\frac{1}{k}\square$	$\frac{1}{k}\square$

Table 4.1. Composition of a function with a polynomial.

Notice that one does not need to save all the entries of the Table **4.1** to compute only the coefficients p_j. Moreover for each entries in the ith row with $i = 2, \ldots, k$, one only needs to consider polynomials of degree $k-i-1$. Overall the extra memory is at least $\frac{3}{2}k(k-1)$.

On the other hand, the number of arithmetic operations following the rule eq. (4.26) are given by the Proposition **4.7**.

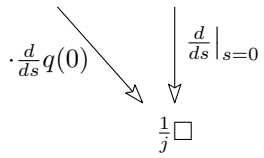

Figure 4.1. Generation rule for entries in Table **4.1** with $j = 2, \ldots, k$.

PROPOSITION 4.7. *Let $K(\theta)$ be a real-periodic function and let $q(s)$ be a real polynomial of degree k. Given $\frac{d^j}{d\theta^j}K(q(0))$ for $j = 0, \ldots, k$. The polynomial $K \circ q$ can be performed with at least $\frac{3}{2}k(k-1)$ extra memory, $\Theta(k^4)$ multiplications and additions.*

Proof. Notice that $k(k+1)$ multiplications and $(k+1)^2$ additions are needed to perform the product of two polynomials of degree k. Also k multiplications are needed to perform the derivative of a polynomial of degree k multiplied by a scalar. In order to bound the number of operations we must distinct three different situations of the Table **4.1**.

1. The column $a_{3..k,2}$. $\sum_{i=1}^{k-2}(k-i+1) = \frac{1}{2}(k^2+k-6)$ multiplications.

2. The diagonal $a_{3..k,3..k}$.

   - $\sum_{j=1}^{k-2}(k-j-1)(k-j+1)+1 = \frac{1}{6}(2k^3-3k^2+k-6)$ multiplications.
   - $\sum_{j=1}^{k-2}(k-j-1)^2+1 = \frac{1}{6}(2k^3-9k^2+19k-18)$ additions.

3. The rest.

   - $\sum_{j=1}^{k-2}\sum_{i=j+1}^{k-2}(k-i-1)(k-i+1)+(k-i-2)+1 = \frac{1}{12}(7k^4-56k^3+71k^2+38k-24)$ multiplications.
   - $\sum_{j=1}^{k-2}\sum_{i=j+1}^{k-2}(k-i-1)^2+(k-i)+1 = \frac{1}{12}(5k^4-36k^3+85k^2-102k+72)$ additions.

Overall $\frac{7}{12}k^4+\Theta(k^3)$ multiplications and $\frac{5}{12}k^4+\Theta(k^3)$ additions. □

The case of K compose with $\widetilde{W}$ requires the jet propagation of an exponential which is obtained by a recurrence. Concretely, $e(s) = s\exp q(s)$ has

coefficients $e_0 = 0$, $e_1 = \exp q_0$ and

$$e_{j+1} = \frac{1}{j}\sum_{k=0}^{j-1}(j-k)q_{j-k}e_{k+1}, \qquad j \geqslant 1,$$

which has a linear contribution w.r.t. the degree of the polynomial q.

The next Theorem **4.8** summarises the previous explanations. It assumes that $\frac{d^i}{d\theta^i}K(q_0)$ of Table **4.1** are given as input. Once we fix the computational representation of a periodic function we will be able to express these mappings.

THEOREM 4.8. *For a fixed θ, the computational complexity to compute the compositions $K(\theta, s) = \sum_{j=0}^{m-1} K_j(\theta)(b_0 s)^j$ between $W(\theta, s) = \sum_{j=0}^{k-1} W^j(\theta)(bs)^j$ and $\widetilde{W}(\theta, s)$ is $\Theta(mk^4)$, and space $\Omega(k^2)$ assuming $\frac{d^i}{d\theta^i}K_j(W_1^0(\theta))$ as input for $i = 0, \ldots, k-1$.*

Fourier representation

A mapping $K\colon \mathbb{T} \to \mathbb{R}$ is called periodic when $K(\theta + 1) = K(\theta)$ for all θ in $\mathbb{T}$. In order to get a computer representation of that kind of maps we can either take a mesh in $\theta = (\theta_k)_{k=0}^{n_\theta - 1}$ and their evaluations by K, $\check{K} = (\check{K}_k)_{k=0}^{n_\theta-1} \in \mathbb{R}^{n_\theta}$ or we can take advantage of the periodicity and represent it in a trigonometric basis. The Discrete Fourier Transform (DFT) is defined when $\theta_k = (k/n_\theta)_{k=0}^{n_\theta-1}$ by $\widehat{K} = (\widehat{K}_k)_{k=0}^{n_\theta-1} \in \mathbb{C}^{n_\theta}$ so that

$$\check{K}_k = \sum_{j=0}^{n_\theta-1} \widehat{K}_j e^{-2\pi \mathtt{i} jk/n_\theta} \tag{4.27}$$

or equivalently by

$$\widehat{K}_k = \frac{1}{n_\theta}\sum_{j=0}^{n_\theta-1} \check{K}_j e^{2\pi \mathtt{i} jk/n_\theta}. \tag{4.28}$$

In the real case the complex numbers $\widehat{K}$ satisfies a symmetry namely Hermitian symmetry, i.e. $\widehat{K}_k = \widehat{K}^*_{n_\theta - k}$ which implies $\widehat{K}_0$ is real and when n_θ is even $\widehat{K}_{n_\theta/2}$ is also real. Then we can define real numbers $(a_0; a_k, b_k)_{k=1}^{\lfloor n_\theta/2 \rfloor - 1}$ if n_θ is odd or $(a_0, a_{n_\theta/2}; a_k, b_k)_{k=1}^{n_\theta/2-1}$ defined by

$$a_0 = \operatorname{Re}\widehat{K}_0,\ a_{n_\theta/2} = \operatorname{Re}\widehat{K}_{n_\theta/2},\ a_k = 2\operatorname{Re}\widehat{K}_k \text{ and } b_k = -2\widehat{K}_k$$

with $1 \leqslant k < \lfloor n_\theta/2 \rfloor$. Thus, K can be approximated by

$$K(\theta) = \frac{a_0}{2} + \frac{a_{n_\theta/2}}{2}\cos(\pi n_\theta \theta) + \sum_{k=1}^{\lfloor n_\theta/2 \rfloor - 1} a_k \cos(2\pi k\theta) + b_k \sin(2\pi k\theta) \tag{4.29}$$

where the coefficient $a_{n_\theta/2}$ only appears when n_θ is even. Therefore eq. (4.29) is equivalent to eq. (4.27) but rather than $2n_\theta$ real numbers, only half of them are needed. Henceforth, any real periodic mapping K is computational storage by an array of length n_θ whose values are represented either in mesh points or in Fourier coefficients. Fast Fourier Transform (FFT), which is just a faster algorithm to implement the DFT in the sense that rather $\Theta(n_\theta^2)$ computational complexity it can be performed with $\Theta(n_\theta \log n_\theta)$, is applied to change from one representation to the other. There are different ways to order these Fourier coefficients in the array depending on the main important thing to be optimised in terms of performance of the FFT, and if it is intended to offer the option of FFT for several angles. For instance, [FJ05] uses in its function `fftw_plan_r2r_1d` the following order of the Fourier coefficients in a real array $(v_0, \ldots, v_{n_\theta-1})$.

$$\begin{aligned} v_0 &= a_0, \\ v_k &= 2a_k \text{ and } v_{n_\theta-k} = -2b_k \quad \text{for } 1 \leqslant k < \lfloor n_\theta/2 \rfloor, \\ v_{n_\theta/2} &= a_{n_\theta/2} \end{aligned}$$

where the index $n_\theta/2$ is only taken into consideration if, and only if, n_θ is even. Another standard order is just $(a_0, a_{n_\theta/2}; a_k, b_k)$ in sequential order or $(a_0; a_k, b_k)$ if n_θ is odd.

Norms and smoothness

The functions W^j in Algorithm **4.6** are not expected to be analytic due to the composition with the delay function (even if it is analytic). Fourier series are good for the analytic and finite differentiability case. Among the most effective norms in Fourier series are the weighted ℓ^1 norms. For instance,

$$\begin{aligned} \|K\|_{w\ell^1,n} &= \sum_{k=0}^{\lfloor n_\theta/2 \rfloor - 1} ((n_\theta - k)^n + k^n)|\widehat{K}_k| \\ &= 2(n_\theta/2)^n |a_{n_\theta/2}| + 2(n_\theta)^n |a_0| + \\ &\quad \frac{1}{2} \sum_{k=1}^{\lfloor n_\theta/2 \rfloor - 1} ((n_\theta - k)^n + k^n)(a_k^2 + b_k^2)^{1/2}. \end{aligned}$$

where the coefficient $n_\theta/2$ only appears if, and only if, n_θ is even. The smoothness of K can be approximated in terms of how the Fourier coefficients decay. Riemann-Lebesgue's Lemma tells us that if K is real, continuous, and periodic, $\widehat{K}_k \to 0$ as $k \to \infty$, and in general if K is m times differentiable, then $|\widehat{K}_k| \leqslant C/|k|^m$ for $k \neq 0$ and some constant $C > 0$. To determine

approximately m when it is small, we can use the continuous Littlewood-Paley Theorem [dlLP02] which states that K is in α-Hölder space with $\alpha \in \mathbb{R}_+$ if, and only if, for each $\eta \geqslant 0$ there is constant $C > 0$ such that for all $t > 0$.

$$\left\| \left(\frac{\partial}{\partial t} \right)^{\eta} e^{-t\sqrt{-\Delta}\theta} \right\|_{L^\infty(\mathbb{T})} \leqslant C t^{\alpha-\eta}.$$

Composition in Fourier

Composition of real Fourier series may require to know the values not in the standard equispaced mesh. A direct composition of real Fourier series requires a computational complexity $\Theta(n_\theta^2)$. However it can be performed with $\Theta(n_\theta \log n_\theta)$ by the NFFT3, see [KKP09]. It allows to express $K\colon \mathbb{T} \to \mathbb{R}$ with the same coefficients in eq. (4.27), and perform its evaluation in an even number of nonequispaced nodes $(\theta_k)_{k=0}^{n_\theta-1} \subset \mathbb{T}$ by

$$K(\theta_k) = \sum_{j=0}^{n_\theta-1} \widehat{K}_j e^{-2\pi \mathtt{i}(j-n_\theta/2)(\theta_k-1/2)}. \tag{4.30}$$

The corrections of θ_k in eq. (4.30) is because NFFT3 considers $\mathbb{T} \cong [-1/2, 1/2)$ rather than $[0, 1)$. It uses some window functions for a first approximation as a cut-off in the frequency domain and also for a second approximation as a cut-off in time domain. It takes under control (by bounds) these approximations to ensure the solution is a good approximation. Joining these result with Proposition **4.7** we can rewrite Theorem **4.8** as

THEOREM 4.9. *The computational complexity to compute the composition* $K(\theta, s) = \sum_{j=0}^{m-1} K_j(\theta)(b_0 s)^j$ *between* $W(\theta, s) = \sum_{j=0}^{k-1} W^j(\theta)(bs)^j$, *and* $\widetilde{W}(\theta, s) = \sum_{j=0}^{k-1} \widetilde{W}^j(\theta)(bs)^j$ *in Algorithm* ***4.6*** *with* K_j, W^j *and* $\widetilde{W}^j$ *expressed with* n_θ *Fourier coefficients is* $\Theta(mk^4 n_\theta + mkn_\theta \log n_\theta)$.

Automatic Differentiation in Fourier

For the s^0 case, i.e. Algorithm **4.5**, the composition of Fourier series is needed. However, for the other orders we need to perform the composition with a polynomial in s with coefficient Fourier series and the output must be an object of the same kind, i.e. a Taylor-Fourier expansion.

Theorem **4.8** tells us that the composition $K \circ W(\theta, s)$ can numerically be done independently of the periodic mapping representation. Nevertheless, differentiation is a notoriously ill-posed problem due to of the lack of information in the discretesed problem. Thus, Table **4.1** is a good option when no advantage of the computer periodic representation exists or $k \ll m$.

Using the representation eq. (4.29), we can use the jet propagation of sine and cosine by recurrence. That is, if $q(s)$ is a polynomial, then $\sin q(s)$ and $\cos q(s)$ are given by $s_0 = \sin q_0$, $c_0 = \cos q_0$ and for $j \geqslant 1$,

$$s_j = \frac{1}{j}\sum_{k=0}^{j-1}(j-k)q_{j-k}c_k, \qquad c_j = -\frac{1}{j}\sum_{k=0}^{j-1}(j-k)q_{j-k}s_k. \tag{4.31}$$

Therefore the computational cost to obtain the sine and cosine of a polynomial is linear w.r.t. its degree.

Theorem **4.10** says that the composition of K with W or $\widetilde{W}$ are rather than $\Theta(mk^4n_\theta + mkn_\theta \log n_\theta)$ like in Theorem **4.9** just $\Theta(mkn_\theta^2)$. Therefore if $k \ll m$, the approach given by Theorem **4.9** has a better complexity although Theorem **4.10** will be more stable for larger k.

THEOREM 4.10. *The computational complexity to compute the composition* $K(\theta, s) = \sum_{j=0}^{m-1} K_j(\theta)(b_0 s)^j$ *between* $W(\theta, s) = \sum_{j=0}^{k-1} W^j(\theta)(bs)^j$ *and* $\widetilde{W}(\theta, s) = \sum_{j=0}^{k-1} \widetilde{W}^j(\theta)(bs)^j$ *in Algorithm* ***4.6*** *with* K_j, W^j *and* $\widetilde{W}^j$ *expressed with* n_θ *Fourier coefficients is* $\Theta(mkn_\theta^2)$.

4.7 The main Theorems

The next two Theorems establish first the existence of the limit cycle and then the existence (and also uniqueness) of the rest of the expression of $W(\theta, s)$ with the form like eq. (4.12). Both results are given in *a posteriori* format. In particular, it gives by free the continuation method. Theorem **4.12** shows that at each order we loose differentiability in the solution. We conjecture that the solution will be C^∞ as $\varepsilon \to 0$. Although we did not prove that, we have numerically seen that for further order we need more Fourier coefficients as well as ε must be smaller at each new order.

THEOREM 4.11 (Limit Cycle). *For any given integer* $L > 0$, *there is* $\varepsilon_0 > 0$ *such that when* $0 \leqslant \varepsilon \leqslant \varepsilon_0$, *there exist an* $\omega \neq 0$ *and an* L*-times differentiable map* $W^0 \colon \widetilde{\mathbb{T}} \to \widetilde{\mathbb{T}} \times \mathbb{R}$, *with* L*th derivative Lipschitz, which solve eq.* (4.14).

Moreover, for an initial guess $(\omega^0, W^{0,0})$ *satisfying the periodic condition i eq.* (4.15) *and the invariance equation eq.* (4.14) *with an error function* E^0, *there exist a unique* (ω, W^0) *nearby solving the same equations exactly with bounds*

$$\|W^{0,0} - W^0\|_{C^l} \leqslant C\|E^0\|_{C^0}^{1-l/L}, \qquad 0 \leqslant l < L \tag{4.32}$$

$$|\omega^0 - \omega| \leqslant C\|E^0\|_{C^0}, \tag{4.33}$$

for some constant C possibly depending on ε, ω_0, λ_0, l, L, and bounds of $\|W^{0,0}\|_{C^{L+\mathrm{Lip}}}$. In fact, W^0 has derivatives up to any order.

THEOREM 4.12 (Isochoron). *For any given integers $N \geqslant 2$ and $L \geqslant 2+N$, there is $\varepsilon_0 > 0$ such that when $0 \leqslant \varepsilon \leqslant \varepsilon_0$, there exist $\omega \neq 0$, $\lambda < 0$, and $W\colon \widetilde{\mathbb{T}} \times \mathbb{R} \to \widetilde{\mathbb{T}} \times \mathbb{R}$ of the form*

$$W(\theta, s) = W^0(\theta) + W^1(\theta)s + \sum_{j=2}^{N-1} W^j(\theta)s^j + W^>(\theta, s).$$

which solve the equation eq. (4.9).

Where $W^0\colon \widetilde{\mathbb{T}} \to \widetilde{\mathbb{T}} \times \mathbb{R}$ is L times differentiable with Lth derivative Lipschitz. For $1 \leqslant j < N$, $W^j\colon \widetilde{\mathbb{T}} \to \widetilde{\mathbb{T}} \times \mathbb{R}$ is $(L-1)$ times differentiable with $(L-1)$th derivative Lipschitz and $W^>$ is of at least Nth order in s and is $(L-2-N)$ times differentiable in θ and s, with $(L-2-N)$th derivative Lipschitz.

Moreover, if $(\omega^0, W^{0,0}, \lambda^0, W^{1,0}, W^{>,0})$ satisfy the invariance equations eq. (4.14), eq. (4.16), and eq. (4.22), with error functions $E^0(\theta)$, $E^1(\theta)$, and $E^>(\theta, s)$, respectively, then there are ω, $W^0(\theta)$, λ, $W^1(\theta)$, $W^>(\theta, s)$ which solve eqs. (4.14), (4.16), and (4.22). Therefore, eq. (4.9) is solved by ω, λ, and $W(\theta, s)$ as in eq. (4.12) of above form. For $0 \leqslant l \leqslant L-3$, we have

$$\begin{aligned} &\|W(\theta, s) - \sum_{j=0}^{N-1} W^{j,0}(\theta)s^j - W^{>,0}(\theta, s)\|_{C^l} \\ &\qquad \leqslant C\left(\sum_{j=0}^{N-1} \|E^j\|_{C^0}|s|^j + \|E^>\|_{0,N}|s|^N\right)^{1-\frac{l}{(L-2-N)}}, \end{aligned} \tag{4.34}$$

$$\begin{aligned} |\omega - \omega^0| &\leqslant C\|E^0\|_{C^0}, \\ |\lambda - \lambda^0| &\leqslant C\|E^1\|_{C^0}, \end{aligned} \tag{4.35}$$

for some constant C depending on ε, ω_0, λ_0, N, l, L, and bounds for $\|W^{0,0}\|_{L+\mathrm{Lip}}$ and $\|W^{1,0}\|_{L-1+\mathrm{Lip}}$.

Section **4.4.3** tells that for small ε (we did not quantify it), we do not need the extension in the invariance equations for the finite order. Therefore, once the two previous theorem were proved, we would also have the next two results.

COROLLARY 4.13. *When ε is small enough, eq. (4.4) admits a limit cycle close to the limit cycle of the unperturbed equation. If ω, W^0 solve the invariance eq. (4.24), then $K \circ W^0(\theta)$ gives a parametrisation of the limit cycle of eq. (4.4), i.e. for any θ, $K \circ W^0(\theta + \omega t)$ solves eq. (4.4) for all t.*

We can also find a 2-parameter family of solutions close to the limit cycle:

COROLLARY 4.14. *For small ε, there are isochrons for the limit cycle of equation eq. (4.4). If ω, λ, and $W\colon \widetilde{\mathbb{T}}\times\mathbb{R}\to\widetilde{\mathbb{T}}\times\mathbb{R}$ solves the extended invariance eq. (4.9), then there exists $0<s_0<\frac{1}{2}$, such that $K\circ W(\theta,s)$, $|s|\leqslant s_0$ gives a parametrisation of the isochrons in a neighbourhood of the limit cycle, i.e. for any θ and s, with $|s|\leqslant s_0$, $K\circ W(\theta+\omega t, se^{\lambda}t)$ solves eq. (4.4) for all $t\geqslant 0$.*

4.7.1 Overview of the proof

We are going to consider an operator for each of the orders so that they are going to satisfy the invariance equations in eq. (4.9). In particular, the operator for the 0th order must involves the periodicity eq. (4.15), the 1st order will fix the speed rate via a normalisation condition eq. (4.19).

To define such contractions, we must fix suitable spaces and norms. We conjecture the solution can only be finite differentiable. Hence, we will consider the space of functions from a Banach space Y to another one X with uniformly bounded continuous Lth derivative, denoted by $C^L(Y,X)$, and whose norm is

$$\|f\|_{C^L}=\max_{0\leqslant j\leqslant L}\sup_{\xi\in Y}\|D^jf(\xi)\|_{Y^{\otimes j}\to X}.$$

It becomes a Banach space as well as the closed subset, denoted by C^L_B, of C^L with elements bounded by the constant $B>0$. We will also denote $C^{L+\mathrm{Lip}}(Y,X)$ the subspace of C^L with Lth derivative Lipschitz. In that case, its norm is defined as the maximum between the one in C^L and

$$\operatorname{Lip}D^Lf=\sup_{\xi_1\neq\xi_2}\frac{\|D^Lf(\xi_1)-D^Lf(\xi_2)\|_{Y^{\otimes L}\to X}}{\|\xi_1-\xi_2\|_Y}.$$

Similarly, $C^{L+\mathrm{Lip}}_B$ is the closed subset of the space $C^{L+\mathrm{Lip}}$ whose elements are bounded by $B>0$.

To prove the convergence of the fixed-point method for the invariance equations in section **4.4.2**, we will use a well-known result in [Lan73, Proposition A2] quoted in Lemma **4.15**. It can be interpreted as $C^{L+\mathrm{Lip}}_1(Y,X)$ is closed under pointwise weak topology on X.

LEMMA 4.15 (Lanford, [Lan73]). *Let $(u_n)_{n\in\mathbb{N}}$ be a sequence of functions on a Banach space Y with values on another one X admitting derivatives up to kth order. If for all n and y*

i. $\|D^ju_n(y)\|\leqslant 1$ *for all* $j=0,1,2,\dots,k$.

ii. $D^k u_n$ *is Lipschitz with Lipschitz constant* 1.

iii. $(u_n(y))$ *converges weakly to a unit* $u(y)$.

Then,

1. *u has a Lipschitz kth derivative with Lipschitz constant 1.*
2. $D^j u_n(y)$ *converges weakly to* $D^j u(y)$ *for all* y *and* $j = 1, 2, \dots, k$.

   `N.B.:` *For all* $(y_1, \dots, y_j) \in Y^{\otimes j}$, *the sequence* $(D^j u_n(y)(y_1, \dots, y_j))$ *converges in the weak topology to* $D^j u(y)(y_1, \dots, y_j)$.

The interpolation inequalities will allow us to prove C^0-contractions for each of the operator involves in the system of invariance equations. For completeness, let us quote the statement as a Lemma.

LEMMA 4.16 ([dlLO99]). *Let* U *be a convex and bounded open subset of a Banach space* E, F *is a Banach space. Let* r, s, t *be positive numbers,* $0 \leqslant r < s < t$ *and* $\mu = \frac{t-s}{t-r}$. *There is a constant* $M_{r,t}$, *such that if* $f \in C^t(U, F)$, *then*

$$\|f\|_{C^s} \leqslant M_{r,t} \|f\|_{C^r}^{\mu} \|f\|_{C^t}^{1-\mu}.$$

4.7.2 Proof for the limit cycle, Theorem 4.11

Proposition **4.3** gives an explicit solution for the invariance equation eq. (4.14) of W^0 which is solvable because eq. (4.15). Therefore let us define the operator Γ^0 (which depends on ε)

$$\begin{aligned} \Gamma^0(a, Z)(\theta) &\coloneqq \begin{pmatrix} \Gamma_1^0(a, Z) \\ \Gamma_2^0(a, Z)(\theta) \\ \Gamma_3^0(a, Z)(\theta) \end{pmatrix} \\ &\coloneqq \begin{pmatrix} \omega_0 + \varepsilon \int_0^1 \overline{Y}_1(Z(\theta), \widetilde{Z}(\theta; a), \varepsilon)\, d\theta \\ \frac{1}{\Gamma_1^0(a,\ Z)} \left(\omega_0 \theta + \varepsilon \int_0^\theta \overline{Y}_1(Z(\sigma), \widetilde{Z}(\sigma; a), \varepsilon)\, d\sigma\right) \\ \varepsilon \int_0^\infty e^{\lambda_0 t} \overline{Y}_2(Z(\theta - at), \widetilde{Z}(\theta - at; a), \varepsilon)\, dt \end{pmatrix}. \end{aligned} \tag{4.36}$$

Then if Γ^0 has a fixed point (a^*, Z^*), then eq. (4.14) is solved, at the same time that periodic condition eq. (4.15) is satisfied.

Let $D^0 = I^0 \times \mathcal{C}_0^{L+\mathrm{Lip}}$ be the domain of Γ^0 where for a constant $B^0 > 2$,

$$\begin{aligned} I^0 &\coloneqq \{a \in \mathbb{R} \colon |a - \omega_0| \leqslant |\omega_0|/2\}, \\ \mathcal{C}_0^{L+\mathrm{Lip}} &\coloneqq \{f \in C_{B^0}^{L+\mathrm{Lip}}(\widetilde{\mathbb{T}}, \widetilde{\mathbb{T}} \times \mathbb{R}) \colon f(\theta + 1) = f(\theta) + \left(\begin{smallmatrix} 1 \\ 0 \end{smallmatrix}\right), \text{ for all } \theta\}. \end{aligned}$$

Let us first remark that it makes sense to consider a C^l space. Assume, for a moment, that (ω, W^0) satisfies the invariance equation, eq. (4.14). Then $K \circ W^0$ gives a parametrisation of the limit cycle, and, in particular, it solves the SDDE

$$\begin{cases} \frac{d}{dt} K \circ W^0(\theta(t)) = X(K \circ W^0(\theta(t)), \widetilde{K \circ W^0}(\theta(t)), \varepsilon), \\ \frac{d}{dt}\theta(t) = \omega. \end{cases}$$

Hence, if W^0 is L-times differentiable, the RHS is L-times differentiable, then also the LHS. Since K is a local diffeomorphism, W^0 is $(L+1)$-times differentiable. In fact, it is differentiable up to any order.

Now, let us split the conditions of Lemma **4.15** in different steps.

LEMMA 4.17. *There is $\varepsilon_1^0 > 0$ such that for all $0 < \varepsilon \leqslant \varepsilon_1^0$, $\Gamma^0(D^0) \subset D^0$.*

Proof. Notice that $\overline{Y}_1(Z(\theta), \widetilde{Z}(\theta; a), \varepsilon)$ is uniformly bounded in D^0. Let ε be small enough so that $\Gamma_1^0(a, Z)$ is in I^0. On the other hand, for all $(a, Z) \in D^0$,

$$\begin{aligned} \Gamma_2^0(a, Z)(\theta + 1) &= \Gamma_2^0(a, Z)(\theta) + 1, \\ \Gamma_3^0(a, Z)(\theta + 1) &= \Gamma_3^0(a, Z)(\theta). \end{aligned}$$

It remains to bound the derivatives of Γ_2^0 and Γ_3^0.

$$\frac{d}{d\theta}\Gamma_2^0(a, Z)(\theta) = \frac{1}{\Gamma_1^0(a, Z)}\big(\omega_0 + \varepsilon \overline{Y}_1(Z(\theta), \widetilde{Z}(\theta; a), \varepsilon)\big).$$

Faà di Bruno's formula (see [AR67]), for $2 \leqslant n \leqslant L$, $\frac{d^n}{d\theta^n}\Gamma_2^0(a, Z)(\theta)$ will be a polynomial of a common factor $\frac{\varepsilon}{\Gamma_1^0(a,\ Z)}$, each term will contain products of derivatives of $\overline{Y}_1$, Z, and $\overline{r \circ K}$ up to order $(n-1)$. By the smoothness of $\overline{Y}_1$, and $\overline{r \circ K}$, for $(a, Z) \in D^0$, if we choose B^0 to be larger than 2, then for small enough ε, $\Gamma_2^0(a, Z)(\theta)$ on $\mathbb{T}$ has derivatives up to order L bounded by B^0 and Lth derivative Lipschitz with Lipschitz constant less than B^0.

To establish bounds for the derivatives of $\Gamma_3^0(a, Z)(\theta)$, we apply a similar argument. For $1 \leqslant n \leqslant L$, $\frac{\partial^n}{\partial\theta^n}\overline{Y}_2(Z(\theta - at), \widetilde{Z}(\theta - at; a), \varepsilon)$ will be a polynomial with each term a product of derivatives of $\overline{Y}_2$, Z, and $\overline{r \circ K}$ up to order n. With regularity of $\overline{Y}_2$, and $\overline{r \circ K}$, for $(a, Z) \in D^0$, $|\frac{\partial^n}{\partial\theta^n}\overline{Y}_2(Z(\theta - at), \widetilde{Z}(\theta - at), \varepsilon)|$ will be bounded. Therefore, for small enough ε, $\Gamma_3^0(a, Z)$ has derivatives up to order L bounded by B^0 and its Lth derivative is Lipschitz with Lipschitz constant less than B^0.

If we take ε_1^0 such that above conditions are satisfied at the same time, then for $\varepsilon \leqslant \varepsilon_1^0$, we have $\Gamma^0(D^0) \subset D^0$. □

LEMMA 4.18. *There is $\varepsilon_2^0 > 0$, such that for all $0 < \varepsilon \leqslant \varepsilon_2^0$ the operator Γ^0 in eq.* (4.36) *is a contraction with the norm in D^0 defined by*

$$d((a, Z), (a', Z')) \coloneqq |a - a'| + \|Z - Z'\|_\infty. \tag{4.37}$$

Proof. We must show that there is $0 < \mu_0 < 1$ such that

$$d(\Gamma^0(a, Z), \Gamma^0(a', Z')) < \mu_0 d((a, Z), (a', Z')). \tag{4.38}$$

By definition, $d(\Gamma^0(a, Z), \Gamma^0(a', Z'))$ is equal to

$$|\Gamma_1^0(a, Z) - \Gamma_1^0(a', Z')| + \|(\Gamma_2^0(a, Z) - \Gamma_2^0(a', Z'), \Gamma_3^0(a, Z)) - \Gamma_3^0(a', Z'))\|_\infty \tag{4.39}$$

More explicitly,

$$\varepsilon \left| \int_0^1 \left[\overline{Y}_1(Z(\theta), \widetilde{Z}(\theta; a), \varepsilon) - \overline{Y}_1(Z'(\theta), \widetilde{Z}'(\theta; a'), \varepsilon) \right] d\theta \right| \tag{4.40}$$

plus the maximum between

$$\begin{aligned} \sup_{\theta \in \mathbb{T}} \Bigg| & \omega_0 \theta \left[\frac{1}{\Gamma_1^0(a, Z)} - \frac{1}{\Gamma_1^0(a', Z')} \right] + \\ & \varepsilon \int_0^\theta \left[\overline{Y}_1(Z(\sigma), \widetilde{Z}(\sigma; a), \varepsilon) - \overline{Y}_1(Z'(\sigma), \widetilde{Z}'(\sigma; a'), \varepsilon) \right] d\sigma \Bigg|, \end{aligned} \tag{4.41}$$

and

$$\begin{aligned} \varepsilon \sup_{\theta \in \mathbb{T}} \Bigg| \int_0^\infty e^{\lambda_0 t} \big[& \overline{Y}_2(Z(\theta - at), \widetilde{Z}(\theta - at; a), \varepsilon) - \\ & \overline{Y}_2(Z'(\theta - a't), \widetilde{Z}'(\theta - a't; a'), \varepsilon) \big] \, dt \Bigg|. \end{aligned} \tag{4.42}$$

Let us start giving a (non-sharp) bound for the difference $|\overline{Y}_1(Z(\theta), \widetilde{Z}(\theta; a), \varepsilon) - \overline{Y}_1(Z'(\theta), \widetilde{Z}'(\theta; a'), \varepsilon)|$ which is equal to

$$|\overline{Y}_1(Z(\theta), Z(\theta - a\overline{r \circ K} \circ Z(\theta)), \varepsilon) - \overline{Y}_1(Z'(\theta), Z'(\theta - a'\overline{r \circ K} \circ Z'(\theta)), \varepsilon)|. \tag{4.43}$$

Adding and subtracting terms, eq. (4.43) is bounded by

$$|\overline{Y}_1(Z(\theta), \widetilde{Z}(\theta), \varepsilon) - \overline{Y}_1(Z'(\theta), \widetilde{Z}(\theta), \varepsilon)| + \tag{ℓ_1}$$

$$|\overline{Y}_1(Z'(\theta), Z(\theta - a\overline{r \circ K} \circ Z(\theta)), \varepsilon) - \overline{Y}_1(Z'(\theta), Z'(\theta - a\overline{r \circ K} \circ Z(\theta)), \varepsilon)| + \tag{ℓ_2}$$

$$|\overline{Y}_1(Z'(\theta), Z'(\theta - a\overline{r \circ K} \circ Z(\theta)), \varepsilon) - \overline{Y}_1(Z'(\theta), Z'(\theta - a'\overline{r \circ K} \circ Z(\theta)), \varepsilon)| + \tag{ℓ_3}$$

$$|\overline{Y}_1(Z'(\theta), Z'(\theta - a'\overline{r \circ K} \circ Z(\theta)), \varepsilon) - \overline{Y}_1(Z'(\theta), Z'(\theta - a'\overline{r \circ K} \circ Z'(\theta)), \varepsilon)|. \tag{ℓ_4}$$

By the mean value Theorem, then

$$\begin{aligned}(\ell_1) &\leqslant \|D_1\overline{Y}_1\|_\infty\|Z-Z'\|_\infty,\\ (\ell_2) &\leqslant \|D_2\overline{Y}_1\|_\infty\|Z-Z'\|_\infty,\\ (\ell_3) &\leqslant \|D\overline{Y}_1\|_\infty\|DZ'\|_\infty\|\overline{r\circ K}\|_\infty|a-a'|,\end{aligned}$$

and

$$(\ell_4) \leqslant \|D\overline{Y}_1\|_\infty\|DZ'\|_\infty|a'|\|D(\overline{r\circ K})\|_\infty\|Z-Z'\|_\infty.$$

Because of the assumption that (a,Z) and (a',Z') are in the set D^0, then $|\overline{Y}_1(Z(\theta),\widetilde{Z}(\theta;a),\varepsilon)-\overline{Y}_1(Z'(\theta),\widetilde{Z}'(\theta;a'),\varepsilon)|$ is finally bounded by

$$\|D\overline{Y}_1\|_\infty\big[(2+B^0|a'|\|D(\overline{r\circ K})\|_\infty)\|Z-Z'\|_\infty+B^0\|\overline{r\circ K}\|_\infty|a-a'|\big]. \quad (4.44)$$

In particular, $|\Gamma_1^0(a,Z)-\Gamma_1^0(a',Z')|$ in eq. (4.39) is bounded ε times by eq. (4.44) due to its explicit expression in eq. (4.40).

To bound $\|\Gamma_2^0(a,Z)-\Gamma_2^0(a',Z')\|_\infty$ in eq. (4.39), let us bound the expression eq. (4.41) adding and subtracting the term

$$\frac{\varepsilon}{\Gamma_1^0(a,Z)}\int_0^\theta \overline{Y}_1(Z'(\sigma),\widetilde{Z}'(\sigma;a'),\varepsilon)\,d\sigma,$$

eq. (4.41) turns out to be bounded by

$$\begin{aligned}&\frac{\varepsilon}{|\Gamma_1^0(a,Z)|}\int_0^1|\overline{Y}_1(Z(\theta),\widetilde{Z}(\theta),\varepsilon)\,d\theta-\overline{Y}_1(Z'(\theta),\widetilde{Z}'(\theta),\varepsilon)|\,d\theta\\ &+\frac{|\Gamma_1^0(a,Z)-\Gamma_1^0(a',Z')|}{|\Gamma_1^0(a,Z)\Gamma_1^0(a',Z')|}\left[\varepsilon\int_0^1|\overline{Y}_1(Z'(\theta),\widetilde{Z}'(\theta;a'),\varepsilon)|\,d\theta+|\omega_0|\right]\end{aligned} \quad (4.45)$$

which, because eq. (4.44) and the definition of $|\Gamma_1^0(a,Z)-\Gamma_1^0(a',Z')|$ in eq. (4.40), is bounded by (and so also $\|\Gamma_2^0(a,Z)-\Gamma_2^0(a',Z')\|_\infty$)

$$\frac{\varepsilon|\omega_0|+\varepsilon^2\|\overline{Y}_1\|_\infty+\varepsilon|\Gamma_1^0(a',Z')|}{|\Gamma_1^0(a,Z)\Gamma_1^0(a',Z')|}eq.\ (4.44). \quad (4.46)$$

For eq. (4.42) we are going to proceed as before. In this case, adding and subtracting, the term $|\overline{Y}_2(Z(\theta-at),\widetilde{Z}(\theta-at;a),\varepsilon)-\overline{Y}_2(Z'(\theta-a't),\widetilde{Z}'(\theta-$

$a't; a'), \varepsilon)|$ is bounded by

$$|\overline{Y}_2(Z(\theta-at), \widetilde{Z}(\theta-at;a), \varepsilon) - \overline{Y}_2(Z'(\theta-at), \widetilde{Z}(\theta-at;a), \varepsilon)| + \qquad (\ell_1)$$

$$|\overline{Y}_2(Z'(\theta-at), \widetilde{Z}(\theta-at;a), \varepsilon) - \overline{Y}_2(Z'(\theta-a't), \widetilde{Z}(\theta-at;a), \varepsilon)| + \qquad (\ell_2)$$

$$\begin{aligned}&|\overline{Y}_2(Z'(\theta-a't), Z(\theta-at-a\overline{r\circ K}\circ Z(\theta-at)), \varepsilon) - \\ &\overline{Y}_2(Z'(\theta-a't), Z'(\theta-at-a\overline{r\circ K}\circ Z(\theta-at)), \varepsilon)| +\end{aligned} \qquad (\ell_3)$$

$$\begin{aligned}&|\overline{Y}_2(Z'(\theta-a't), Z'(\theta-at-a\overline{r\circ K}\circ Z(\theta-at)), \varepsilon) - \\ &\overline{Y}_2(Z'(\theta-a't), Z'(\theta-a't-a\overline{r\circ K}\circ Z(\theta-at)), \varepsilon)| +\end{aligned} \qquad (\ell_4)$$

$$\begin{aligned}&|\overline{Y}_2(Z'(\theta-a't), Z'(\theta-a't-a\overline{r\circ K}\circ Z(\theta-at)), \varepsilon) - \\ &\overline{Y}_2(Z'(\theta-a't), Z'(\theta-a't-a'\overline{r\circ K}\circ Z(\theta-at)), \varepsilon)| +\end{aligned} \qquad (\ell_5)$$

$$\begin{aligned}&|\overline{Y}_2(Z'(\theta-a't), Z'(\theta-a't-a'\overline{r\circ K}\circ Z(\theta-at)), \varepsilon) - \\ &\overline{Y}_2(Z'(\theta-a't), Z'(\theta-a't-a'\overline{r\circ K}\circ Z'(\theta-at)), \varepsilon)| +\end{aligned} \qquad (\ell_6)$$

$$\begin{aligned}&|\overline{Y}_2(Z'(\theta-a't), Z'(\theta-a't-a'\overline{r\circ K}\circ Z'(\theta-at)), \varepsilon) - \\ &\overline{Y}_2(Z'(\theta-a't), Z'(\theta-a't-a'\overline{r\circ K}\circ Z'(\theta-a't)), \varepsilon)|.\end{aligned} \qquad (\ell_7)$$

By the mean value Theorem, then

$$\begin{aligned}(\ell_1) &\leqslant \|D_1\overline{Y}_2\|_\infty \|Z - Z'\|_\infty,\\ (\ell_2) &\leqslant t\|D_2\overline{Y}_2\|_\infty \|DZ'\|_\infty |a-a'|,\\ (\ell_3) &\leqslant \|D_2\overline{Y}_2\|_\infty \|Z - Z'\|_\infty,\\ (\ell_4) &\leqslant t\|D_2\overline{Y}_2\|_\infty \|DZ'\|_\infty |a-a'|,\\ (\ell_5) &\leqslant \|D_2\overline{Y}_2\|_\infty \|DZ'\|_\infty \|\overline{r\circ K}\|_\infty |a-a'|,\\ (\ell_6) &\leqslant \|D_2\overline{Y}_2\|_\infty \|DZ'\|_\infty |a'| \|D(\overline{r\circ K})\|_\infty \|Z-Z'\|_\infty,\end{aligned}$$

and

$$(\ell_7) \leqslant t\|D_2\overline{Y}_2\|_\infty \|DZ'\|_\infty^2 |a'| \|D(\overline{r\circ K})\|_\infty |a-a'|.$$

Under the assumption that (a, Z) and (a', Z') are in D^0, we obtain the bound

$$\begin{aligned}\|D\overline{Y}_2\|_\infty \big[&(2 + B^0|a'|\|D(\overline{r\circ K})\|_\infty)\|Z - Z'\|_\infty + \\ &\big(B^0\|\overline{r\circ K}\|_\infty + tB^0(2 + B^0|a'|\|D(\overline{r\circ K})\|_\infty)\big)|a-a'|\big].\end{aligned} \qquad (4.47)$$

We can have a bound for eq. (4.42) because of the observation that for $\lambda_0 < 0$,

$$\int_0^\infty e^{\lambda_0 t}\,dt = \frac{1}{|\lambda_0|},\ \text{and}\ \int_0^\infty te^{\lambda_0 t}\,dt = \frac{1}{\lambda_0^2}.$$

Thus, $\|\Gamma_3^0(a,Z) - \Gamma_3^0(a',Z')\|_\infty$ is finally bounded by

$$\frac{\varepsilon}{|\lambda_0|}\|D\overline{Y}_2\|_\infty\big[(2+B^0|a'|\|D(\overline{r\circ K})\|_\infty)\|Z-Z'\|_\infty + \big(B^0\|\overline{r\circ K}\|_\infty + \frac{B^0}{|\lambda_0|}(2+B^0|a'|\|D(\overline{r\circ K})\|_\infty)\big)|a-a'|\big]. \tag{4.48}$$

Due to eqs. (4.44), (4.46), and (4.48), we have arrived to an expression like

$$d(\Gamma^0(\omega,Z),\Gamma^0(\omega',Z')) \leqslant c_1|a-a'| + c_2\|Z-Z'\|_\infty$$

where

$$c_1 = \varepsilon B^0\|\overline{r\circ K}\|_\infty\left[\|D\overline{Y}_1\|_\infty\left(1+\frac{|\omega_0|+\varepsilon\|\overline{Y}_1\|_\infty+|\Gamma_1^0(a',Z')|}{|\Gamma_1^0(a,Z)\Gamma_1^0(a',Z')|}\right) - \frac{\|D\overline{Y}_2\|_\infty}{|\lambda_0|}\right] + \varepsilon\frac{B^0}{\lambda_0^2}\|D\overline{Y}_2\|_\infty\big(2+B^0|a'|\|D(\overline{r\circ K})\|_\infty\big),$$

and

$$c_2 = \varepsilon(2+B^0|a'|\|D(\overline{r\circ K})\|_\infty)\left[\|D\overline{Y}_1\|_\infty\left(1+\frac{|\omega_0|+\varepsilon\|\overline{Y}_1\|_\infty+|\Gamma_1^0(a',Z')|}{|\Gamma_1^0(a,Z)\Gamma_1^0(a',Z')|}\right) - \frac{\|D\overline{Y}_2\|_\infty}{|\lambda_0|}\right].$$

Since a, a', $\Gamma_1^0(a,Z)$, and $\Gamma_1^0(a',Z')$ are all in I^0, their absolute value can be bounded by $\frac{3}{2}|\omega_0|$. Thus,

$$c_1 = \varepsilon B^0\|\overline{r\circ K}\|_\infty\left[\|D\overline{Y}_1\|_\infty\frac{19|\omega_0|+4\varepsilon\|\overline{Y}_1\|_\infty}{9|\omega_0|} - \frac{\|D\overline{Y}_2\|_\infty}{|\lambda_0|}\right] + \varepsilon\frac{B^0}{2\lambda_0^2}\|D\overline{Y}_2\|_\infty\big(4+3B^0|\omega_0|\|D(\overline{r\circ K})\|_\infty\big),$$

and

$$c_2 = \frac{\varepsilon}{2}(4+3B^0|\omega_0|\|D(\overline{r\circ K})\|_\infty)\left[\|D\overline{Y}_1\|_\infty\frac{19|\omega_0|+4\varepsilon\|\overline{Y}_1\|_\infty}{9|\omega_0|} - \frac{\|D\overline{Y}_2\|_\infty}{|\lambda_0|}\right].$$

Because c_1 and c_2 are bounded by ε multiplied by some constants, they can be made small with ε small. Therefore, if ε is sufficiently small, we can find a $\mu_0 < 1$, such that eq. (4.38) is true and then Γ^0 in eq. (4.36) is a contraction. □

Remark 4.19 (for Lemma **4.18**).

- $\|D\overline{Y}_i\|_\infty$ are interpreted as the maximum of $\|D_j\overline{Y}_i\|_\infty$ for $i,j \in \{1,2\}$.
- If $r(x) = \tau > 0$ is constant, then the bounds for c_1 and c_2 become

$$c_1 = \varepsilon B^0 \left[\tau \|D\overline{Y}_1\|_\infty \frac{19|\omega_0| + 4\varepsilon\|\overline{Y}_1\|_\infty}{9|\omega_0|} + \|D\overline{Y}_2\|_\infty \frac{2 - \tau|\lambda_0|}{\lambda_0^2} \right],$$

and

$$c_2 = 2\varepsilon \left[\|D\overline{Y}_1\|_\infty \frac{19|\omega_0| + 4\varepsilon\|\overline{Y}_1\|_\infty}{9|\omega_0|} - \frac{\|D\overline{Y}_2\|_\infty}{|\lambda_0|} \right].$$

We have shown that taking an $0 < \varepsilon \leqslant \min\{\varepsilon_1^0, \varepsilon_2^0\}$ with ε_1^0 coming from Lemma **4.17** and ε_2^1 from Lemma **4.18**, then for all $(\omega^0, W^{0,0}(\theta)) \in D^0$, such as $\omega = \omega_0$ and $W^{0,0}(\theta) = \binom{\theta}{0}$. There is a (unique) limit by Γ^0. This limit is actually in D^0 as well. Note that this does not contradict the non-uniqueness due to the phase shift because we have fixed a phase.

For the second part of Theorem **4.11**, we know that

$$\begin{aligned} d\big((\omega^0, W^{0,0}), (\omega, W^0)\big) &= \lim_{k\to\infty} d\big((\omega^0, W^{0,0}), (\Gamma^0)^k(\omega^0, W^{0,0})\big) \\ &\leqslant \sum_{k=0}^{\infty} (\mu_0)^k d\big((\omega^0, W^{0,0}), \Gamma^0(\omega^0, W^{0,0})\big) \\ &\leqslant \frac{1}{1-\mu_0} d\big((\omega^0, W^{0,0}), \Gamma^0(\omega^0, W^{0,0})\big). \end{aligned} \tag{4.49}$$

It remains to estimate $d\big((\omega^0, W^{0,0}), \Gamma^0(\omega^0, W^{0,0})\big)$ by $\|E^0\|_\infty$. The error function for an initial condition $(\omega^0, W^{0,0})$ is defined as the error of the invariance equation, eq. (4.14). That is, $E^0 \equiv (E_1^0, E_2^0)$ with

$$E^0(\theta) \coloneqq \left[\omega^0 \partial_\theta - \begin{pmatrix} 0 & 0 \\ 0 & \lambda_0 \end{pmatrix} \right] W^{0,0}(\theta) - \begin{pmatrix} \omega_0 \\ 0 \end{pmatrix} - \varepsilon \overline{Y}(W^{0,0}(\theta), \widetilde{W}^{0,0}(\theta; \omega^0), \varepsilon),$$

Then $d\big((\omega^0, W^{0,0}), \Gamma^0(\omega^0, W^{0,0})\big)$ is bounded by

$$\left| \omega_0 + \varepsilon \int_0^1 \overline{Y}_1(W^{0,0}(\theta), \widetilde{W}^{0,0}(\theta; \omega^0), \varepsilon)\, d\theta - \omega^0 \right| + \tag{ℓ_1}$$

$$\sup_{\theta\in\mathbb{T}} \left| \frac{1}{\Gamma_1^0(\omega^0, W^0)} \left(\omega_0\theta + \varepsilon \int_0^\theta \overline{Y}_1(W^{0,0}(\sigma), \widetilde{W}^{0,0}(\sigma; \omega^0), \varepsilon)\, d\sigma \right) - W_1^{0,0}(\theta) \right| + \tag{ℓ_2}$$

$$\sup_{\theta\in\mathbb{T}} \left| \varepsilon \int_0^\infty e^{\lambda_0 t} \overline{Y}_2(W^{0,0}(\theta - \omega^0 t), \widetilde{W}^{0,0}(\theta - \omega^0 t; \omega^0), \varepsilon)\, dt - W_2^{0,0}(\theta) \right|. \tag{ℓ_3}$$

Then

$$
\begin{aligned}
(\ell_1) &\leqslant \left|\int_0^1 E_1^0(\theta)\,d\theta\right|,\\
(\ell_2) &\leqslant \sup_\theta \frac{1}{|\Gamma_1^0(\omega^0,\ W^0)|}\left(\left|\int_0^\theta E_1^0(\sigma)\,d\sigma\right| + \|W_1^{0,0}\|_\infty\left|\int_0^1 E_1^0(\theta)\,d\theta\right|\right), \qquad (\ell_2')\\
(\ell_3) &\leqslant \sup_\theta\left|\int_0^\infty e^{\lambda_0 t}E_2^0(\theta-\omega^0 t)\,dt\right|.
\end{aligned}
$$

Since $\Gamma_1^0(\omega^0,\ W^0)$ is in I^0 and $W^{0,0}$ is bounded by B^0, then

$$
(\ell_2') \leqslant \frac{2}{|\omega_0|}\sup_\theta\left(\left|\int_0^\theta E_1^0(\sigma)\,d\sigma\right| + B^0\left|\int_0^1 E_1^0(\theta)\,d\theta\right|\right).
$$

Combining it with eq. (4.49), we arrive to a bound which only depends on ε, B^0, ω_0, λ_0, and the ones for μ_0 coming from Lemma **4.18**,

$$
d\big((\omega^0,W^{0,0}),(\omega,W^0)\big) \leqslant \frac{1}{1-\mu_0}\left[\frac{|\omega_0|+2+2B^0}{|\omega_0|}\|E_1^0\|_\infty + \frac{1}{|\lambda_0|}\|E_2^0\|_\infty\right]. \tag{4.50}
$$

Finally to get eq. (4.32) we use the interpolation inequality as follows

$$
\begin{aligned}
\|W^{0,0}-W^0\|_{C^l} &\leqslant c(l,L)\|W^{0,0}-W^0\|_{C^0}^{1-\frac{l}{L}}\|W^{0,0}-W^0\|_{C^L}^{\frac{l}{L}}\\
&\leqslant c(l,L)\|W^{0,0}-W^0\|_{C^0}^{1-\frac{l}{L}}(2B^0)^{\frac{l}{L}},
\end{aligned}
$$

for some constant $c(l,L)>0$.

4.7.3 Proof for the isochrons, Theorem 4.12

1st order proof; W^1 and λ

Using Proposition **4.3** in eq. (4.16) we can consider the operator Γ^1 defined by

$$
\begin{aligned}
\Gamma^1(b,F_1,F_2)(\theta) &= \begin{pmatrix}\Gamma_1^1(b,F)\\ \Gamma_2^1(b,F)(\theta)\\ \Gamma_3^1(b,F)(\theta)\end{pmatrix}\\
&= \begin{pmatrix}\lambda_0+\varepsilon\int_0^1 \overline{Y}_2^1(\theta,b,F,\varepsilon)d\theta\\ -\varepsilon\int_0^\infty e^{bt}\overline{Y}_1^1(\theta+\omega t,b,F,\varepsilon)\,dt\\ C(b,F)+\frac{\varepsilon}{\omega}\int_0^\theta \overline{Y}_2^1(\sigma,b,F,\varepsilon)-\big[\int_0^1 \overline{Y}_2^1(\theta,b,F,\varepsilon)\,d\theta\big]F_2(\sigma)\,d\sigma\end{pmatrix},
\end{aligned} \tag{4.51}
$$

where

$$C(b,F) \coloneqq 1 - \frac{\varepsilon}{\omega}\int_0^1\int_0^\theta \overline{Y}^1{}_2(\sigma,b,F,\varepsilon)\,d\sigma\,d\theta + \frac{\varepsilon}{\omega}\left[\int_0^1 \overline{Y}^1{}_2(\theta,b,F,\varepsilon)\,d\theta\right]\int_0^1\int_0^\theta F_2(\sigma)\,d\sigma\,d\theta \tag{4.52}$$

is a constant to ensure that $\Gamma_3^1(b,F)$ satisfies the normalisation condition considered in eq. (4.19), i.e. $\int_0^1 \Gamma_3^1(b,F)(\theta)\,d\theta = 1$.

Therefore a fixed-point for the operator Γ^1 verifies the invariance equation, eq. (4.16) and the normalisation condition in eq. (4.19).

Let $D^1 = I^1 \times \mathcal{C}_1^{L+\mathrm{Lip}}$ be the domain of Γ^1 where for a constant $B^1 > 0$,

$$I^1 \coloneqq \{b \in \mathbb{R}\colon |b-\lambda_0| \leqslant |\lambda_0|/3\},$$
$$\mathcal{C}_1^{L+\mathrm{Lip}} \coloneqq \left\{ f \in C_{B^1}^{L-1+\mathrm{Lip}}(\widetilde{\mathbb{T}}, \widetilde{\mathbb{T}}\times\mathbb{R})\colon f(\theta+1) = f(\theta), \text{ and } \int_0^1 f_2(\theta)\,d\theta = 1 \right\}.$$

Formally I^1 should be a subset of $\mathbb{C}$ since we have an eigenvalue problem. However, λ_0 is real and since we are interested in the slowest manifold, it will be enough to consider I^1 as subset of $\mathbb{R}$.

Similarly to section **4.7.2**, we split the conditions in Lemma **4.15**.

LEMMA 4.20. *There is $\varepsilon_1^1 > 0$ such that for all $0 < \varepsilon \leqslant \varepsilon_1^1$, $\Gamma^1(D^1) \subset D^1$.*

Proof. First of all, since $\overline{Y}^1{}_2(\theta,b,F,\varepsilon)$ is bounded, for small ε let us say ϵ_1, we can have $\Gamma_1^1(b,F)$ in I^1.

Because of the periodicity in the already known W^0 and the periodicity w.r.t. the first component of $\overline{r\circ K}$, then $\overline{Y}^1{}_1(\theta+1,b,F,\varepsilon) = \overline{Y}^1{}_1(\theta,b,F,\varepsilon)$. And also

$$\Gamma_2^1(b,F)(\theta+1) = \Gamma_2^1(b,F)(\theta).$$

To see the boundness of the nth derivative of $\Gamma_2^1(b,F)(\theta)$, with $0 \leqslant n < L$, i.e., of

$$\frac{d^n}{d\theta^n}\Gamma_2^1(b,F)(\theta) = -\varepsilon\int_0^\infty e^{bt}\frac{\partial^n}{\partial\theta^n}\overline{Y}^1{}_1(\theta+\omega t,b,F,\varepsilon)\,dt.$$

By the dominated convergence Theorem, it suffices to see $\frac{\partial^n}{\partial\theta^n}\overline{Y}^1{}_1(\theta+\omega t,b,F,\varepsilon)$ is bounded. By Faà di Bruno's formula (see [AR67]), $\frac{\partial^n}{\partial\theta^n}\overline{Y}^1{}_1(\theta+\omega t,b,F,\varepsilon)$ is bounded because the smoothness of $\overline{Y}$, $\overline{r\circ K}$, and $W^0(\theta)$, whenever F is in $C_{B^1}^{L-1+\mathrm{Lip}}$. Furthermore, due to the same argument, $\frac{d^{L-1}}{d\theta^{L-1}}\Gamma_2^1(b,F)(\theta)$ is Lipschitz.

To see the periodicity of $\Gamma_3^1(b,F)(\theta)$, we first compute its derivative, i.e.,

$$\frac{d}{d\theta}\Gamma_3^1(b,F)(\theta) = \frac{\varepsilon}{\omega}\overline{Y}_2^1(\theta,b,F,\varepsilon) - \frac{\varepsilon}{\omega}\left(\int_0^1 \overline{Y}_2^1(\theta,b,F,\varepsilon)\,d\theta\right)F_2(\theta)$$

which is periodic. Hence, to show periodicity of $\Gamma_3^1(b,F)(\theta)$, it suffices to see that $\Gamma_3^1(b,F)(0) = \Gamma_3^1(b,F)(1)$, which is true because $\int_0^1 F_2(\theta)d\theta = 1$. The choice of the constant $C(b,F)$ ensures the normalisation condition, that is, $\int_0^1 \Gamma_3^1(b,F)(\theta)d\theta = 1$.

Now for $2 \leqslant n < L$

$$\frac{d^n}{d\theta^n}\Gamma_3^1(b,F)(\theta) = \frac{\varepsilon}{\omega}\Bigg[\frac{d^{(n-1)}}{d\theta^{(n-1)}}\overline{Y}_2^1(\theta,b,F,\varepsilon) - \left(\int_0^1 \overline{Y}_2^1(\theta,b,F,\varepsilon)\,d\theta\right)\frac{d^{(n-1)}}{d\theta^{(n-1)}}F_2(\theta)\Bigg],$$

which will be bounded due to the smoothness of $\overline{Y}$, $\overline{r\circ K}$, and $W^0(\theta)$, as well as because F is in $C_{B^1}^{L-1+Lip}$. Similarly, we conclude $\frac{d^{L-1}}{d\theta^{L-1}}\Gamma_3^1(b,F)(\theta)$ to be Lipschitz.

Since ε appeared in front of all the expressions of the derivatives, there is $\epsilon_2 > 0$ depending on derivative bounds of $\overline{Y}$, $\overline{r\circ K}$, B^0, and B^1. Such a ϵ_2 can be chosen uniformly of the choice of $(b,F) \in D^1$. Therefore $(\Gamma_2^1(b,F),\Gamma_3^1(b,F))$ can be $C_{B^1}^{L-1+\mathrm{Lip}}$ for all $\varepsilon \leqslant \min\{\epsilon_1,\epsilon_2\} =: \varepsilon_1^1$. □

LEMMA 4.21. *There is $\varepsilon_2^1 > 0$, such that for all $0 < \varepsilon \leqslant \varepsilon_2^1$ the operator Γ^1 in eq. (4.51) is a contraction with the norm in D^1 defined by*

$$d((b,F),(b',F')) \coloneqq |b-b'| + \|F-F'\|_\infty. \tag{4.53}$$

Proof. We must show that there is $0 < \mu_1 < 1$ such that

$$d(\Gamma^1(b,F),\Gamma^1(b',F')) < \mu_1 d((b,F),(b',F')). \tag{4.54}$$

By definition, $d(\Gamma^1(b,F),\Gamma^1(b',F'))$ can be bounded by

$$\varepsilon\left|\int_0^1 \overline{Y}_2^1(\theta,b,F,\varepsilon) - \overline{Y}_2^1(\theta,b',F',\varepsilon)\,d\theta\right| \tag{4.55}$$

plus the maximum between

$$\varepsilon\sup_{\theta\in\mathbb{T}}\left|\int_0^\infty e^{bt}\overline{Y}_1^1(\theta+\omega t,b,F,\varepsilon) - e^{b't}\overline{Y}_1^1(\theta+\omega t,b',F',\varepsilon)\,dt\right|, \tag{4.56}$$

and

$$\sup_{\theta\in\mathbb{T}}\frac{\varepsilon}{|\omega|}\Bigg|\int_0^\theta \overline{Y}^1_2(\sigma,b,F,\varepsilon)-\left[\int_0^1 \overline{Y}^1_2(\theta,b,F,\varepsilon)\,d\theta\right]F_2(\sigma)\,d\sigma- \int_0^\theta \overline{Y}^1_2(\sigma,b',F',\varepsilon)+\left[\int_0^1 \overline{Y}^1_2(\theta,b',F',\varepsilon)\,d\theta\right]F_2'(\sigma)\,d\sigma\Bigg|+ |C(F,b)-C(F',b')|. \tag{4.57}$$

Because of eq. (4.17), $\overline{Y}^1$ has the form

$$\overline{Y}^1(\theta,\lambda,W^1,\varepsilon)=A(\theta)W^1(\theta)+B(\theta;\lambda)W^1(\theta-\omega r\circ K\circ W^0(\theta)).$$

Introducing the notation

$$A(\theta)=\begin{pmatrix}A_{11}(\theta) & A_{12}(\theta)\\ A_{21}(\theta) & A_{22}(\theta)\end{pmatrix},\quad \text{and}\quad B(\theta;\lambda)=\begin{pmatrix}B_{11}(\theta;\lambda) & B_{12}(\theta;\lambda)\\ B_{21}(\theta;\lambda) & B_{22}(\theta;\lambda)\end{pmatrix}.$$

Then $\overline{Y}^1(\theta,\lambda,W^1,\varepsilon)$ can explicitly be expressed as

$$\begin{aligned}\overline{Y}^1_1(\theta,\lambda,W^1,\varepsilon)=&A_{11}(\theta)W^1_1(\theta)+A_{12}(\theta)W^1_2(\theta)\\ &+B_{11}(\theta;\lambda)W^1_1(\theta-\omega\overline{r\circ K}\circ W^0(\theta))\\ &+B_{12}(\theta;\lambda)W^1_2(\theta-\omega\overline{r\circ K}\circ W^0(\theta)),\end{aligned}$$

and

$$\begin{aligned}\overline{Y}^1_2(\theta,\lambda,W^1,\varepsilon)=&A_{21}(\theta)W^1_1(\theta)+A_{22}(\theta)W^1_2(\theta)\\ &+B_{21}(\theta;\lambda)W^1_1(\theta-\omega\overline{r\circ K}(W^0(\theta)))\\ &+B_{22}(\theta;\lambda)W^1_2(\theta-\omega\overline{r\circ K}(W^0(\theta))).\end{aligned}$$

Since b and b' are in I^1, we estimate

$$\|B(\theta;b)\|_\infty\leqslant e^{-\frac{4}{3}\lambda_0\|\overline{r\circ K}\|_\infty}\|D_2\overline{Y}\|_\infty,$$

and

$$\|B(\theta;b)-B(\theta;b')\|_\infty\leqslant\|D_2\overline{Y}\|_\infty e^{-\frac{4}{3}\lambda_0\|\overline{r\circ K}\|}\|\overline{r\circ K}\|_\infty|b-b'|.$$

Hence a bound for $\|\overline{Y}^1(\theta,b,F,\varepsilon)-\overline{Y}^1(\theta,b',F',\varepsilon)\|_\infty$ and for its components will be

$$\begin{aligned}&\|A\|_\infty\|F-F'\|_\infty+\|B(\theta;b)\|_\infty\|F-F'\|_\infty+\|B(\theta;b)-B(\theta;b')\|_\infty\|F'\|_\infty\\ &\qquad\leqslant(\|A\|_\infty+e^{-\frac{4}{3}\lambda_0\|\overline{r\circ K}\|_\infty}\|D_2\overline{Y}\|_\infty)\|F-F'\|_\infty+\\ &\qquad\qquad B^1\|D_2\overline{Y}\|_\infty e^{-\frac{4}{3}\lambda_0\|\overline{r\circ K}\|_\infty}\|\overline{r\circ K}\|_\infty|b-b'|\end{aligned}\tag{4.58}$$

Similarly $\|\overline{Y}_1^1(\theta, b, F, \varepsilon)\|_\infty$ and its components, is bounded by

$$B^1(\|A\|_\infty + e^{-\frac{4}{3}\lambda_0\|\overline{r\circ K}\|_\infty}\|D_2\overline{Y}\|_\infty),$$

Now we can bound eq. (4.55) as

$$|\Gamma_1^1(b, F) - \Gamma_1^1(b', F')| \leqslant \varepsilon eq.\ (4.58). \tag{4.59}$$

To bound $|\Gamma_2^1(b, F) - \Gamma_2^1(b', F')|$ let us just adding, and subtracting terms to get

$$\begin{aligned} e^{bt}\overline{Y}_1^1(\theta + \omega t, b, F, \varepsilon) - e^{b't}\overline{Y}_1^1(\theta + \omega t, b', F', \varepsilon) = \\ e^{bt}(\overline{Y}_1^1(\theta + \omega t, b, F, \varepsilon) - \overline{Y}_1^1(\theta + \omega t, b', F', \varepsilon)) + \\ (e^{bt} - e^{b't})\overline{Y}_1^1(\theta + \omega t, b', F', \varepsilon). \end{aligned}$$

Since b and b' are in I^1, then $|\int_0^\infty e^{bt} - e^{b't}\, dt| \leqslant \frac{9}{4\lambda_0^2}|b - b'|$. Hence, $|\Gamma_2^1(b, F) - \Gamma_2^1(b', F')|$ is finally bounded by

$$\begin{aligned} &\frac{3\varepsilon}{2|\lambda_0|}(\|A\|_\infty + e^{-\frac{4}{3}\lambda_0\|\overline{r\circ K}\|_\infty}\|D_2\overline{Y}\|_\infty)\|F - F'\|_\infty + \\ &\qquad \frac{3B^1\varepsilon}{2|\lambda_0|}\left[e^{-\frac{4}{3}\lambda_0\|\overline{r\circ K}\|_\infty}\|D_2\overline{Y}\|_\infty\left(\|\overline{r\circ K}\|_\infty + \frac{3}{2|\lambda_0|}\right) + \frac{3\|A\|_\infty}{2|\lambda_0|}\right]|b - b'| \end{aligned}$$

Finally, $|\Gamma_3^1(b, F) - \Gamma_3^1(b', F')|$ can be bounded similarly, in this case, by adding and subtracting by the term

$$\int_0^1 \overline{Y}_1^1(\theta, b, F, \varepsilon)\, d\theta F'(\sigma)$$

which leads to a bound for the integrals in eq. (4.57)

$$\begin{aligned} &(1 + 2B^1)(\|A\|_\infty + e^{-\frac{4}{3}\lambda_0\|\overline{r\circ K}\|_\infty}\|D_2\overline{Y}\|_\infty)\|F - F'\|_\infty \\ &\qquad B^1(1 + B^1)\|D_2\overline{Y}\|_\infty e^{-\frac{4}{3}\lambda_0\|\overline{r\circ K}\|_\infty}\|\overline{r\circ K}\|_\infty|b - b'|. \end{aligned} \tag{4.60}$$

The same previous bound allows to estimate $|C(F, b) - C(F', b')|$ and then is,

$$eq.\ (4.57) \leqslant \frac{2\varepsilon}{|\omega|} eq.\ (4.60).$$

Combine all the estimations above, we can find constants c_1 and c_2 such that,

$$d(\Gamma^1(b, F), \Gamma^1(b', F')) \leqslant \varepsilon(c_1|b - b'| + c_2\|F - F'\|_\infty).$$

Therefore, for small enough ε, we will have a contraction. □

With the two previous lemmas we have proved that taking an $0 < \varepsilon \leqslant \min\{\varepsilon_1^1, \varepsilon_2^1\}$ where ε_1^1 comes from lemma **4.20** and ε_2^1 from lemma **4.21**, then for all $(\lambda^0, W^{1,0}(\theta)) \in D^1$, for instance $\lambda^0 = \lambda_0$ and $W^{1,0}(\theta) = \left(\begin{smallmatrix} 0 \\ 1 \end{smallmatrix}\right)$ there is a unique limit in C^0 by the operator Γ^1 which solves eq. (4.16).

Similar to eq. (4.49)

$$d\big((\lambda^0, W^{1,0}), (\lambda, W^1)\big) \leqslant \frac{1}{1-\mu_1} d\big((\lambda^0, W^{1,0}), \Gamma^1(\lambda^0, W^{1,0})\big). \tag{4.61}$$

And we must provide an estimation of $d\big((\lambda^0, W^{1,0}), \Gamma^1(\lambda^0, W^{1,0})\big)$ in terms of the norm of the error function of the invariance equation eq. (4.16), i.e. $\|E^1\|$ where $E^1 \equiv (E_1^1, E_2^1)$ is

$$E^1(\theta) \coloneqq \left[\omega\partial_\theta - \begin{pmatrix} \lambda & 0 \\ 0 & \lambda - \lambda_0 \end{pmatrix}\right] W^{1,0}(\theta) - \varepsilon \overline{Y}^1(\theta, \lambda, W^1, \varepsilon)$$

with $\overline{Y}^1(\theta, \lambda, W^1, \varepsilon)$ given in eq. (4.17). Thus $d\big((\lambda^0, W^{1,0}), \Gamma^1(\lambda^0, W^{1,0})\big)$ admits a first estimation

$$\left|\lambda_0 + \varepsilon \int_0^1 \overline{Y}_2^1(\theta, \lambda^0, W^{1,0}, \varepsilon)\, d\theta - \lambda^0\right| + \tag{ℓ_1}$$

$$\sup_{\theta\in\mathbb{T}} \left|W_1^{1,0}(\theta) + \varepsilon \int_0^\infty e^{\lambda^0 t} \overline{Y}_1^1(\theta + \omega t, \lambda^0, W^{1,0}, \varepsilon)\, dt\right| + \tag{ℓ_2}$$

$$\begin{aligned} \sup_{\theta\in\mathbb{T}} \Bigg| C(\lambda^0, W^{1,0}) + \frac{\varepsilon}{\omega} \int_0^\theta \overline{Y}_2^1(\sigma, \lambda^0, W^{1,0}, \varepsilon) - \\ \left[\int_0^1 \overline{Y}_2^1(\theta, \lambda^0, W^{1,0}, \varepsilon)\, d\theta\right] W_2^{1,0}(\sigma)\, d\sigma - W_2^{1,0}(\theta)\Bigg|. \end{aligned} \tag{ℓ_3}$$

Then

$$(\ell_1) \leqslant \left|\int_0^1 E_2^1(\theta)\, d\theta\right|, \qquad \text{(since } \textstyle\int_0^1 W_2^{1,0}(\theta)\, d\theta = 1\text{)}$$

and

$$(\ell_2) \leqslant \left|\int_0^\infty e^{\lambda^0 t} E_1^1(\theta + \omega t)\, dt\right|.$$

To bound (ℓ_3), let us start making the following observation

$$\begin{aligned} \frac{1}{\omega} \int_0^\theta E_2^1(\sigma)\, d\sigma = W_2^{1,0}(\theta) - W_2^{1,0}(0) + \\ \frac{\lambda^0 - \lambda_0}{\omega} \int_0^\theta W_2^{1,0}(\sigma)\, d\sigma - \frac{\varepsilon}{\omega} \int_0^\theta \overline{Y}_2^1(\sigma, \lambda^0, W^{1,0}, \varepsilon)\, d\sigma. \end{aligned}$$

In particular, since $W_2^{1,0}(1) = W_2^{1,0}(0)$ and $\int_0^1 W_2^{1,0}(\theta)\,d\theta = 1$, then

$$\int_0^1 E_2^1(\theta)\,d\theta = \lambda^0 - \lambda_0 - \varepsilon \int_0^1 \overline{Y}_2^1(\theta, \lambda^0, W^{1,0}, \varepsilon)\,d\theta.$$

Thus, it turns out that we can consider equivalent expressions in (ℓ_3). More precisely,

$$\begin{aligned}
&\frac{\varepsilon}{\omega}\int_0^\theta \overline{Y}_2^1(\sigma, \lambda^0, W^{1,0}, \varepsilon) - \left[\int_0^1 \overline{Y}_2^1(\theta, \lambda^0, W^{1,0}, \varepsilon)\,d\theta\right] W_2^{1,0}(\sigma)\,d\sigma = \\
&\quad \frac{\varepsilon}{\omega}\int_0^\theta \overline{Y}_2^1(\sigma, \lambda^0, W^{1,0}, \varepsilon) + \frac{1}{\omega}\left[\int_0^1 E_2^1(\theta)\,d\theta - (\lambda^0 - \lambda_0)\right] W_2^{1,0}(\sigma)\,d\sigma = \\
&\qquad W_2^{1,0}(\theta) - W_2^{1,0}(0) - \frac{1}{\omega}\int_0^\theta E_2^1(\sigma)\,d\sigma + \frac{1}{\omega}\int_0^1 E_2^1(\theta)\,d\theta \int_0^\theta W_2^{1,0}(\sigma)\,d\sigma.
\end{aligned}$$

With the previous identities applied now in $C(\lambda^0, W^{1,0})$, which is defined in eq. (4.52), it is equal to

$$\begin{aligned}
&1 - \int_0^1 \left[W_2^{1,0}(\theta) - W_2^{1,0}(0) - \frac{1}{\omega}\int_0^\theta E_2^1(\sigma)\,d\sigma + \frac{1}{\omega}\int_0^1 E_2^1(\theta)\,d\theta \int_0^\theta W_2^{1,0}(\sigma)\,d\sigma\right] d\theta \\
&\qquad = W_2^{1,0}(0) + \frac{1}{\omega}\int_0^1 \int_0^\theta E_2^1(\sigma)\,d\sigma - \frac{1}{\omega}\int_0^1 E_2^1(\theta)\,d\theta \int_0^1 \int_0^\theta W_2^{1,0}(\sigma)\,d\sigma.
\end{aligned}$$

We have then arrived to

$$\begin{aligned}
(\ell_3) = \frac{1}{|\omega|}\sup_{\theta\in\mathbb{T}}\Bigg|&\int_0^1 \int_0^\theta E_2^1(\sigma) - \int_0^1 E_2^1(\alpha)\,d\alpha W_2^{1,0}(\sigma)\,d\sigma\,d\theta - \\
&\int_0^\theta E_2^1(\sigma) - \int_0^1 E_2^1(\theta)\,d\theta W_2^{1,0}(\sigma)\,d\sigma\Bigg|
\end{aligned}$$

which gives us the bound $(\ell_3) \leqslant \frac{2+2B^1}{|\omega|}\|E_2^1\|_\infty$ since $W^{1,0} \in C_1^{L+\mathrm{Lip}}$.

Combining the previous bounds for (ℓ_1), (ℓ_2) and (ℓ_3) we get a bound for eq. (4.61), that is,

$$\begin{aligned}
d\big((\lambda^0, W^{1,0}), \Gamma^1(\lambda^0, W^{1,0})\big) &\leqslant \frac{1}{|\lambda^0|}\|E_1^1\|_\infty + \left(1 + \frac{2+2B^1}{|\omega|}\right)\|E_2^1\|_\infty \\
&\leqslant \frac{3}{2|\lambda_0|}\|E_1^1\|_\infty + \left(1 + \frac{2+2B^1}{|\omega|}\right)\|E_2^1\|_\infty.
\end{aligned} \tag{4.62}$$

Therefore, we can find a constant C, depending on ε, B^1, ω, and λ_0 such that eq. (4.61) holds and so also eq. (4.35).

Finite order proof; W^j

For a theoretical propose, we do not need to formally proof the existence and uniqueness of W^j with $j \geqslant 2$ to proe the higher order terms. However, we are going to specify the operator, its domain and the fact that for small ε, it will become a C^0-contraction. At this moment, we know (ω, W^0), (λ, W^1) and W^i with $0 \leqslant i < j$ (induction hypothesis). We are going to find W^j. To obtain the invariance equation to be satisfied for W^j, which we put earlier in equation eq. (4.20). We consider the jth order terms in eq. (4.9). Note that the coefficient for s^j in $\widetilde{W}(\theta, s)$, is

$$-\omega DW^0(\theta - \omega\overline{r \circ K} \circ W^0(\theta))D(\overline{r \circ K}) \circ W^0(\theta)W^j(\theta)$$

Therefore, $\overline{Y}^j(\theta, \lambda, W^0, W^j, \varepsilon)$ is of the form:

$$\begin{aligned} &D_1\overline{Y}(W^0(\theta), \widetilde{W}(\theta), \varepsilon)W^j(\theta) - \\ &\omega D_2\overline{Y}(W^0(\theta), \widetilde{W}(\theta), \varepsilon)DW^0(\theta - \omega\overline{r \circ K} \circ W^0(\theta)D(\overline{r \circ K}) \circ W^0(\theta)W^j(\theta). \end{aligned}$$

We also note that $R^j(\theta; \lambda)$ will be some expression in the derivatives of $\overline{Y}$ evaluated at $(W^0(\theta), \widetilde{W}(\theta), \varepsilon)$, multiplied with $W^0, \ldots, W^{j-1}$. Therefore, $R^j(\theta; \lambda)$ will have the same regularity as W^{j-1}. We will see inductively by the following argument that W^j is $(L-1)$ times differentiable with $(L-1)$th derivative Lipschitz.

We define the following operator Γ^j,

$$\Gamma^j(G)(\theta) = \begin{pmatrix} -\varepsilon \int_0^\infty e^{\lambda jt}\left(\overline{Y}^j_1(\theta + \omega t, G, \varepsilon) + R^j_1(\theta + \omega t; \lambda)\right) dt \\ -\varepsilon \int_0^\infty e^{(\lambda j - \lambda_0)t}\left(\overline{Y}^j_2(\theta + \omega t, G, \varepsilon) + R^j_2(\theta + \omega t; \lambda)\right) dt \end{pmatrix}$$

whose domain of definition is for $B^j > 0$

$$\mathcal{C}^{L-1+\mathrm{Lip}}_j \coloneqq \{f \in C^{L-1+\mathrm{Lip}}_{B^j}(\widetilde{\mathbb{T}}, \widetilde{\mathbb{T}} \times \mathbb{R})\colon f(\theta + 1) = f(\theta)\},$$

Assume that we have already obtained W^k in $\mathcal{C}^k$ for $0 \leqslant k < j$, we have the following:

LEMMA 4.22. *There is* $\varepsilon^j_1 > 0$ *such that for all* $0 < \varepsilon \leqslant \varepsilon^j_1$, $\Gamma^j(\mathcal{C}^{L-1+\mathrm{Lip}}_j) \subset \mathcal{C}^{L-1+\mathrm{Lip}}_j$.

This follows from that $\lambda < 0$ and $(\lambda j - \lambda_0) < 0$ for $j \geqslant 2$ and the regularity of $W^0, \ldots, W^j$, $\overline{Y}^j$, and R^j, and all the derivative could be bounded thanks to the ε in front of them. Since it is very similar to the analysis of W^0 and W^1, we will omit the detailed proof here.

We also know that Γ^j is a C^0 contraction for small ε.

LEMMA 4.23. *There is $\varepsilon_2^j > 0$ such that for all $0 < \varepsilon \leqslant \varepsilon_2^j$, Γ^j is a contraction in C^0 distance.*

This follows easily from that $\lambda < 0$ and $(\lambda j - \lambda_0) < 0$ for $j \geqslant 2$, and $\overline{Y}^j$ is linear in W^j. Thus, similarly to Lemma **4.18** or Lemma **4.21** there is $0 < \mu_j < 1$, such that

$$\|\Gamma(G) - \Gamma(G')\|_\infty \leqslant \mu_j \|G - G'\|_\infty.$$

Taking any initial guess $W^{j,0} \in \mathcal{C}^j$, we would take $W^{j,0}(\theta) = \binom{0}{0}$, the sequence $(\Gamma^j)^n(W^{j,0})$ has a limit in $\mathcal{C}^j$, we denote it by W^j. W^j is a fixed point of operator Γ^j and it solves eq. (4.20). W^j is unique in the sense of C^0, close to the initial guess, by the contraction argument. We will see quantitative estimates below.

We know that

$$\|W^j - W^{j,0}\|_\infty \leqslant \frac{1}{1-\mu_j} \|W^{j,0} - \Gamma^j(W^{j,0})\|_\infty.$$

With similar argument as in the error estimation of W^0 and W^1, we have

$$\begin{aligned} |W_1^{j,0}(\theta) - \Gamma_1^j(W^{j,0})(\theta)| &\leqslant -\frac{1}{j\lambda} \|E_1^j\|_\infty, \\ |W_2^{j,0}(\theta) - \Gamma_2^j(W^{j,0})(\theta)| &\leqslant -\frac{1}{j\lambda - \lambda_0} \|E_2^j\|_\infty. \end{aligned}$$

Therefore, we have

$$\|W^j - W^{j,0}\|_\infty \leqslant \frac{1}{1-\mu_j} \left(-\frac{1}{j\lambda} \|E_1^j\|_\infty - \frac{1}{j\lambda - \lambda_0} \|E_2^j\|_\infty \right) \leqslant C \|E^j\|_\infty. \quad (4.63)$$

We stress that in above, C depend on j, ε, and the SDDE, however, C does not depend on $W^{j,0}$.

Remainder proof; $W^>$

From now on, we will write:

$$W(\theta, s) = W^\leqslant(\theta, s) + W^>(\theta, s), \quad (4.64)$$

where $W^\leqslant(\theta, s) = \sum_{j=0}^{N-1} W^j(\theta) s^j$. Theoretically it is enough to take $N = 2$ although one may want to get for larger N's in practical computations. To make the analysis feasible, we do a cut-off to the equation satisfied by $W^>$ in eq. (4.22). It is needed in our method. This is not too restrictive. Indeed, we

have seen when we apply our results to the original locally defined problem in section **4.4.3**, what happens for s with large absolute value is not important.

Now let $c(t) = (\theta + \omega t, se^{\lambda t})$ be the characteristics, we define an operator as follows:

$$\Gamma^{>}(H)(\theta, s) = -\varepsilon \int_0^{\infty} \begin{pmatrix} 1 & 0 \\ 0 & e^{-\lambda_0 t} \end{pmatrix} Y^{>}(H, c(t), \varepsilon)\phi(se^{\lambda t})\, dt. \tag{4.65}$$

A fixed point of $\Gamma^{>}$ solves the extended invariance equation, eq. (4.22). The domain of $\Gamma^{>}$, denoted by $D^{>}$, consists in the space of continuous functions $H\colon \widetilde{\mathbb{T}} \times \mathbb{R} \to \widetilde{\mathbb{T}} \times \mathbb{R}$, where $\partial_\theta^l \partial_s^m H_i(\theta, s)$, $i = 1, 2$, exists for all (θ, s) in $\widetilde{\mathbb{T}} \times \mathbb{R}$ if $l + m \leqslant L^{>}$ and moreover it has a bounded norm $\| \cdot \|_{L^{>},N}$ with bound $B > 0$. The norm is defined by

$$\|H\|_{L^{>},N} = \max_{l+m\leqslant L^{>}, i=1,2} \begin{cases} \sup\limits_{(\theta,s)\in\widetilde{\mathbb{T}}\times\mathbb{R}} |\partial_\theta^l \partial_s^m H_i(\theta, s)||s|^{-(N-m)} & \text{if } m \leqslant N, \\ \sup\limits_{(\theta,s)\in\widetilde{\mathbb{T}}\times\mathbb{R}} |\partial_\theta^l \partial_s^m H_i(\theta, s)| & \text{if } m > N. \end{cases} \tag{4.66}$$

Under above notations in eq. (4.64), we have

$$\begin{aligned} \widetilde{W}(\theta, s) &= W(\theta - \omega\overline{r \circ K} \circ W(\theta, s), e^{-\lambda\overline{r\circ K}\circ W(\theta,s)}) \\ &= W^{\leqslant}(\theta - \omega\overline{r \circ K} \circ W(\theta, s), e^{-\lambda\overline{r\circ K}\circ W(\theta,s)}) \\ &\quad + W^{>}(\theta - \omega\overline{r \circ K} \circ W(\theta, s), e^{-\lambda\overline{r\circ K}\circ W(\theta,s)}), \end{aligned}$$

and we define

$$\widetilde{W}^{>}(\theta, s) \coloneqq W^{>}\big(\theta - \omega\overline{r \circ K} \circ (W^{\leqslant} + W^{>})(\theta, s), e^{-\lambda\overline{r\circ K}\circ(W^{\leqslant}+W^{>})(\theta,s)}\big). \tag{4.67}$$

LEMMA 4.24. *There is $\varepsilon_1^{>} > 0$ such that for all $0 < \varepsilon \leqslant \varepsilon_1^{>}$, $\Gamma^{>}(D^{>}) \subset D^{>}$.*

Proof. We must prove that for $i = 1, 2$, and $l + m \leqslant L^{>}$, the derivatives $\partial_\theta^l \partial_s^m \Gamma_i^{>}(H)(\theta, s)$ exist and also that $\|\Gamma^{>}(H)\|_{L^{>},N}$ is bounded by the constant B. Let us define, similarly to eq. (4.67),

$$\widetilde{H}(\theta, s) \coloneqq H(\theta - \omega\overline{r \circ K} \circ (W^{\leqslant} + H)(\theta, s), se^{-\lambda\overline{r\circ K}\circ(W^{\leqslant}+H)(\theta,s)}).$$

We first claim that if $\|H\|_{L^{>},N} \leqslant B$, then we can find a constant C, which does not depend on the choice of H, such that for $l + m \leqslant L^{>}$, $i = 1, 2$, and for all $(\theta, s) \in \widetilde{\mathbb{T}} \times [-1, 1]$,

$$\begin{cases} |\partial_\theta^l \partial_s^m \widetilde{H}_i(\theta, s)| \leqslant C|s|^{(N-m)} & \text{if} \quad m \leqslant N, \\ |\partial_\theta^l \partial_s^m \widetilde{H}_i(\theta, s)| \leqslant C & \text{if} \quad m > N, \end{cases} \tag{4.68}$$

where C may vary from line to line. But we will take C to be the maximum of all C's at each steps. To prove the previous claim, let us notice that $\|H\|_{L^>,N} \leqslant B$ implies that for $l+m \leqslant L^>$ and $(\theta,s) \in \widetilde{\mathbb{T}} \times \mathbb{R}$,

$$\begin{cases} |\partial_\theta^l \partial_s^m H_i(\theta,s)| \leqslant B|s|^{(N-m)} & \text{if} \quad m \leqslant N, \\ |\partial_\theta^l \partial_s^m H_i(\theta,s)| \leqslant B & \text{if} \quad m > N. \end{cases}$$

Then

$$|\widetilde{H}_i(\theta,s)| \leqslant B|s|^N e^{-\lambda N \overline{r\circ K}\circ(W^{\leqslant}+H)(\theta,s)}.$$

By boundedness of $\overline{r\circ K}$, we have $|\widetilde{H}_i(\theta,s)| \leqslant C|s|^N$.

$$\begin{aligned} \frac{\partial}{\partial\theta}\widetilde{H}_i(\theta,s) = \partial_\theta H_i\big(\theta - \omega\overline{r\circ K}\circ(W^{\leqslant}+H)(\theta,s), se^{-\lambda\overline{r\circ K}\circ(W^{\leqslant}+H)(\theta,s)}\big)\cdot \\ \big(1-\omega D(\overline{r\circ K})\circ(W^{\leqslant}+H)(\theta,s)\partial_\theta(W^{\leqslant}+H)(\theta,s)\big) \\ + \partial_s H_i\big(\theta - \omega\overline{r\circ K}\circ(W^{\leqslant}+H)(\theta,s), se^{-\lambda\overline{r\circ K}\circ(W^{\leqslant}+H)(\theta,s)}\big)\cdot \\ s(-\lambda)D(\overline{r\circ K})\circ(W^{\leqslant}+H)(\theta,s)\partial_\theta(W^{\leqslant}+H)(\theta,s)e^{-\lambda\overline{r\circ K}\circ(W^{\leqslant}+H)(\theta,s)}. \end{aligned}$$

Then, we have

$$\begin{aligned} \left|\frac{\partial}{\partial\theta}\widetilde{H}_i(\theta,s)\right| \leqslant B|s|^N e^{-\lambda N\|\overline{r\circ K}\|_\infty}(1+|\omega|\|D(\overline{r\circ K})\|_\infty\|\partial_\theta(W^{\leqslant}+H)\|_\infty)+ \\ B|s|^{N-1}e^{-\lambda(N-1)\|\overline{r\circ K}\|_\infty}|s||\lambda|\|D(r\circ K)\|_\infty e^{-\lambda\|r\circ K\|_\infty}\|\partial_\theta(W^{\leqslant}+H)\|_\infty. \end{aligned}$$

The regularity of $W^{\leqslant}$, H, $\overline{r\circ K}$ lead to

$$\left|\frac{\partial}{\partial\theta}\widetilde{H}_i(\theta,s)\right| \leqslant C|s|^N.$$

Above C may depend on B, but it will not depend on the choice of $H \in D^>$. Similarly,

$$\begin{aligned} \frac{\partial}{\partial_s}\widetilde{H}_i(\theta,s) = \partial_\theta H_i(\theta - \omega\overline{r\circ K}\circ(W^{\leqslant}+H)(\theta,s), se^{-\lambda\overline{r\circ K}\circ(W^{\leqslant}+H)(\theta,s)})\cdot \\ (-\omega)D(\overline{r\circ K})\circ(W^{\leqslant}+H)(\theta,s)\partial_s(W^{\leqslant}+H)(\theta,s) \\ + \partial_s H_i(\theta - \omega\overline{r\circ K}\circ W^{\leqslant}+H)(\theta,s), se^{-\lambda\overline{r\circ K}\circ(W^{\leqslant}+H)(\theta,s)})\cdot \\ \big(1+s(-\lambda)D(\overline{r\circ K})\circ(W^{\leqslant}+H)(\theta,s)\partial_s(W^{\leqslant}+H)(\theta,s)\big)e^{-\lambda\overline{r\circ K}\circ(W^{\leqslant}+H)(\theta,s)}. \end{aligned}$$

Then,

$$\begin{aligned} \left|\frac{\partial}{\partial s}\widetilde{H}_i(\theta,s)\right| \leqslant B|s|^{N-1}e^{-\lambda(N-1)\|\overline{r\circ K}\|_\infty} \\ + B|s|^N e^{-\lambda N\|\overline{r\circ K}\|_\infty}\big(|\lambda|+|\omega|\big)\|D(\overline{r\circ K})\|_\infty\|\partial_s(W^{\leqslant}+H)\|_\infty. \end{aligned}$$

Since we have $|s| \leqslant 1$, regularity of $W^{\leqslant}$ and H lead to

$$\left|\frac{\partial}{\partial s}\widetilde{H}_i(\theta, s)\right| \leqslant C|s|^{N-1}$$

where C does not depend on the choice of H as long as $\|H\|_{L^{>},N} \leqslant B$. The proof of the claim is then finished by induction.

Now we observe that we can bound the integrand in the operator $\Gamma^{>}$, eq. (4.65). Indeed, we claim that there exists a constant C, such that if $\|H\|_{L^{>},N} \leqslant B$, then $\|Y(H, \theta, s, \varepsilon)\phi(s)\|_{L^{>},N} \leqslant C$.

Note that by definition of the cut-off function ϕ, it suffices to consider $s \in [-1, 1]$. Also

$$Y^{>}(H, \theta, s, \varepsilon) = \overline{Y}\big((W^{\leqslant} + H)(\theta, s), (\widetilde{W^{\leqslant} + H})(\theta, s), \varepsilon\big) - \sum_{i=0}^{N-1} \overline{Y}^i(\theta)s^i,$$

where

$$\overline{Y}^i(\theta) = \frac{1}{i!}\frac{\partial^i}{\partial s^i}\big(\overline{Y}((W^{\leqslant} + H)(\theta, s), (\widetilde{W^{\leqslant} + H})(\theta, s), \varepsilon)\big)|_{s=0}.$$

Adding and subtracting terms in above expression turns out $Y^{>}(H, \theta, s, \varepsilon)$ to be equal to

$$\begin{aligned}&\overline{Y}((W^{\leqslant} + H)(\theta, s), (\widetilde{W^{\leqslant} + H})(\theta, s), \varepsilon) - \\ &\overline{Y}(W^{\leqslant}(\theta, s), \widetilde{W^{\leqslant}}(\theta, s), \varepsilon) +\end{aligned} \tag{ℓ_1}$$

$$\begin{aligned}&\overline{Y}(W^{\leqslant}(\theta, s), \widetilde{W^{\leqslant}}(\theta, s), \varepsilon) - \\ &\overline{Y}(W^{\leqslant}(\theta, s), W^{\leqslant}(\theta - \omega\overline{r \circ K} \circ W^{\leqslant}(\theta, s), se^{-\lambda\overline{r\circ K}\circ W^{\leqslant}(\theta,s)}), \varepsilon) +\end{aligned} \tag{ℓ_2}$$

$$\begin{aligned}&\overline{Y}(W^{\leqslant}(\theta, s), W^{\leqslant}(\theta - \omega\overline{r \circ K} \circ W^{\leqslant}(\theta, s), se^{-\lambda\overline{r\circ K}\circ W^{\leqslant}(\theta,s)}), \varepsilon) \\ &\quad - \sum_{i=0}^{N-1} \overline{Y}^i(\theta)s^i,\end{aligned} \tag{ℓ_3}$$

with

$$\widetilde{W^{\leqslant}}(\theta, s) \coloneqq W^{\leqslant}\big(\theta - \omega\overline{r \circ K} \circ (W^{\leqslant} + H)(\theta, s), se^{-\lambda\overline{r\circ K}\circ(W^{\leqslant}+H)(\theta,s)}\big).$$

Let us establish bounds for (ℓ_1), (ℓ_2), and (ℓ_3).

$$\begin{aligned}(\ell_1) = \int_0^1 &D_1\overline{Y}\big((1-t)W^{\leqslant}(\theta, s) + t(W^{\leqslant} + H)(\theta, s), (\widetilde{W^{\leqslant} + H})(\theta, s), \varepsilon\big)H(\theta, s) \\ &+ D_2\overline{Y}\big(W^{\leqslant}(\theta, s), (1-t)\widetilde{W^{\leqslant}}(\theta, s) + t(\widetilde{W^{\leqslant} + H})(\theta, s), \varepsilon\big)\widetilde{H}(\theta, s)\, dt.\end{aligned}$$

By the regularity of $\overline{Y}$ and $W^{\leqslant}$, and $\|H\|_{L^{>},N} \leqslant B$, using that $\widetilde{H}$ satisfy eq. (4.68), we conclude that $\|(\ell_1)\phi(s)\|_{L^{>},N} \leqslant C$.

Similarly (ℓ_2) is equal to

$$\int_0^1 D_2\overline{Y}\big(W^{\leqslant}(\theta,s), W^{\leqslant}(\theta-\omega\overline{r\circ K}\circ(W^{\leqslant}+tH)(\theta,s), se^{-\lambda\overline{r\circ K}\circ(W^{\leqslant}+tH)(\theta,s)}),\varepsilon)\cdot$$
$$\big[\partial_\theta W^{\leqslant}(\theta-\omega\overline{r\circ K}\circ(W^{\leqslant}+tH)(\theta,s), se^{-\lambda\overline{r\circ K}\circ(W^{\leqslant}+tH)(\theta,s)}),\varepsilon)$$
$$(-\omega)D(\overline{r\circ K})\circ(W^{\leqslant}+tH)(\theta,s)+$$
$$\partial_s W^{\leqslant}(\theta-\omega\overline{r\circ K}\circ(W^{\leqslant}+tH)(\theta,s), se^{-\lambda\overline{r\circ K}\circ(W^{\leqslant}+tH)(\theta,s)}),\varepsilon)$$
$$se^{-\lambda\overline{r\circ K}\circ(W^{\leqslant}+tH)(\theta,s)}D(\overline{r\circ K})\circ(W^{\leqslant}+tH)(\theta,s)(-\lambda)\big]H(\theta,s)\,dt,$$

Similar to (ℓ_1) case, we have that $\|(\ell_2)\phi(s)\|_{L^{>},N} \leqslant C$.

For (ℓ_3), let us notice that $\sum_{i=0}^{N-1}\overline{Y}^i(\theta)s^i$ is the truncated Taylor expansion at $s=0$ for

$$\overline{Y}(W^{\leqslant}(\theta,s), W^{\leqslant}(\theta-\omega\overline{r\circ K}(W^{\leqslant}(\theta,s)), se^{-\lambda\overline{r\circ K}(W^{\leqslant}(\theta,s))}),\varepsilon), \tag{4.69}$$

According to Taylor's Formula with remainder, see [LdlL10], we just need to show that for $m \leqslant N$

$$\frac{\partial^{N-m}}{\partial s^{N-m}}\frac{\partial^l}{\partial\theta^l}\frac{\partial^m}{\partial s^m}eq.\ (4.69),$$

and for $m > N$,

$$\frac{\partial^m}{\partial s^m}\frac{\partial^l}{\partial\theta^l}(\ell_3),$$

are bounded for all θ, $|s| \leqslant 1$, and $l+m \leqslant L^{>}$. This is true if we assume that the lower order term has more regularity, more precisely, $L-1 \geqslant L^{>}+N$. We will take $L^{>} = L-1-N$ to optimise regularity. Therefore, we have $\|(\ell_3)\phi(s)\|_{L^{>},N} \leqslant C$ and the claim is proved.

Hence, according to eq. (4.65), if $m \leqslant N$, for small ε, we have that

$$|\partial_\theta^l\partial_s^m\Gamma_i^{>}(H)(\theta,s)| \leqslant \varepsilon\left|\int_0^\infty e^{-\lambda_0 t}C|s|^{N-m}e^{\lambda(N-m)t}e^{\lambda mt}\,dt\right| \leqslant B|s|^{N-m},$$

if $m > N$, for small ε, we have that

$$|\partial_\theta^l\partial_s^m\Gamma_i^{>}(H)(\theta,s)| \leqslant \varepsilon\left|\int_0^\infty e^{-\lambda_0 t}Ce^{\lambda mt}\,dt\right| \leqslant B,$$

Therefore, for small ε, $\|\Gamma_i^{>}(H)\|_{L^{>},N} \leqslant B$, when $\|H\|_{L^{>},N} \leqslant B$. □

LEMMA 4.25. *There is $\varepsilon_2^> > 0$ such that for all $0 < \varepsilon \leqslant \varepsilon_2^>$, $\Gamma^>$ in eq. (4.65) is a contraction in $\|\cdot\|_{0,N}$ defined in eq. (4.66).*

Proof. Recall that $\|H\|_{0,N} = \sup_{\theta,s} |H(\theta,s)||s|^{-N}$. We consider

$$\begin{aligned}\Gamma^>(H)(\theta,s) - \Gamma^>(H')(\theta,s)\\ = -\varepsilon \int_0^\infty \begin{pmatrix} 1 & 0 \\ 0 & e^{-\lambda_0 t} \end{pmatrix} (Y^>(H, c(t), \varepsilon) - Y^>(H', c(t), \varepsilon))\phi(se^{\lambda t})\, dt\end{aligned}$$

Known the low order terms let us denote $W = W^{\leqslant} + H$ and $W' = W^{\leqslant} + H'$. Then

$$\begin{aligned}Y^>(H, c(t), \varepsilon) - Y^>(H', c(t), \varepsilon)\\ = \overline{Y}(W(c(t)), \widetilde{W}(c(t)), \varepsilon) - \overline{Y}(W'(c(t)), \widetilde{W}'(c(t)), \varepsilon).\end{aligned}$$

with $c(t) = (\theta + \omega t, se^{\lambda t})$.

Note that for all θ, s,

$$|W(\theta,s) - W'(\theta,s)| = |H(\theta,s) - H'(\theta,s)| \leqslant \|H - H'\|_{L^>,N}|s|^N.$$

And adding and subtracting terms we have that $\widetilde{W}(\theta,s) - \widetilde{W}'(\theta,s)$, which is equal to

$$\begin{aligned}W(\theta - \omega\overline{r\circ K} \circ W(\theta,s), se^{-\lambda\overline{r\circ K}\circ W(\theta,s)}) -\\ W'(\theta - \omega\overline{r\circ K} \circ W'(\theta,s), se^{-\lambda\overline{r\circ K}\circ W'(\theta,s)})\end{aligned}$$

is bounded uniformly in θ and s by

$$\begin{aligned}&\Big|W(\theta - \omega\overline{r\circ K} \circ W(\theta,s), se^{-\lambda\overline{r\circ K}\circ W(\theta,s)}) -\\ &W'(\theta - \omega\overline{r\circ K} \circ W(\theta,s), se^{-\lambda\overline{r\circ K}\circ W(\theta,s)})\Big| +\\ &\Big|W'(\theta - \omega\overline{r\circ K} \circ W(\theta,s), se^{-\lambda\overline{r\circ K}\circ W(\theta,s)}) -\\ &W'(\theta - \omega\overline{r\circ K} \circ W'(\theta,s), se^{-\lambda\overline{r\circ K}\circ W(\theta,s)})\Big| +\\ &\Big|W'(\theta - \omega\overline{r\circ K} \circ W'(\theta,s), se^{-\lambda\overline{r\circ K}\circ W(\theta,s)}) -\\ &W'(\theta - \omega\overline{r\circ K} \circ W'(\theta,s), se^{-\lambda\overline{r\circ K}\circ W'(\theta,s)})\Big| \leqslant M_1\|H - H'\|_{0,N}|s|^N,\end{aligned}$$

where

$$M_1 = e^{-\lambda N\|\overline{r\circ K}\|_\infty} + (\|DW^{\leqslant}\|_\infty + \|DH'\|_\infty)\|D(\overline{r\circ K})\|_\infty(|\omega| + |\lambda||s|e^{-\lambda\|\overline{r\circ K}\|_\infty}).$$

Then,

$$|\Gamma^>(H)(\theta,s) - \Gamma^>(H')(\theta,s)| \leqslant \varepsilon\|H - H'\|_{0,N}|s|^N \int_0^\infty e^{(\lambda N-\lambda_0)t} M\phi(se^{\lambda t})dt,$$

where

$$M = \|D_1\overline{Y}\|_\infty + \|D_2\overline{Y}\|_\infty M_1.$$

Now, notice that by definition of D^1, we have that $\lambda \in [\frac{4\lambda_0}{3}, \frac{2\lambda_0}{3}]$, then $\lambda N - \lambda_0 < 0$ if $N \geqslant 2$. Under this assumption, we have for all θ, s,

$$|\Gamma^>(H)(\theta,s) - \Gamma^>(H')(\theta,s)| \leqslant -\frac{\varepsilon M}{\lambda N - \lambda_0}\|H - H'\|_{0,N}|s|^N.$$

If ε is small enough, we have for all θ, s,

$$|\Gamma^>(H)(\theta,s) - \Gamma^>(H')(\theta,s)| \leqslant \mu\|H - H'\|_{0,N}|s|^N.$$

Hence for small enough ε,

$$\|\Gamma^>(H) - \Gamma^>(H')\|_{0,N} \leqslant \mu\|H - H'\|_{0,N},$$

and $\Gamma^>$ becomes is a contraction. Note that smallness condition for ε only depends on N, B^j, $j = 0,\dots,N-1$, ω, λ, $\overline{Y}$, and $\overline{r\circ K}$. □

Now for any initial guess $W^{<,0}$, the sequence $(\Gamma^>)^n(W^{>,0})$ in the function space $D^>$, will converge pointwise to a function $W^>$, which is indeed a fixed point of $\Gamma^>$, by [Lan73], we know that $W^>$ is $(L^> - 1)$ times differentiable, with $(L^> - 1)$-th derivative Lipschitz.

It remains to do the error analysis. Now the error function is defined as

$$E^>(\theta,s) \coloneqq \left[\omega\partial_\theta + \begin{pmatrix}\lambda s & 0\\ 0 & \lambda s - \lambda_0\end{pmatrix}\right]W^{>,0}(\theta,s) - \varepsilon Y^>(W^{>,0},\theta,s,\varepsilon)\phi(s),$$

along the characteristics $c(t) = (\theta + \omega t, se^{\lambda t})$, we have

$$E^>(c(t)) = \left[\omega\partial_\theta + \begin{pmatrix}\lambda s & 0\\ 0 & \lambda s - \lambda_0\end{pmatrix}\right]W^{>,0}(c(t)) - \varepsilon Y^>(W^{>,0},c(t),\varepsilon)\phi(se^{\lambda t}).$$

Hence,

$$\Gamma^>(W^{>,0})(\theta,s) - W^{>,0}(\theta,s) = \int_0^\infty \begin{pmatrix}1 & 0\\ 0 & e^{-\lambda_0 t}\end{pmatrix} E^>(c(t))\,dt.$$

Based on proof of Lemma **4.24**, we know that $\|E^{>}\|_{0,N}$ is bounded, therefore, for the maximum norm,

$$\|\Gamma^{>}(W^{>,0}) - W^{>,0}\|_{0,N} \leqslant \frac{1}{\lambda_0 - \lambda N}\|E^{>}\|_{0,N}|s|^N,$$

and then

$$\|W^{>} - W^{>,0}\|_{0,N} \leqslant \frac{1}{(1-\mu)(\lambda_0 - \lambda N)}\|E^{>}\|_{0,N}|s|^N. \tag{4.70}$$

If we take account of error estimations in eqs. (4.50), (4.62), (4.63), and (4.70), we see that $l = 0$ case of eq. (4.34) is proved. Inequality in eq. (4.34) for $l \neq 0$ is obtained using interpolation inequalities. Indeed, the norm

$$\|W(\theta, s) - W^{0,0}(\theta) - W^{1,0}(\theta)s - W^{>,0}(\theta, s)\|_{C^l}$$

is bounded by

$$\sum_{j=0}^{N-1} |s|^j \|W^j - W^{j,0}\|_{C^l} + \|W^{>} - W^{>,0}\|_{C^l} \leqslant$$
$$\sum_{j=0}^{N-1} c_j |s|^j \|E^j\|_{C^0}^{1-\frac{l}{L-2-N}} + c_{>}(|s|^N \|E^{>}\|_{0,N})^{1-\frac{l}{L-2-N}}.$$

for some constants c_j and $c_{>}$ independent of $W^{j,0}$ for $0 \leqslant j < N$, $W^{>,0}$, ω^0 and λ^0. Taking their maximum we get the upper bound eq. (4.34).

4.8 Numerical experiment

The van der Pol oscillator [vdP20] is an oscillator with non-linear damping governed by the second-order differential equation [HG15].

The state-dependent perturbation of the van Der Pol oscillator has the form

$$\begin{aligned} \dot{x}(t) &= y(t), \\ \dot{y}(t) &= \mu(1 - x(t)^2)y(t) - x(t) + \varepsilon x(t - r(x(t))), \end{aligned} \tag{4.71}$$

with, for instance, $\mu = 1$ and $\varepsilon = 10^{-4}$. For the delay function $r(x)$ we are going to consider two case. A pure state-dependent delay case or just a constant delay case. That is, $r(x) = \beta e^{2x}$ or just $r(x) = \beta$ with $\beta = 0.006$.

The first step consists in computing the change of coordinate K, the frequency ω_0 of the limit cycle and its speed rate $\lambda_0 < 0$ for $\varepsilon = 0$. A limit cycle close to $(x, y) = (2, 0)$ with frequency $\omega_0 = 0.1500760842377394$ and $\lambda_0 = -1.0593769948418550$ allows to run Algorithm **4.1** and so generate its isochrons in Figure **4.2**.

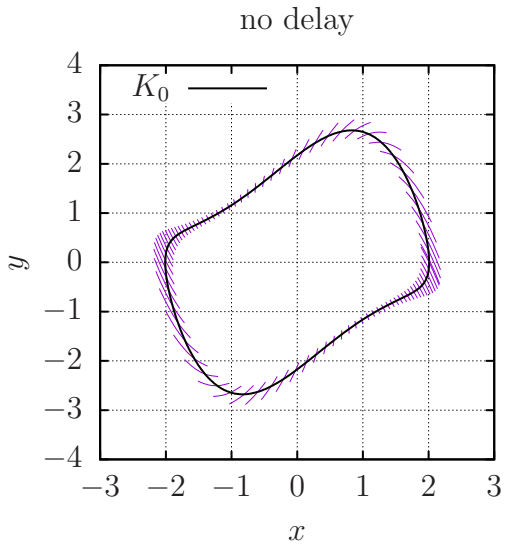

Figure 4.2. Limit cycle and its isochrons for the unperturbed, eq. (4.71).

4.8.1 State-dependent delay perturbation

Using Algorithm **4.5** for the state-dependent $r(x) = \beta e^{2x}$, with a tolerance of 10^{-11} in double-precision we obtain W^0 and $\omega = 0.1500677573762797$. We notice a speed factor of 2.25 using the NFFT3 w.r.t. to the simulation with a direct implementation of the Fourier composition, that is, the one that we use in section **4.6.3** for the orders s^j with $j \geqslant 1$ but with polynomials of degree 0.

After that we can go forward and use Algorithm **4.6** compute the W^1, and λ that with the same tolerance we get $\lambda = -1.059382672350053$. Then using the criterion in section **4.6.2** for the scaling factor we can reach the first 4 next orders whose isochrons are plotted in Figure **4.3**. In that case the mean speed factor using the two different numerical composition of Fourier series, that is Theorems **4.9** and **4.10** is around 1.3 of the former approach. Both two approaches differ essentially in round-off or value smaller than the tolerance requested.

4.8.2 Constant delay perturbation

Our method also applies to the constant delay case $r(x) = \beta$. In particular, in some aspects the constant delay case is simpler. Indeed the expression of $\widetilde{W}$ is just $\widetilde{W}(\theta, s) = W(\theta - \omega\beta, se^{-\lambda\beta})$. However the composition w.r.t. K is

still needed to do it with jet transport for the step item **4** of Algorithm **4.6**.

In this simulation and with the same tolerance of 10^{-11} in double-precision, we get $\omega = 0.1500677573212776$, $\lambda = -1.059382495053311$ and 10 order in less than 4 minutes. Figure **4.3** shows the isochrons for the constant delay case.

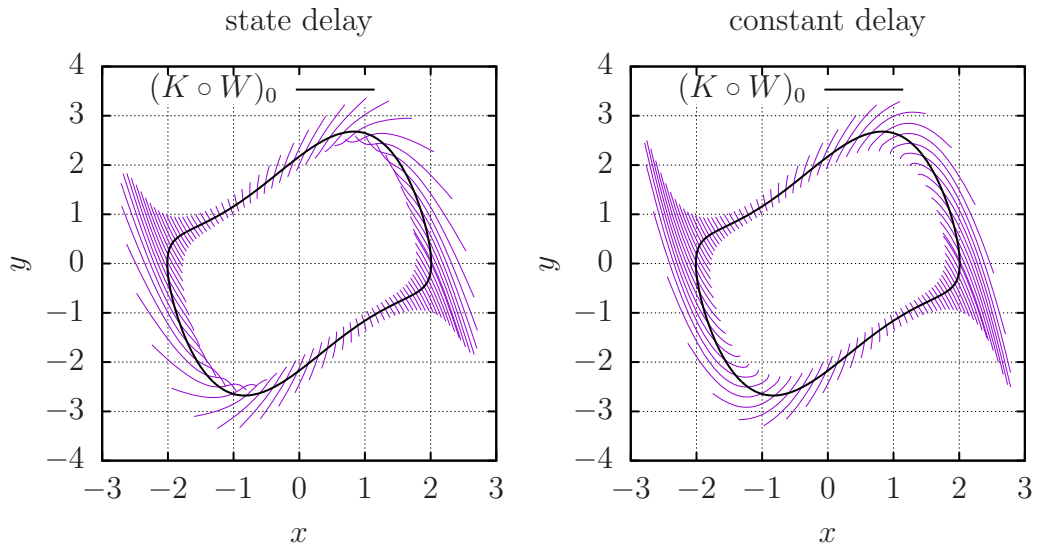

Figure 4.3. Limit cycle and its isochrons for the perturbed case $K \circ W$ of eq. (4.71) with state-dependent map $r(x) = \beta e^{2x}$, and constant map $r(x) = \beta$.

Conclusions and future work

In reference to the introduction of Chapter **2**, this thesis is a splicing point in the author's life.

Thanks to that point, we have had the chance to write down a formal interpretation of the notion of jet transport in high order variational flows. In particular, we have proved in Chapter **1** that independently of the numerical method that integrates an ordinary differential equation (ODE) with their variational equations, that is, the ODE itself and the (normalised) variation w.r.t. the initial conditions or parameters are exactly the same like integrating the same initial ODE with jet transport, not only at the end of the integration also in the intermediate steps. That justifies, for instance, stepsize control of the integrator with jets.

We have provided formal proofs for the classical methods of integration such as Runge-Kutta methods and Taylor method. Despite of the simplicity in the proofs, we did not find any so clear proofs for this result which seems to be basic to understand the jet transport in higher orders. The good understanding of the jet transport in numerical integrators allowed to consider the Poincaré map of an arbitrary ODE and its high order derivatives which are exactly obtained via jet transport on the numerical integrator.

There are two kind of Poincaré maps; the ones that are obtained by a temporal section and the ones coming from a spatial section. The former do not present any trouble in the use of jet transport but the latter have a limitation in use of jet transport. In essence the problem is due to the fact that the spatial derivatives and the temporal ones are mixed in this case. That implies that the integrator must be able to capture the same order of differentiability that is being requested in the jet transport. While Runge-Kutta methods and other similar methods have a limitation in the order, Taylor method can be performed in any temporal order and then it allows to agreed with the one for jet transport.

Because of the exactness in the use of jet transport, we can claim that the computation of the parametrisation method via jet trasnport in multi-precision arithmetic is exactly the same than if we added the full system of

variational equations in the integration.

The result in this project opens many new ones that can be understanding by the use of jet transport. For instance, normal forms in higher orders, control theory in higher orders, accurate integrator with suitable stepsize control, and parametrisation method of tori in higher dimension as well as its continuation.

In Chapter **2**, we have seen that the use of an interpolation method, based on a linear combination of the spatial points applies for jet transport which means that the results in Chapter **1** can be extended for delay differential equations (DDEs). In that chapter, we have focused on the constant delay case and we explained in detail the results in [GJS18] which proofs theoretically the equilibrium points and their stability are the same as the DDE which takes the delay equals to zero for a specific kind of constant DDE. However, these kind of results do not quantify the stability and after some preliminary simulations we thought to be interested in providing a further study in the quantification of the stability in terms of the delay. Using the jet transport we avoided to solve the transcendental characteristic equation, which allows to quantify the stability in its solution with major real part.

Chapter **3** continues the results in Chapter **2** and they are applied in the numerical computation of periodic and quasi-periodic solutions as well as in their stability and continuation. In that context the linear system to solve in a Newton approach can become large but due to the compactness of the Poincaré map in the DDE the iterative linear solver and the corresponding preconditioners have become a good alternative to use a matrix-free Newton method.

Because of the timings in the results (which are different in the writing of the thesis), we establish as coming projects the use of the results of Chapters **1** and **2** for the parametrisation of constant DDEs of (un)stable of (quasi)periodic orbits for higher orders, Lyapunov exponents, etc. In the case of manifold computation for DDEs, we know in advance that the unstable manifold will be finite dimensional and the stable one will be infinite dimensional but some of the directions will be more important than others, and they can be quantify by the associated element in the spectrum. Therefore, as we have done in Chapter **4** it makes sense to firstly focus on the slowest stable direction.

Chapter **4** has been allowed us to get the parametrisation of the slowest stable manifold of state-dependent delay differential equations (SDDEs) that are obtained as a perturbation of an ordinary differential equations. Although

it is a perturbation result, it turns on again the field of SDDE that in the last years have been a kind of stuck. We strongly believe that the novel techniques developed in Chapter **4** opens a lot of potential new results, specially due to its *a posteriori* formulation. In particular, new research directions will be in the existence and computation of the full infinite stable manifold, the use of Lindstedt series for SDDEs, and bifurcation theory.

Besides all the potential new projects coming from the previous chapters, we would like to mention other projects that we are working on now and we expect to have results soon. For instance, the project with À. Jorba and J.P. Lessard for the existence of choreographies for state-dependent motion of bodies whose speed of gravitational interaction is finite. The one with R. Calleja, A. Celletti, R. de la Llave for the rigorous proof of torus in the spin-orbit problem with tidal torque. And also the one with J. Jaquette and À. Jorba about rigorous integrators.

Bibliography

[ADLBZB10] R. Armellin, P. Di Lizia, F. Bernelli-Zazzera, and M. Berz. Asteroid close encounters characterization using differential algebra: the case of Apophis. *Celestial Mech. Dynam. Astronom.*, 107(4):451–470, 2010.

[AFJ+08] E. M. Alessi, A. Farrés, À. Jorba, C. Simó, and A. Vieiro. Efficient usage of self validated integrators for space applications. Ariadna final report, contract no. 20783/07/nl/cb, ESTEC (European Space Agency), 2008.

[AFJ+09] E.M. Alessi, A. Farrés, À. Jorba, C. Simó, and A. Vieiro. Jet transport and applications to neos. In *Proceedings of the 1st IAA Planetary Defense Conference: Protecting Earth from Asteroids*, Granada (Spain), 2009.

[AR67] R. Abraham and J. Robbin. *Transversal mappings and flows*. An appendix by Al Kelley. W. A. Benjamin, Inc., New York-Amsterdam, 1967.

[BBN99] R. Baltensperger, J.-P. Berrut, and B. Noël. Exponential convergence of a linear rational interpolant between transformed Chebyshev points. *Math. Comp.*, 68(227):1109–1120, 1999.

[BG15] M. Berljafa and S. Güttel. Generalized rational Krylov decompositions with an application to rational approximation. *SIAM J. Matrix Anal. Appl.*, 36(2):894–916, 2015.

[BT04] J.-P. Berrut and L. N. Trefethen. Barycentric Lagrange interpolation. *SIAM Rev.*, 46(3):501–517, 2004.

[But87] J. C. Butcher. *The numerical analysis of ordinary differential equations*. A Wiley-Interscience Publication. John Wiley & Sons, Ltd., Chichester, 1987. Runge-Kutta and general linear methods.

[BZ13] A. Bellen and M. Zennaro. *Numerical methods for delay differential equations*. Numerical Mathematics and Scientific Computation. Oxford University Press, Oxford, 2013. First paperback reprint of the 2003 original [MR1997488].

[Car81] J. Carr. *Applications of centre manifold theory*, volume 35 of *Applied Mathematical Sciences*. Springer-Verlag, New York-Berlin, 1981.

[CFdlL05] X. Cabré, E. Fontich, and R. de la Llave. The parameterization method for invariant manifolds. III. Overview and applications. *J. Differential Equations*, 218(2):444–515, 2005.

[CJ00] E. Castellà and À. Jorba. On the vertical families of two-dimensional tori near the triangular points of the bicircular problem. *Celestial Mech. Dynam. Astronom.*, 76(1):35–54, 2000.

[Cle62] C. W. Clenshaw. *Chebyshev series for mathematical functions*. National Physical Laboratory Mathematical Tables, Vol. 5. Department of Scientific and Industrial Research. Her Majesty's Stationery Office, London, 1962.

[Cor93] P. B. Corkum. Plasma perspective on strong field multiphoton ionization. *Phys. Rev. Lett.*, 71:1994–1997, Sep 1993.

[Cor14] P. Corkum. Recollision physics. *Phyricsl Today*, 64:36–41, 03 2014.

[CRR64] J. Cronin, P. B. Richards, and L. H. Russell. Some periodic solutions of a four-body problem. I. *Icarus*, 3:423–428, 1964.

[DB08] G. Dahlquist and Å. Björck. *Numerical methods in scientific computing. Vol. I.* Society for Industrial and Applied Mathematics (SIAM), Philadelphia, PA, 2008.

[DGKS76] J. W. Daniel, W. B. Gragg, L. Kaufman, and G. W. Stewart. Reorthogonalization and stable algorithms for updating the Gram-Schmidt QR factorization. *Math. Comp.*, 30(136):772–795, 1976.

[DLABZB14] P. Di Lizia, R. Armellin, F. Bernelli-Zazzera, and M. Berz. High order optimal control of space trajectories with uncertain boundary conditions. *Acta Astronautica*, 93:217 – 229, 2014.

[DLAL08] P. Di Lizia, R. Armellin, and M. Lavagna. Application of high order expansions of two-point boundary value problems to astrodynamics. *Celestial Mech. Dynam. Astronom.*, 102(4):355–375, 2008.

[dlLO99] R. de la Llave and R. Obaya. Regularity of the composition operator in spaces of Hölder functions. *Discrete Contin. Dynam. Systems*, 5(1):157–184, 1999.

[dlLP02] R. de la Llave and N. P. Petrov. Regularity of conjugacies between critical circle maps: an experimental study. *Experiment. Math.*, 11(2):219–241, 2002.

[DP86] J. R. Dormand and P. J. Prince. Runge-Kutta triples. *Comput. Math. Appl. Ser. A*, 12(9):1007–1017, 1986.

[FJ05] M. Frigo and S. G. Johnson. The design and implementation of FFTW3. *Proceedings of the IEEE*, 93(2):216–231, 2005. Special issue on "Program Generation, Optimization, and Platform Adaptation".

[FR81] V. Franceschini and L. Russo. Stable and unstable manifolds of the Hénon mapping. *J. Statist. Phys.*, 25(4):757–769, 1981.

[GC91] A. Griewank and G.F. Corliss, editors. *Automatic Differentiation of Algorithms: Theory, Implementation, and Application*. SIAM, Philadelphia, Penn., 1991.

[GH01] N. Guglielmi and E. Hairer. Implementing Radau IIA methods for stiff delay differential equations. *Computing*, 67(1):1–12, 2001.

[GH08] N. Guglielmi and E. Hairer. Computing breaking points in implicit delay differential equations. *Adv. Comput. Math.*, 29(3):229–247, 2008.

[Gim15] J. Gimeno. On time Delay Differential Equations. Master's thesis, Universitat de Barcelona, 2015.

[GJS18] J. Gimeno, À. Jorba, and J. Sardanyés. On the effect of time lags on a saddle-node remnant in hyperbolic replicators. *J. Phys. A*, 51(38):385601, 12, 2018.

[GMJ17] C. M. Groothedde and J. D. Mireles James. Parameterization method for unstable manifolds of delay differential equations. *J. Comput. Dyn.*, 4(1-2):21–70, 2017.

[Guc75] J. Guckenheimer. Isochrons and phaseless sets. *J. Math. Biol.*, 1(3):259–273, 1974/75.

[GW08] A. Griewank and A. Walther. *Evaluating derivatives*. Society for Industrial and Applied Mathematics (SIAM), Philadelphia, PA, second edition, 2008. Principles and techniques of algorithmic differentiation.

[Hay50] N. D. Hayes. Roots of the transcendental equation associated with a certain difference-differential equation. *J. London Math. Soc.*, 25:226–232, 1950.

[HCF+16] À. Haro, M. Canadell, J.-L. Figueras, A. Luque, and J.-M. Mondelo. *The parameterization method for invariant manifolds*, volume 195 of *Applied Mathematical Sciences*. Springer, [Cham], 2016. From rigorous results to effective computations.

[HdlL13] G. Huguet and R. de la Llave. Computation of limit cycles and their isochrons: fast algorithms and their convergence. *SIAM J. Appl. Dyn. Syst.*, 12(4):1763–1802, 2013.

[HG15] A. Hou and S. Guo. Stability and Hopf bifurcation in van der Pol oscillators with state-dependent delayed feedback. *Nonlinear Dynam.*, 79(4):2407–2419, 2015.

[HNrW93] E. Hairer, S. P. Nø rsett, and G. Wanner. *Solving ordinary differential equations. I*, volume 8 of *Springer Series in Computational Mathematics*. Springer-Verlag, Berlin, second edition, 1993. Nonstiff problems.

[Hua60] S. S. Huang. Very restricted four-body problem. Technical note TN D-501, Goddard Space Flight Center, NASA, 1960.

[HVL93] J. K. Hale and S. M. Verduyn Lunel. *Introduction to functional-differential equations*, volume 99 of *Applied Mathematical Sciences*. Springer-Verlag, New York, 1993.

[HW10] E. Hairer and G. Wanner. *Solving ordinary differential equations. II*, volume 14 of *Springer Series in Computational Mathematics*. Springer-Verlag, Berlin, 2010. Stiff and differential-algebraic problems, Second revised edition, paperback.

[IJ90] G. Iooss and D. D. Joseph. *Elementary stability and bifurcation theory*. Undergraduate Texts in Mathematics. Springer-Verlag, New York, second edition, 1990.

[JC19] M. Jorba-Cuscó. *Periodic time dependent Hamiltonian systems and applications*. PhD thesis, Universitat de Barcelona, 2019.

[Jor01] À. Jorba. Numerical computation of the normal behaviour of invariant curves of n-dimensional maps. *Nonlinearity*, 14(5):943–976, 2001.

[JPN10] À. Jorba and E.-M. Pérez-Nueno. Propagation of the uncertainty region for a particle around the Earth. Final report, Deimos Space SL, 2010.

[JZ05] À. Jorba and M. Zou. A software package for the numerical integration of ODEs by means of high-order Taylor methods. *Experiment. Math.*, 14(1):99–117, 2005.

[KCUM14] A. Kamor, C. Chandre, T. Uzer, and F. Mauger. Recollision scenario without tunneling: Role of the ionic core potential. *Physical review letters*, 112:133003, 04 2014.

[KKP09] J. Keiner, S. Kunis, and D. Potts. Using NFFT 3—a software library for various nonequispaced fast Fourier transforms. *ACM Trans. Math. Software*, 36(4):Art. 19, 30, 2009.

[KL12] G. Kiss and J.-P. Lessard. Computational fixed-point theory for differential delay equations with multiple time lags. *J. Differential Equations*, 252(4):3093–3115, 2012.

[KMCU14] A. Kamor, F. Mauger, C. Chandre, and T. Uzer. How key periodic orbits drive recollisions in a circularly polarized laser field. *Physical Review Letters*, 25:253002, 07 2014.

[Knu98] D. E. Knuth. *The art of computer programming. Vol. 2*. Addison-Wesley, Reading, MA, third edition, 1998. Seminumerical algorithms.

[KS17] T. Kapela and C. Simó. Rigorous KAM results around arbitrary periodic orbits for Hamiltonian systems. *Nonlinearity*, 30(3):965–986, 2017.

[Kuz04] Y.A. Kuznetsov. *Elements of applied bifurcation theory*, volume 112 of *Applied Mathematical Sciences*. Springer-Verlag, New York, third edition, 2004.

[Lan73] O. E. Lanford. Bifurcation of periodic solutions into invariant tori: The work of ruelle and takens. In Ivar Stakgold, Daniel D. Joseph, and David H. Sattinger, editors, *Nonlinear Problems in the Physical Sciences and Biology*, pages 159–192, Berlin, Heidelberg, 1973. Springer-Verlag, New York-Berlin.

[LdlL10] X. Li and R. de la Llave. Convergence of differentiable functions on closed sets and remarks on the proofs of the "converse approximation lemmas". *Discrete Contin. Dyn. Syst. Ser. S*, 3(4):623–641, 2010.

[LELR97] T. Luzyanina, K. Engelborghs, K. Lust, and D. Roose. Computation, continuation and bifurcation analysis of periodic solutions of delay differential equations. *Internat. J. Bifur. Chaos Appl. Sci. Engrg.*, 7(11):2547–2560, 1997.

[LSY98] R. B. Lehoucq, D. C. Sorensen, and C. Yang. *ARPACK users' guide*, volume 6 of *Software, Environments, and Tools*. Society for Industrial and Applied Mathematics (SIAM), Philadelphia, PA, 1998. Solution of large-scale eigenvalue problems with implicitly restarted Arnoldi methods.

[MADLZ15] A. Morselli, R. Armellin, P. Di Lizia, and F. B. Zazzera. A high order method for orbital conjunctions analysis: Monte carlo collision probability computation. *Advances in Space Research*, 55(1):311 – 333, 2015.

[MCU10] F. Mauger, C. Chandre, and T. Uzer. Recollisions and correlated double ionization with circularly polarized light. *Phys. Rev. Lett.*, 105:083002, Aug 2010.

[MKCU12] F. Mauger, A. Kamor, C. Chandre, and T Uzer. Delayed double ionization as a signature of hamiltonian chaos. *Phys. Rev. E*, 85:066205, 06 2012.

[Nau12] U. Naumann. *The art of differentiating computer programs*, volume 24 of *Software, Environments, and Tools*. Society for Industrial and Applied Mathematics (SIAM), Philadelphia, PA, 2012. An introduction to algorithmic differentiation.

[NCUW15] M. J. Norman, C. Chandre, T. Uzer, and P. Wang. Nonlinear dynamics of ionization stabilization of atoms in intense laser fields. *Phys. Rev. A*, 91:023406, Feb 2015.

[Nis16] J. Nishiguchi. On parameter dependence of exponential stability of equilibrium solutions in differential equations with a single constant delay. *Discrete Contin. Dyn. Syst.*, 36(10):5657–5679, 2016.

[Nus78] R. D. Nussbaum. Differential-delay equations with two time lags. *Mem. Amer. Math. Soc.*, 16(205):vi+62, 1978.

[PPGM18] D. Pérez-Palau, G. Gómez, and J. J. Masdemont. A new subdivision algorithm for the flow propagation using polynomial algebras. *Commun. Nonlinear Sci. Numer. Simul.*, 61:37–53, 2018.

[Saa03] Y. Saad. *Iterative methods for sparse linear systems*. Society for Industrial and Applied Mathematics, Philadelphia, PA, second edition, 2003.

[SGJM95] C. Simó, G. Gómez, À. Jorba, and J. Masdemont. The bicircular model near the triangular libration points of the RTBP. In *From Newton to chaos (Cortina d'Ampezzo, 1993)*, volume 336 of *NATO Adv. Sci. Inst. Ser. B Phys.*, pages 343–370. Plenum, New York, 1995.

[SZ18] R. Szczelina and P. Zgliczyński. Algorithm for rigorous integration of delay differential equations and the computer-assisted proof of periodic orbits in the Mackey-Glass equation. *Found. Comput. Math.*, 18(6):1299–1332, 2018.

[TW91] L. N. Trefethen and J. A. C. Weideman. Two results on polynomial interpolation in equally spaced points. *J. Approx. Theory*, 65(3):247–260, 1991.

[VADLL14] M. Valli, R. Armellin, P. Di Lizia, and M. R. Lavagna. Nonlinear filtering methods for spacecraft navigation based on differential algebra. *Acta Astronautica*, 94(1):363 – 374, 2014.

[vdP20] B. van der Pol. A theory of the amplitude of free and forced triode vibrations. *Radio Review.*, 1(701-710):754–762, 1920.

[Ver78] J. H. Verner. Explicit Runge-Kutta methods with estimates of the local truncation error. *SIAM J. Numer. Anal.*, 15(4):772–790, 1978.

[WDLA+15] A. Wittig, P. Di Lizia, R. Armellin, K. Makino, F. Bernelli-Zazzera, and M. Berz. Propagation of large uncertainty sets in orbital dynamics by automatic domain splitting. *Celestial Mech. Dynam. Astronom.*, 122(3):239–261, 2015.